

T H E U N I V E R S I T Y O F M I C H I G A N

COLLEGE OF ENGINEERING
Department of Civil Engineering

STRUCTURAL DESIGN
OF
ASPHALT PAVEMENTS

Mihai Rafiroiu
Lecturer in Civil Engineering

Polytechnic Institute
Timosara, Romania

partially supported by:

Funds from the Second International Conference
on the Structural Design of Asphalt Pavements

Department of Civil Engineering
The University of Michigan

July 1974

1. Introduction

This report is part of a study on aspects of Materials Resource Management in Highway Construction. In order to find a practical system (procedure) for economical design and selection of materials for road structures, the structural design of asphalt pavements will be discussed. The report has 5 main parts:

2. The Problem.
3. Stresses and Strains in Homogeneous Masses.
4. Stresses and Strains in Layered Systems.
5. Deriving a New Design Method.
6. Conclusions.

2. The Problem

As it was shown in Report No. 1, Chapter 2, the construction materials transportation represents about 60% of all transportation costs or 9 to 18% of the total investment in the highway. It should also be noted that the costs of the pavement amount to 24 to 50% of the total investment and no reduction of the pavement cost is possible without a good understanding of the behavior of

the road body under current loads.

The topic of this report deals with a semiempirical approach for a new design method based on the energy consumed during the loading of the pavement.

The new design method will be used in further investigations, in order to get an appropriate procedure for the economical design of the pavement and the reduction of pavement construction costs by taking into account all future maintenance operations and costs. The new design method will be also used in order to assess the needed quantities of materials upon the highway sections before any optimization of the materials transportation is done.

In this report only part 3, entitled "Stresses and Strains in Homogeneous Masses" deals with things already known. All further developments were done by the author of this report even if quotations from the technical literature are given.

3. Stresses and Strains in Homogeneous Masses

The distribution of the stresses below a concentrated or circular load has been studied by many researchers. The general equations have been obtained for an ideal material which is perfectly elastic and homogeneous and obeys Hooke's law [Ref. 4, page 21].

Many experiments have demonstrated that these assumptions are generally acceptable for a low level of stresses and displacements because the measured values of the stresses and strains reasonably agree with the computed ones.

The theory of elasticity [Ref. 14, page 174] demonstrates that

the stresses in axial symmetric and homogeneous masses can be computed with equations (1) where ϕ is an arbitrary function which has to fit some boundary conditions.

The general equations for the stresses are the following:

$$\begin{aligned}\sigma_r &= \frac{\partial}{\partial z} \left(\mu \cdot \nabla^2 \phi - \frac{\partial^2 \phi}{\partial r^2} \right) \\ \sigma_\theta &= \frac{\partial}{\partial z} \left(\mu \cdot \nabla^2 \phi - \frac{1}{r} \cdot \frac{\partial \phi}{\partial r} \right) \\ \sigma_z &= \frac{\partial}{\partial z} \left[(2-\mu) \cdot \nabla^2 \phi - \frac{\partial^2 \phi}{\partial z^2} \right] \\ \tau_{rz} &= \frac{\partial}{\partial r} \left[(1-\mu) \cdot \nabla^2 \phi - \frac{\partial^2 \phi}{\partial z^2} \right]\end{aligned}\tag{1}$$

where all parameters are defined as shown in Fig. 1.

The boundary conditions used in order to define the function ϕ are generally reduced to one:

$$\left(\frac{\partial^2}{\partial r^2} + \frac{1}{r} \cdot \frac{\partial}{\partial r} + \frac{\partial^2}{\partial z^2} \right) \left(\frac{\partial^2 \phi}{\partial r^2} + \frac{1}{r} \frac{\partial \phi}{\partial r} + \frac{\partial^2 \phi}{\partial z^2} \right) = 0\tag{2}$$

usually written as follows:

$$\nabla^2 (\nabla^2 \phi) = 0\tag{2.a}$$

The literature in this area shows that one can use many different

solutions for ϕ and no restrictions are formulated to limit the use of new expressions for ϕ , except those in (2) or (2.a), which means that any function ϕ used has to be at least a biharmonic function.

As is well known, these types of functions are called stress functions.

The general equations for the strains can be also formulated in the same way as the stresses but it was demonstrated by Gallerkine [Ref. 14, page 176] that one can get the strains with more accuracy by using equations (3), where ϕ_1 , ϕ_2 and ϕ_3 are scalar biharmonic functions:

$$\begin{aligned} u &= B \cdot \frac{\partial w}{\partial x} + \nabla^2 \phi_1 \\ v &= B \cdot \frac{\partial w}{\partial y} + \nabla^2 \phi_2 \\ w &= B \cdot \frac{\partial w}{\partial z} + \nabla^2 \phi_3 \end{aligned} \tag{3}$$

where:

$$\begin{aligned} w &= \frac{\partial \phi_1}{\partial x} + \frac{\partial \phi_2}{\partial y} + \frac{\partial \phi_3}{\partial z} \\ B &= \frac{1}{2 \cdot (1 - \mu)} \end{aligned} \tag{4}$$

and ϕ_1 , ϕ_2 and ϕ_3 have to satisfy the condition in (2) or (2.a). The parameters in (3) are defined as shown in Fig. 2.

It is to be added that, according to Ref. 14, pages 300-302,

the idea is to use the principle of the minimal energy, where the potential energy must be expressed in terms of deformation components, namely in terms of displacements at the top level of the halfspace, the integration being extended throughout all the mass of the halfspace.

It is well known that Boussinesq used in his developments an Airy function for ϕ and his results may be written as follows [Ref. 4, page 22]:

$$\left. \begin{aligned} \sigma_z &= p \cdot \left[1 - \frac{z^3}{(a^2 + z^2)^{3/2}} \right] \\ \sigma_r &= \frac{p}{2} \cdot \left[1 + 2 \cdot \mu - \frac{2 \cdot (1 + \mu) \cdot z}{(a^2 + z^2)^{1/2}} + \frac{z^3}{(a^2 + z^2)^{3/2}} \right] \end{aligned} \right\} (5)$$

where all parameters are defined as shown in Fig. 3.

One can complete the equations (5) (that are given on a vertical axis passing through the center of the circular load) with the equation necessary for shear stress computing [Ref. 14, page 108]:

$$\tau_{rz} = \tau_{zr} = \frac{1}{2} (\sigma_z - \sigma_r) \quad (6)$$

the equation (6) being the simplest possible.

Boussinesq's problem was solved for different cases of loading. Only two of them will be presented herein.

The first case deals with an uniform loaded circular area as shown in Fig. 4.

The deflection under the center of the loaded area (w_0) is

given by equation (7) [Ref. 14, page 257]:

$$w_o = \frac{2 \cdot (1 - \mu^2)}{\pi \cdot a \cdot E} \cdot P \quad (7)$$

where:

μ is the Poisson's ratio of the loaded mass

E - Young's modulus for the same mass

a - radius of the circular area

P - total load on the circular area; it can be computed with relation in (8):

$$P = \frac{\pi}{4} \cdot D^2 \cdot p \quad (8)$$

where:

D is the diameter of the circular area, and

p - the unit load on the circular plate.

In terms of D and p, equation (7) can be presented as follows:

$$w_o = \frac{(1 - \mu^2)}{E} \cdot p \cdot D \quad (9)$$

The deflection at the edge of the plate (w_a) is given by equation (10) presented also in terms of D and p [Ref. 14, page 258]:

$$w_a = \frac{2}{\pi} \cdot \frac{(1 - \mu^2)}{E} \cdot p \cdot D \quad (10)$$

The ratio w_o/w_a is:

$$\frac{w_o}{w_a} = \frac{\pi}{2} = 1.57 \quad (11)$$

which means that w_a is almost two-thirds of w_o .

It should be said that the edge of the loaded area corresponds to an inflection point on the deflection curve as shown in Fig. 4.

The second case deals with a "semispherical" loaded circular area as shown in Fig. 5.

The deflection under the center of the loaded area (w_o^s) is given by [Ref. 14, page 260]:

$$w_o^s = \frac{3 \cdot \pi}{8} \cdot \frac{(1 - \mu^2)}{E} \cdot p \cdot D \quad (12)$$

and the deflection under the edge of the loaded area (w_a^s):

$$w_a^s = \frac{3 \cdot \pi}{16} \cdot \frac{(1 - \mu^2)}{E} \cdot p \cdot D \quad (13)$$

It means that, for this particular type of loading, the ratio w_o^s/w_a^s will be:

$$\frac{w_o^s}{w_a^s} = \frac{3 \cdot \pi}{8} \cdot \frac{16}{3 \cdot \pi} = 2 \quad (14)$$

which means that w_a^s is one-half of w_o^s .

This fact is very important for all further investigations done in this report.

But BEZUHOV [Ref. 14, page 260] adds:

"If the radius of the deformed surface at the top level of the mass is 'large' in comparison with the radius of the loaded area (and usually this is the situation), equation (15) can be considered, from a practical point of view, as being the equation

of a certain spherical surface."

Equation (15) is given below:

$$w_r^s = w_o^s - 0.75 \cdot \pi \cdot \frac{(1 - \mu^2)}{E} \cdot p \cdot \frac{r^2}{D} \quad (15)$$

where r represents the distance from the center of the plate to a point situated inside the loaded area.

The assertion is very important for the developments which will be made through this work, because the computation of the tensile stresses at the bottom of the layers will be much simplified.

4. Stresses and Strains in Layered Systems

4.1. Introduction

The problem of stresses and strains in layered systems has been under study for a long time and will continue well into the future. A great many papers, articles and reports have been published on this matter and only a few will be reviewed here.

The author of this report will present mainly his concepts, and only the most recent developments will be presented in more detail.

4.2. Notations

- D - diameter of the loaded area (assumed as a circular plate), at the top of the pavement, in units of length;
- a - radius of the loaded area, in units of length;

- P - gross or total load on the circular plate (total load on single wheel), in units of force;
- p - unit load on the circular plate, in units of force per unit of area;
- N - present annual traffic, in EWL (Equivalent Wheel Load);
- N_R - annual traffic increase rate, dimensionless;
- N_T - total estimated traffic for the service life of the pavement, in EWL;
- K_W - wheel equivalency factor, dimensionless;
- K_S - season equivalency factor, dimensionless;
- S_1 - service life of the pavement, in years;
- r - horizontal distance from the center of the load, in units of length;
- Z - depth under the center of the plate, generally expressed by the relative depth Z/D , in units of length or dimensionless;
- E_i - Young's modulus of the material in layer i, in units of force per unit of area;
- μ_i - Poisson's ratio of the material in layer i, dimensionless;
- h_i - thickness of layer i, in units of length;
- γ_i - natural density of the material in layer i, in units of weight per unit of volume;
- ϕ_i - angle of internal friction of the material in layer i, in degrees;
- ψ_{ij} - angle of superficial friction between two layers i and j, in degrees;
- f_{ij} - friction factor, at the interface of two layers i and j, dimensionless, ($f_{ij} = \tan \psi_{ij}$)

- A_i - area of assumed spherical surface at the top of layer i , in units of area;
- α_i - distribution factor of the load, at the top level of layer i , dimensionless;
$$A_i = \pi \cdot \frac{(\alpha_i \cdot D)^2}{4}$$
- λ_i - multiplier, representing the ratio between the diameter of the surface A_i and D ; dimensionless;
- σ_z - vertical stress at depth z , under the center of the plate, in units of force per unit of area;
- $\sigma_y = \sigma_r$ - radial stress at depth z , under the center of the plate, in units of force per unit of area;
- τ_z - shear stress at depth z , under the center of the plate, in units of force per unit of area;
- τ_z^{\max} - maximum tangential stress which can be mobilized at depth z , in units of force per unit of area;
- ϵ_z - unit vertical strain at depth z , under the center of the plate, dimensionless;
- σ_i^v - vertical compressive stress at the top of layer i , under the center of the plate, in units of force per unit of area;
- σ_i^m - maximum bending stress in layer i , in units of force per unit of area;
- τ_i^m - maximum shear stress in layer i , in units of force per unit of area;
- σ_i^r - maximum radial stress at the bottom of layer i (equal to radial stress at the top of layer underneath), in units of force per unit of area;
- σ_i^f - maximum friction stress at the bottom of layer i (equal to friction stress at the top of layer underneath), in units of force per unit of area;

- σ_i^{va} - average compressive stress in layer i , under the center of the plate, in units of force per unit of area;
- σ_i^{gp} - compressive stress at the bottom of layer i , due to the natural weight of the above layers;
- τ_i^a - allowable vertical shear stress along the circumference of the assumed loaded area, for layer i , in units of force per unit of area;
- p_i^{ad} - permitted pressure (compressive stress) at the top of layer i , in units of force per unit of area;
- M_x - bending moment along axis x , in units of force times units of length;
- T_x - total shear force along axis x , in units of force;
- R_i - radius of curvature at the top level of layer i , in units of length;
- w_a - permitted deflection at the surface of the pavement in the center of the loaded area, in units of length;
- w_i^j - deflection at the top level of layer i , under the edge of the surface A_j , where j is the index of another layer, in units of length;
- w_i^{pj} - partial deflection due to the compression of layer i , under the edge of the surface A_j , in units of length;
- W_e - exterior energy transferred by the load during the deformation of the highway body, in units of force times units of length;
- W_{int} - interior energy gained by the highway body during deformation, in units of force times units of length;
- W_t - subgrade energy gained during deformation, in units of force times units of length;

- W_{sr} - pavement energy, gained during deformation, in units of force times units of length;
- W_{si} - layer energy, gained in layer i during deformation, in units of force times units of length;
- F_d - correction factor, used in the computation of the permitted deflection of the surface, in the center of the loaded area; $F_d = 1$ if one uses the International Units of Measure; $F_d = 0.3937$ if one uses the American Units of Measure;
- F_r - deflection reduction factor, which represents the ratio between the average deflection of the surface, inside the loaded area, and the deflection under the center of the plate; dimensionless;
- β - correction factor, used in the computation of the deflection reduction factor, dimensionless;
- c - correction factor, used in stress computation formula, dimensionless;
- b - correction factor, used in equivalent layer thickness computation, dimensionless;
- F_s - safety factor, dimensionless;
- F_l - "lack of fit" factor, dimensionless;
- Z_f - frost penetration depth, in units of length.

4.3. Study on Stresses and Strains in Flexible Pavements

Fundamental Assumptions

In order to develop a particular theory concerning the distribution of stresses and strains in flexible pavements, several assumptions were made as follows:

- Each layer acts as a continuous, isotropic, homogeneous,

linearly elastic medium infinite in horizontal extent;

- The surface loading can be represented by a uniformly distributed vertical stress acting over a circular area;

- The surface loading is elastic;

- The interface conditions between layers can be represented as being partially rough; which means that friction stresses can occur between layers;

- Inertia forces are negligible;

- The principle of superposition is valid (in the pavement analysis);

- The influence of the other wheels, than that which is taken into account, is negligible;

- Each layer, except the subgrade, behaves as a slab of a low rigidity, for a given range of stresses and strains;

- Deformations throughout the system are small;

- The vertical deflection is extremely small in comparison with the thickness of the layers;

- The temperature, the moisture contents and the frost penetration can be taken into consideration by their influence on the moduli of the layers and Poisson's ratios;

- The failure of flexible pavements is essentially a fatigue phenomenon, though the distress mechanisms which appear to be most prevalent are: (1) failure resulting from repeated applications of vehicular loads; (2) distortion which is traffic associated, and (3) fracture resulting from non-traffic associated factors.

The behavior of the highway body under the given load is imagined to be as shown in Fig. 6.

Each layer is characterized by its Young's modulus, Poisson's ratio and thickness, except for the subgrade whose thickness is infinite.

Each layer, except the subgrade, is assumed to be stressed by both the load transmitted through layers above and by the bending of the layer resulting from its following the deflection of the subgrade. This double loading of the layer is due to the relatively low friction stresses that can be mobilized at the interface of each layer.

For this reason, the most important surface which is to be characterized is the deformed surface at the top of the subgrade, which is concordance with the theory of elasticity (Ref. 14, pages 300-302, quoted above).

For the m-layered system, one can present the stresses under the center of the load as shown in Fig. 7.

As boundary conditions at the interface between two layers in contact one can write:

$$\sigma_i^{ri} = \sigma_{i-1}^{rs} = \sigma_i^r \quad (16)$$

$$\sigma_i^{fi} = \sigma_{i-1}^{fs} = \sigma_i^f$$

As a consequence of equations (16) the principal stresses under the center of the loaded plate and for the layer i can be presented as shown in Fig. 8.

4.4. The Equation of the Deformed Surface at the Top of the Subgrade

Many equations have been proposed for characterizing the deformed surface at the top of the subgrade.

Generally, the proposed equations are of the second degree as follows:

$$w_r = \frac{a'}{b' \cdot r^2 + c' \cdot r + d'} \quad (17)$$

where a' , b' , c' and d' are coefficients that differ from those defined in the list of notations.

After studies, Leger (Ref. 3, page 1196) proposed a simplified equation:

$$w_r = \frac{w_o}{a' \cdot r^2 + b'} \quad (18)$$

The main difference between equations (17) and (18) is of the number of external conditions necessary to define the unknown values of the parameters a' , b' , c' and d' .

Leger's equation needs only three external conditions as shown in Table 1.

It should be noted that the conditions in Table 1 are given according to the model presented in Fig. 6 (where the load at the top of the subgrade is assumed to be distributed semispherically) and is in equation (14).

It should also be noted that the shape and the general equation of the surface studied corresponds rather well to the experimental findings of Coffmann (Ref. 2, page 819-862), Brown and Pell (Ref. 2, page 487-504) and Rafiroiu (Ref. 7, page 14-16), and the procedure used for defining the values of the parameters a and b in equation (18) differs from that which was used by Leger.

According to the condition 1 from the Table 1, when $r = 0$, w must be w_0 . Then:

$$w_0 = \frac{w_0}{a' \cdot (0)^2 + b'} \quad (19)$$

and one finds immediately that $b = 1$.

According to the second condition in Table 1, when $r = \frac{\alpha_0 D}{2}$, $w = \frac{w_0}{2}$. Therefore:

$$\frac{w_0}{2} = \frac{w_0}{a' \cdot \frac{\alpha_0 D}{2}^2 + 1} \quad (20)$$

from which:

$$a' = \frac{4}{\alpha_0^2 \cdot D^2} \quad (20.a)$$

Now one can write the complete equation for the deformed surface (the third condition being automatically satisfied):

$$w_r = \frac{w_0}{\frac{4}{\alpha_0^2 \cdot D^2} \cdot r^2 + 1} \quad (21)$$

But it is known that the second derivative of the deflection gives the curvature of the surface at the point of differentiation:

$$\frac{d^2 w}{dr^2} = - \frac{1}{R_r} \quad (22)$$

From equation (21):

$$\frac{dw}{dr} = - \frac{w_0 \cdot \frac{8}{\alpha_0^2 \cdot D^2} \cdot r}{\left(\frac{4}{\alpha_0^2 \cdot D^2} \cdot r^2 + 1 \right)^2} \quad (23)$$

and:

$$\frac{d^2w}{dr^2} = \frac{- \left(\frac{4}{\alpha_0^2 \cdot D^2} \cdot r^2 + 1 \right) \cdot \frac{8}{\alpha_0^2 \cdot D^2} \cdot w_0 + \frac{64}{\alpha_0^2 \cdot D^2} \cdot r^3 \cdot w_0}{\left(\frac{4}{\alpha_0^2 \cdot D^2} \cdot r^2 + 1 \right)^3} \quad (24)$$

for $r = 0$:

$$-\frac{1}{R_0} = - \frac{8}{\alpha_0^2 \cdot D^2} \cdot w_0 \quad (25)$$

and, finally:

$$\boxed{R_0 = \frac{\alpha_0^2 \cdot D^2}{8 \cdot w_0}} \quad (26)$$

Equation (26) corresponds with the experimental findings reported in Ref. 7, page 22.

But, the validity of equation (26) can also be demonstrated by several experimental findings as follows:

- Leger and Autret, in Ref. 3, page 1199 report that the value of the product $R \text{ (m)} \cdot w_0 \text{ (}\frac{1}{100} \text{ mm)}$ varies, as an average, from 6000 to 7500.

- Scala and Dickinson, in Ref. 2, page 971 report that the product R (ft) $\cdot w_o$ ($\frac{1}{100}$ in) varies from 2250 to 12500, the average being 9000 which corresponds in Leger's units of measure to 7000.

- Dehlen, in Ref. 1, page 814 reports different measured values, which, after interpretations, lead to the same values as those found out by Scala and Dickinson.

- Finally, Grant and Walker, in Ref. 3, page 1161, using the same units of measure as Leger, report that the variation of the value of the product $R \cdot w_o$ is to be related to the ratio E_1/E_o , where E_1 would be the average modulus of elasticity of the pavement and to the modulus of the subgrade.

Some computations were made within this work in order to verify whether equation (26) satisfies the experimental findings mentioned above.

Three different types of pavements were considered:

- Gravel on subgrade (two layered system),
- Macadam on gravel and subgrade (three layered system), and
- Asphalt concrete on Macadam, gravel and subgrade (four layered system).

The thickness of the layers were maintained constant:

- 5 cm (2 in) for the asphalt concrete surface work,
- 10 cm (4 in) for the Macadam base course,
- 27 cm (~11 in) for the gravel subbase.

The modulus of the subgrade was varied, in order to get different values for the ratio E_1/E_o .

The results of the computations are given in Table 2.

One can see immediately that the values given by Grant and Walker can be considered a good approach though they had enough experimental data only for E_1/E_0 ratios between 1 and 3. One can also see that equation (26) gives very good results, and it seems closer to experimental findings than that of Grant and Walker. It should also be said that Leger and Autret in Ref. 3, page 1197, give the distribution of $R \cdot w_0$, which shows variation of $R \cdot w_0$ values related to the moisture of the subgrade (dry season--average value = 8200; wet season--average value = 6600).

If the moisture influences the modulus of the subgrade, the lower it is, the lower the radius of curvature is, and this fact agrees with equation (26).

Nevertheless one shall see that equation (26) gives a radius of curvature a little larger than that which can be measured at the peak of the deflection curve and a reduction coefficient will be introduced later.

This is due to the fact that in reality, although the layers have almost the same radius of curvature as the top of the subgrade, there is a certain difference between radius measured at the top of the surface layer and that measured at the top of the subgrade.

4.5. Stresses in Layered Systems

4.5.1. Vertical Stress

As given in equation (5), the vertical stress in a homogeneous mass under a circular plate can be computed by Boussinesq's equation, which may be written as follows (Ref. 4, page 31):

$$\sigma_z = p \cdot \left\{ 1 - \left[\frac{z}{(a^2 + z^2)^{1/2}} \right]^n \right\} \quad (27)$$

wherein n is called "Froehlich's coefficient" or "concentration factor." For the particular case of an homogeneous mass, n = 3.

For layered systems different values for this factor have been suggested, the most used being n = 2 as shown in Ref. 1, page 538.

It has been also suggested by many authors that, for layered systems, Z represents the equivalent depth of a point estimated under the center of the loaded area. It is well known that, for a two layered system (where E₁ is the modulus of the surface course and to the modulus of the subgrade), the equivalent thickness of the surface course is (h_{1eg}):

$$h_{1eg} = b_1 \cdot h_1 \cdot \sqrt[3]{\frac{E_1}{E_0}} = a_1 \cdot h_1 \quad (28)$$

Many values have been the correction factor b₁, but the most used one is b₁ = 0.9 as proposed by Odemark long ago.

If one replaces the actual depth Z with the relative depth (x):

$$x = \frac{Z}{D} \quad (29)$$

and one uses n = 2 for the concentration factor, equation (27) will become:

$$\sigma_z = p \cdot \left[1 - \frac{a_1^2 \cdot x^2}{0.25 + a_1^2 \cdot x^2} \right] \quad (30)$$

In order to check the accuracy of the equation (30) many papers were studied and all experimental data, available in those papers, concerning this peculiar kind of problem were collected (Ref. 1, page 284; Ref. 2, pages 303, 493, 698-701, 713; Ref. 3, pages 411-420, 478-486, and 877-900).

All of these experimental data are presented in Fig. 9.

But, unfortunately, neither Boussinesq's equation, nor equation (30) with $a_1 = 0.9 \cdot \sqrt[3]{E_1/E_0}$, fitted the experimental data. For this reason a new equation was written as shown in (31):

$$\sigma_z = p \cdot \left[1 - c_1 \cdot \frac{a_1^2 \cdot x^2}{0.25 + a_1^2 \cdot x^2} \right] \quad (31)$$

and different values for a_1 and c_1 were used.

In order to speed up the calculation, a computer program was written and it is presented in Appendix 1.

After an accuracy check had been made, new values for a_1 and c_1 were obtained:

$$a_1 = a_2 \cdot \sqrt[3]{\frac{E_i}{E_0}} \quad (32)$$
$$a_2 = 0.84; c_1 = 0.97$$

Therefore, the empirical equation for the computation of the vertical stress is the following:

$$\sigma_z = p \cdot \left[1 - c_1 \cdot \frac{a_2 \cdot \sqrt[3]{\frac{E_1}{E_0}} \cdot x^2}{0.25 + a_2 \cdot \sqrt[3]{\frac{E_1}{E_0}} \cdot x} \right] \quad (33)$$

The accuracy of the results, which can be obtained by using equation (33), was checked by replacing at each particular depth, the actual data with the mean. The results are shown in Fig. 10 and they demonstrate the high accuracy of equation (33).

Although one can appreciate that the differences between coefficients a_1 and c_1 in (33) and those generally used ($a_1 = 0.9 \cdot \sqrt[3]{E_1/E_0}$; $c_1 = 1.00$) are rather small, it should be said that the latter do not fit at all the experimental data for relative depths below 2.0 where usually the subgrade-subbase interface lies and hence the vertical stress on the subgrade is not correctly estimated.

4.5.2. Radial Stress

If we rewrite equation (5) by using the following replacement:

$$A = \frac{z}{\sqrt{a^2 + z^2}} \quad (34)$$

one can get:

$$\sigma_r = \frac{p}{2} \cdot \left[1 + 2 \cdot \mu - 2 \cdot (1 + \mu) \cdot A + A^3 \right] \cdot \quad (35)$$

If we set:

$$B = A^3 \quad (36)$$

equation (35) will become:

$$\sigma_r = \frac{p}{2} \cdot \left[1 + 2 \cdot \mu - 2 \cdot (1 + \mu) \cdot A + B \right] \quad (37)$$

Finally, we can write:

$$A = \sqrt[n]{B} \quad (38)$$

wherein n - for Boussinesq's problem - is equal to 3.

But, in the previous developments regarding the vertical stress, it was found:

$$B_1 = c_1 \cdot \frac{\left(a_2 \cdot \sqrt[3]{\frac{E_1}{E_0}} \cdot x \right)^2}{0.25 + \left(a_2 \cdot \sqrt[3]{\frac{E_1}{E_0}} \cdot x \right)^2} \quad (39)$$

and n = 2. For this reason one can write :

$$A_1 = \sqrt[2]{c_1 \frac{\left(a_2 \cdot \sqrt[3]{\frac{E_1}{E_0}} \cdot x \right)^2}{0.25 + \left(a_2 \cdot \sqrt[3]{\frac{E_1}{E_0}} \cdot x \right)^2}} \quad (40)$$

or:

$$A_1 = \sqrt{C_1} \cdot \frac{a_2 \cdot \sqrt[3]{\frac{E_1}{E_0}} \cdot x}{\sqrt{0.25 + \left(a_2 \cdot \sqrt[3]{\frac{E_1}{E_0}} \cdot x \right)^2}} \quad (41)$$

and therefore:

$$\sigma_r = \frac{p}{2} \cdot \left[1 + 2 \cdot \mu + 2 \cdot (1 + \mu) \cdot A_1 + B_1 \right] \quad (42)$$

The accuracy of equation (42) was checked by also using the experimental data available in the studied literature (Ref. 2, pages 495 and 712) and the results are given in Fig. 11. The computed data agree reasonably well with measurements, especially at the larger relative depths. For this reason one can consider that all developments in equations (34) to (42) are correct, at least from an empirical point of view.

A computer program for the computation of the radial stress at different levels is given in Appendix 2.

4.5.3. Shear Stress

The literature in the area is rather poor in information about shear stresses and no experimental data could be found. This is the reason why only a theoretical development has been done.

It is well known from the theory of elasticity (Ref. 14, page 108, and Ref. 19, page 370) that the maximum shear stress is given by the relationship:

$$\tau_{zr} = \frac{1}{2} \cdot (\sigma_z - \sigma_r) \quad (43)$$

By replacing σ_z and σ_r by equations in (33) and (42) respectively and after simplifying one gets:

$$\tau_{zr} = \frac{p}{2} \cdot \left\{ \frac{1 - 2 \cdot \mu}{2} + (1 + \mu) \cdot A_1 - \frac{3}{2} \cdot B_1 \right\} \quad (44)$$

or

$$\tau_{zr} = \frac{p}{4} \left[(1 - 2 \cdot \mu) + 2 \cdot (1 + \mu) \cdot A_1 - 3 \cdot B_1 \right] \quad (45)$$

Equation (45) was used in the computer program in Appendix 3. The results are shown in Fig. 12 for two values of Poisson's ratio, $\mu = 0.35$ and $\mu = 0.50$.

In order to make a comparison Boussinesq's formula was also used. According to Ref. 19, page 370, Boussinesq's formula is:

$$\tau_{zr} = \frac{p}{2} \left\{ \frac{1 - 2 \cdot \mu}{2} + (1 + \mu) \cdot \frac{z}{a^2 + z^2} - \frac{3}{2} \cdot \frac{z^3}{(a^2 + z^2)^{3/2}} \right\} \quad (46)$$

It is very interesting to observe the Boussinesq's curves have the same shape, but have the maximum values at a depth two times greater than the other curves, and approximately the same values at the depths $z = 0$ and $z = \infty$.

It should also be noted that the maximum values of the shear stress obtained using equation (45) are greater than those using equation (46), namely, in layered systems shear stresses should be greater than through an halfspace under the same loading. It is to be said that high shear stress could reduce considerably the bearing capacity of the pavement, especially when the maximum shear stress lies in a weak material as sandy gravel or sand which has a small angle of internal friction when wet. The writer would like to report his own experience with finding material displaced by the action of shear stresses, in the base course of an asphalt pavement.

The distinctive action of the shear stresses was observed in a three-layered system (5 cm (2 in) asphalt surface course; 30 cm (12 in) sandy gravel base course; and silty clay as subgrade), in the Spring, after a year of heavy traffic.

The equivalent load was 5000 kg per wheel, with about 30 cm (12 in) equivalent diameter of the loaded area and about 5 kg/cm^2 ($\approx 69 \text{ psi}$) tire pressure.

At about 10 cm (4 in) under the top level of the sandy gravel base course, a region about 2 cm thick, obviously disturbed, was observed, the rest of the material remaining well compacted both above and below this region.

This means, in the writer's opinion, that the thin asphalt concrete surface course had not had any important influence either on the bearing capacity of the pavement or on the reduction of the shear stresses, especially because it was intensely cracked. The shear stresses displaced the material at about $0.33 h/d$, which fits almost perfectly with the theoretical findings.

4.5.4 Stress Function

As was shown in Part 3, the stress formulas are derived from the four basic equations (1) by the use of a stress function.

The general requirement for the stress function is that it be biharmonic. But it seems that more than one requirement is necessary.

As a matter of fact, at least one further requirement should be formulated: a stress function should also lead to formulas whose results must agree with experiments.

Nowadays, a limited number of stress functions are used: Airy functions, Bessel functions, polynomials, and exponential functions. Each of them is arbitrarily chosen, and the usual way to derive the stress formulas is to choose one function, introduce it in equation (1) and solve it in such a way that all constants will satisfy the boundary conditions. This is usually called the "inverse procedure."

The "direct procedure" is to integrate the stress formulas to get the general form of the stress function and then, determine the constants by using the boundary conditions.

Although the purpose of this work is not to solve this particular kind of problem, the homogeneity of the procedure used to get the stress formulas suggested to the writer that a stress function should exist even for the "empirical" stress formulas given in equations (33), (42), and (44).

Unfortunately, these formulas are given only for the region right below the center of the loaded area. This is the reason why the following stress function search aims only at finding an expression which would be useful in guiding further choices.

For this particular problem, $r = 0$ and hence:

$$\begin{aligned}\frac{\partial^2 \phi}{\partial r^2} &= 0 \\ \frac{1}{r} \cdot \frac{\partial \phi}{\partial r} &= 0\end{aligned}\tag{47}$$

Therefore:

$$\nabla^2 (\nabla^2 \phi) = \frac{\partial^2}{\partial z^2} \left(\frac{\partial^2 \phi}{\partial z^2} \right) = 0\tag{48}$$

which is the same as:

$$\frac{\partial \sigma_z}{\partial z} = 0\tag{49}$$

for $z = 0$ and $z = \infty$.

Although, from now on, one could use common derivatives through the theoretical developments, the partial derivatives were however maintained in order not to change the general form of the problem.

If one analyzes equation (33) one will see that for $z = 0$:

$$\sigma_z = p = \text{constant} \tag{50}$$

$$\frac{\partial \sigma_z}{\partial z} = 0$$

and for $z = \infty$

$$\left. \begin{array}{l} \sigma_z \rightarrow 0 \\ \frac{\partial \sigma_z}{\partial z} = 0 \end{array} \right\} \tag{51}$$

As a conclusion of the relationships in (50) and (51) one can state that any stress function obtained as a result of a triple integration process applied to the above stress formulas will be a biharmonic function and it will also satisfy the requirement of the experimental agreement.

For a simpler development one will consider that:

$$\begin{aligned} a_1 &= a_2 \cdot \sqrt[3]{\frac{E_1}{E_0}} \\ b &= b_1 \\ c^2 &= 0.25 \end{aligned} \tag{52}$$

and equation (33) becomes:

$$\sigma_z = p \cdot \left[1 - b \cdot \frac{a_1^2 \cdot x^2}{c^2 + a_1^2 \cdot x^2} \right] \quad (53)$$

which will be more convenient for the integration process.

As a conclusion of the relationships in (47) and (48) one can write:

$$\nabla^2 \phi = \frac{\partial^2 \phi}{\partial x^2} \quad (54)$$

We know that:

$$\sigma_z = \frac{\partial}{\partial x} \left[(2 - \mu) \cdot \nabla^2 \phi - \frac{\partial^2 \phi}{\partial x^2} \right] \quad (55)$$

which, in this case, is the same as:

$$\sigma_z = \frac{\partial}{\partial x} \left[(2 - \mu) \cdot \frac{\partial^2 \phi}{\partial x^2} - \frac{\partial^2 \phi}{\partial x^2} \right] \quad (56)$$

or:

$$\sigma_z = \frac{\partial}{\partial x} \left[\frac{\partial^2 \phi}{\partial x^2} \right] \cdot (1 - \mu) \quad (57)$$

Then, we can write:

$$\sigma_z = (1 - \mu) \cdot \frac{\partial^3 \phi}{\partial x^3} \quad (58)$$

and:

$$p \cdot \left[1 - b \frac{a_1^2 \cdot x^2}{c^2 + a_1^2 \cdot x^2} \right] = (1 - \mu) \cdot \frac{\partial^3 \phi}{\partial x^3} \quad (59)$$

The first integration can now be performed:

$$\frac{\partial^2 \phi}{\partial x^2} = \frac{p}{(1 - \mu)} \cdot \int_0^z \left(1 - b \frac{a_1^2 \cdot x^2}{c^2 + a_1^2 \cdot x^2} \right) \cdot dx \quad (60)$$

After integration one gets:

$$\frac{\partial^2 \phi}{\partial x^2} = \frac{p}{1 - \mu} \cdot \left(\left| x + k_1 \right|_0^z - b \cdot a_1^2 \cdot \left| \frac{x}{a_1^2} - \frac{c}{a_1^3} \cdot \tan^{-1} \frac{a_1 \cdot k}{c} + k_2 \right|_0^z \right) \quad (61)$$

The constants k_1 and k_2 are determined by boundary conditions.

$$z = 0; \frac{\partial^2 \phi}{\partial x^2} = 0 \text{ and } k_1 = k_2 = 0 \quad (62)$$

Thus:

$$\frac{\partial^2 \phi}{\partial x^2} = \frac{p}{1 - \mu} \left[(1 - b) \cdot x - \frac{c}{a_1^3} \cdot \tan^{-1} \frac{a_1 \cdot x}{c} \right] \quad (63)$$

Now, one can make the second integration:

$$\frac{\partial \phi}{\partial x} = \frac{p}{1 - \mu} \int_0^z \left[(1 - b) \cdot x - \frac{c}{a_1^3} \cdot \tan^{-1} \frac{a_1 \cdot x}{c} \right] \cdot d_x \quad (64)$$

which is:

$$\frac{\partial \phi}{\partial x} = \frac{p}{1 - \mu} \left\{ (1 - b) \cdot \left. \frac{x^2}{2} + k_3 \right|_0^z - \frac{c}{a_1^3} \left. \left[a_1 \cdot x \cdot \tan^{-1} \frac{a_1 \cdot x}{c} - \frac{c}{2} \cdot \ln (c^2 + a_1^2 \cdot x^2) + k_4 \right] \right|_0^z \right\} \quad (65)$$

The constants k_3 and k_4 are also determined by boundary conditions:

$$z = 0; \frac{\partial \phi}{\partial z} = 0; k_3 = 0; k_4 = \frac{c}{2} \cdot \ln c^2 \quad (66)$$

And now, the last integration:

$$\phi = \frac{p}{1-\mu} \cdot \int_0^z \left\{ (1-b) \cdot \frac{x^2}{2} - \frac{c}{a_1^3} \cdot \left[a_1 \cdot k \cdot \tan^{-1} \frac{a_1 \cdot x}{c} - \frac{c}{2} \cdot \ln (c^2 + a_1^2 \cdot x^2) + \frac{c}{2} \cdot \ln c^2 \right] \right\} \cdot dx \quad (67)$$

After integration one gets:

$$\phi = \frac{p}{1-\mu} \left\{ \frac{(1-b)}{2} \cdot \left[\frac{x^3}{3} + k_5 \right]_0^z - \frac{c}{a_1^2} \cdot \left[\frac{1}{2} \cdot (c^2 + a_1^2 \cdot x^2) \cdot \tan^{-1} \frac{a_1 \cdot x}{c} - \frac{c \cdot a_1 \cdot x}{2} + k_6 \right]_0^z + \frac{c^2}{2 \cdot a_1^3} \cdot \left[\frac{1}{b} \cdot a_1 \cdot x \cdot \ln (c^2 + a_1^2 \cdot x^2) - 2 \cdot a_1 \cdot k + 2 \cdot \tan^{-1} \frac{a_1 \cdot k}{c} + k_7 \right]_0^z \right\} \quad (68)$$

Finally, by boundary conditions:

$$z = 0; \phi = 0; k_5 = 0; k_6 = 0; k_7 = 0 \quad (69)$$

The final form of the stress function, only for the region underneath the center of the loaded area, is:

$$\phi = \frac{p}{1 - \mu} \left\{ \frac{(1 - b)}{6} \cdot x^3 - \frac{c^2}{2 \cdot a_1^2} \cdot \left[c \cdot a_1^2 + 2 \cdot c^2 - \frac{1}{b} \cdot \ln (c^2 + a_1^2 \cdot x^2) \right] \cdot x + \frac{c}{a_1^2} \cdot \left[\frac{c}{a_1} - \frac{1}{2} \cdot (c^2 + a_1^2 \cdot x^2) \right] \cdot \tan^{-1} \frac{a_1 \cdot x}{c} \right\} \quad (70)$$

wherein $x = z/D$ as presented in equation (29).

If it is assumed that $a_1 = 1.0$ and $b = 1.0$, and ξ represents the ratio between z and the radius of the loaded area, equation (70) becomes:

$$\phi_1 = \frac{p}{(1 - \mu)} \cdot \left\{ -\frac{1}{2} \cdot \left[1 + 2 - \ln (1 + \xi^2) \right] \xi + \left[1 - \frac{1}{2} (1 + \xi^2) \right] \cdot \tan^{-1} \xi \right\} \quad (71)$$

or

$$\phi_1 = -\frac{p}{2(1 - \mu)} \left\{ \left[3 - \ln (1 - \xi^2) \right] \cdot \xi + (1 + \xi^2) \cdot \tan^{-1} \xi \right\} \quad (72)$$

This simplified form of the stress function shows that the problem of the stresses in layered systems is a very complicated one and much more investigation is necessary to solve it accurately from either a theoretical or practical point of view.

4.6. Strains in Layered Systems

Although we have both stress formulas and a stress function, the problem cannot be solved throughout the whole highway body. All the formulas or equations given are only for the region underneath the center of the loaded area. This is the reason why a quite different approach for strains computation was done.

Two main assumptions were made:

- The surface at the top level of the subgrade is deformed as shown on the right-hand side of Fig. 6;
- Each layer deforms itself under the load, and the higher the unit vertical stress is the thinner the layer becomes.

If one measures the vertical deflections at the top of each layer, in comparison with the same surface before deformation and at points situated in the same vertical plane as the edges of the A_i areas, one will get the following matrix (see Fig. 6):

$$W = \begin{vmatrix}
 w_0^{m+1} & w_0^m & w_0^{m-1} & \dots & \dots & \dots & w_0^2 & w_0^1 & w_0^0 \\
 w_1^{m+1} & w_1^m & w_1^{m-1} & \dots & \dots & \dots & w_1^2 & w_1^1 & w_1^0 \\
 w_2^{m+1} & w_2^m & w_2^{m-1} & \dots & \dots & \dots & w_2^2 & w_2^1 & w_2^0 \\
 \vdots & \vdots & \vdots & \vdots & \vdots & \vdots & \vdots & \vdots & \vdots \\
 \vdots & \vdots & \vdots & \vdots & \vdots & \vdots & \vdots & \vdots & \vdots \\
 \vdots & \vdots & \vdots & \vdots & \vdots & \vdots & \vdots & \vdots & \vdots \\
 w_{m-1}^{m+1} & w_{m-1}^m & w_{m-1}^{m-1} & \dots & \dots & \dots & w_{m-1}^2 & w_{m-1}^1 & w_{m-1}^0 \\
 w_m^{m+1} & w_m^m & w_m^{m-1} & \dots & \dots & \dots & w_m^2 & w_m^1 & w_m^0
 \end{vmatrix} \quad (73)$$

The computation of the elements of the matrix W can be done only after the computation of the elements belonging to another matrix (W_p). In the latter matrix the elements, noted by w_i^{pi} represent the partial strain which occurs in layer i at the projection of the edge of the surface A_j .

The matrix W_p will be:

$$W_p = \begin{vmatrix}
 w_1^{pm+1} & w_1^{pm} & w_1^{pm-1} & \dots & \dots & \dots & w_1^{p2} & w_1^{p1} & w_1^{p0} \\
 w_2^{pm+1} & w_2^{pm} & w_2^{pm-1} & \dots & \dots & \dots & w_2^{p2} & w_2^{p1} & w_2^{p0} \\
 \vdots & \vdots & \vdots & \vdots & \vdots & \vdots & \vdots & \vdots & \vdots \\
 \vdots & \vdots & \vdots & \vdots & \vdots & \vdots & \vdots & \vdots & \vdots \\
 \vdots & \vdots & \vdots & \vdots & \vdots & \vdots & \vdots & \vdots & \vdots \\
 w_{m-1}^{pm+1} & w_{m-1}^{pm} & w_{m-1}^{pm-1} & \dots & \dots & \dots & w_{m-1}^{p2} & w_{m-1}^{p1} & w_{m-1}^{p0} \\
 w_m^{pm+1} & w_m^{pm} & w_m^{pm-1} & \dots & \dots & \dots & w_m^{p2} & w_m^{p1} & w_m^{p0}
 \end{vmatrix} \quad (74)$$

The computation of the values of the elements in the matrices W and W_p is the following:

a) For the first row in W:

$$w_o^{m+1} = \pi \cdot \frac{1 - \mu_o^2}{E_o} \cdot \frac{p \cdot D}{\alpha_o} \quad (75a)$$

where:

$$\alpha_o = \sqrt{\frac{p}{\frac{2}{3} \sigma_o^v}} \quad (76a)$$

and:

$$w_o^j = w_o^{m+1} \left[1 - \frac{\alpha_j^2}{\alpha_o^2} \right] \quad (75b)$$

$$j = 1, \dots, m$$

where:

$$\alpha_j = \sqrt{\frac{p}{\frac{2}{3} \sigma_j^v}} \quad (76b)$$

except for the surface course whose $\alpha_m = 1.0$ from geometric conditions.

σ_j^v being calculated by the following equation:

$$\sigma_{j-1}^v = p \left\{ 1 - c_1 \frac{\frac{a_1^2}{D^2} \left(\sum_{l=j}^m h_l \cdot \sqrt[3]{\frac{E_l}{E_0}} \right)^2}{0.25 + \frac{a_1^2}{D^2} \left(\sum_{l=j}^m h_l \cdot \sqrt[3]{\frac{E_l}{E_0}} \right)^2} \right\} \quad (77)$$

which is derived from equation (33).

It should be noted that equation (75a) is derived from equation (12) which is obtained from the theory of elasticity, and equation (75b) is derived from equation (15) which is also obtained from the theory of elasticity.

Computations made with the computer-program, Appendix 5, demonstrated that the deflection calculated by using equation (75b) are very close to those calculated by using equation which is based on the theory of elasticity.

Actually, the differences between the results of the two equations are in the range of 0.2 to 0.06 mm (0.003 to 0.009 in.) hence are very small.

b. For each row in W_p :

If ϵ_z is the strain at the level z under the center of the loaded area, according to the theory of elasticity:

$$\epsilon_z = \frac{1}{E} \left[\sigma_z - \mu \cdot (\sigma_x + \sigma_y) \right] \quad (78)$$

In our particular case $\sigma_x = \sigma_y = \sigma_r$. Then:

$$\epsilon_z = \frac{1}{E} \left[\sigma_v - 2 \cdot \mu \cdot \sigma_r \right] \quad (79)$$

If σ_{vi}^{med} and σ_{ri}^{med} are respectively:

$$\sigma_{vi}^{med} = \frac{\sigma_{i-1}^v + \sigma_i^v}{2} \quad (80)$$

$$\sigma_{vi}^{med} = \frac{\sigma_{i+1}^r + \sigma_i^r}{2}$$

one can write:

$$w_i^{pm+1} = \frac{h_i}{E_i} \left(\sigma_{vi}^{med} - 2 \cdot \mu \cdot \sigma_{ri}^{med} \right). \quad (81)$$

In equation (80), the radial stress σ_i^r can be computed from the following equation:

$$\sigma_i^r = \frac{p}{2} \left\{ 1 + 2 \cdot \mu - 2 \cdot (1 + \mu) \cdot \sqrt{c_1} \frac{\sqrt{d_i}}{\sqrt{0.25 + d_i}} + \frac{c_i d_i}{0.25 + d_i} \right\} \quad (82)$$

where:

$$d_i = \left(\frac{a_1}{D} \sum_{l=i}^m h_l \cdot \sqrt[3]{\frac{E_l}{E_0}} \right)^2 \quad (83)$$

Because of the similitude of many terms in the σ_i^v 's and σ_i^r 's formulas, after computations one may write:

$$w_i^{pm+1} = \frac{h_i \cdot (1 + \mu)}{E_i} \left[\sigma_{vi}^{med} - 2 \cdot \mu \cdot p \left(1 - \sqrt{1 - \frac{\sigma_{vi}^{med}}{p}} \right) \right] \quad (84)$$

If one accepts that the partial deflection of a layer is constant within the loaded area A_i , one may write:

$$w_i^{pj} = w_i^{pm+1}, \quad (j = i, \dots, m) \quad (85)$$

The main problem now is to define the partial deflection of a layer outside of the surface A_i . In order to solve this problem two equations were used.

The first equation is suggested by both equations (15) and (21):

$$w_i^{pj} = w_i^{pm+1} \left(\frac{\alpha_i - \alpha_j}{\alpha_i} \right)^2, \quad (j = 1, \dots, i-1) \quad (86)$$

The second equation is suggested by the developments of M. M. Filonenko-Borodits (Ref. 14, page 474):

$$w_i^{pj} = w_i^{pm+1} \cdot \text{EXP} \left(- \frac{\sigma_i^v}{D} \cdot \frac{\alpha_j}{\alpha_i} \right), \quad (j = 1, \dots, i-1) \quad (87)$$

Computations made as part of the computer-program in Appendix 5 demonstrated that there are no real differences between the results of equations (86) and (87), at least for the computation of the radii of curvature.

c. For the rest of m rows in W:

$$w_i^j = w_{i-1}^j + w_i^{pj}, \quad (i = 1, \dots, m) \quad (88)$$

$$j = 1, \dots, m+1$$

The procedure described above and which is based upon the developments concerning the stresses in layered systems allows the computation of the deflections at a net of points situated in the most stressed part of the pavement, namely inside a cylinder whose radius is equal to $\alpha_0 \cdot D/2$.

Outside of this cylinder, the computation of the strains would be very difficult and, in fact, the computation of the deflections of the top surface of the pavement by using equation (21) is sufficient for practice.

The computer-program, given in Appendix 5, was used in order to check the validity of equations (73) through (86).

The basic data for the computations were obtained from Reference 1 (pages 511-573; 655; 404), Reference 2 (pages 303-305, 677-683; 698-701; 872-874; 1084-1085) and Reference 3 (pages 411-420; 478-486; 789-794; 796-797; 877-900; 1133; 590-603). These data were completed with all necessary information from Ref. 5, Ref. 7, Ref. 9, Ref. 10 and Ref. 11.

It should be said that the majority of data given in the references noted above were not ready to be used in the present developments and a process of evaluating the data had to be done. Therefore, a stochastic approach was used especially as only average values were used for the Young's moduli.

The conclusions resulting from the computer processing of these data are the following:

- The vertical compressive stresses under the center of the loaded area were predicted correctly by equation (77) (which is the same as equation (33)) as one can see in Fig. 13.
- The horizontal tensile stresses at the bottom of the layers are about $15/4$ of the measured stresses, as shown in Fig. 14.
- The deflections at the surface of the pavement under the center of the loaded area are about $14/5$ of the measured deflections as shown in Fig. 15.
- If one takes into account the energy necessary for the change of the form of the layers (procedure according to Ref. 7), the deflections computed by using the procedure given in equations (75) to (88) represent about $14/4.8$ of the new deflections as shown in Fig. 16. For this reason the deflections calculated by taking into account the energy necessary to change the form of the layers are expected to be: $\frac{14}{5} \frac{4.8}{14} \approx 1$, therefore from a statistical point of view, equal to those measured.
- If real deflections are $5/14$ of those calculated by equations (75) through (88), the curvature of the layers and implicitly the calculated tensile stresses at the bottom of the layers are expected to be $5/14$ of those calculated by the computer-

program in Appendix 5. Then, the calculated tensile stresses would represent about: $\frac{5}{14} \frac{15}{4} \approx 1.32$ of the measured ones.

It should be noted that Nijboer (in Ref. 2, pages 699-701) has shown that the tensile stresses at the bottom of the layers, calculated by any method resulting from the theory of elasticity, are almost always higher than those measured (deviations up to 35%). This means that any theoretical approach cannot evaluate correctly both the influence of the friction between layers and the real tensile stresses at these levels. Anyway, it seems to be better to overestimate the tensile stresses at the bottom of the layers, because the higher the tensile stresses are the more cracks at the surface of the pavement occur.

It should be noted that all these results may be incorrect as to their exact values. The purpose of their presentation is to put in evidence a qualitative process whose consequences will be studied in the next part of this report.

- The average ratio E_1/E_0 , where E_1 is the average modulus of the pavement and to the modulus of the subgrade, for the set of given data, is 16; the average number of layers is 5; and the average value of the product $R \cdot w$ ($\text{cm} \cdot \frac{1}{100} \text{ mm}$) is 18000, the range of the latter being between 16000 and 20000.

If the results given in Table 2 are interpreted graphically, and if one accepts a possible extrapolation with the increasing number of the layers and the increasing of the E_1/E_0 ratio, one gets the results shown in Fig. 17.

This means to the writer that the products $R \cdot w$ should be a function not only of the E_1/E_0 ratios as suggested by Grant and Walker

in Ref. 3, page 1161, but also of the number of the layers of the pavement. If this is true one can consider that any approach using an "equivalent halfspace" is wrong. It will remain for further developments to demonstrate the validity of the above assertion.

- The last conclusion is that the tensile stresses at the bottom of the layers measured under the center of the load put in evidence that the real radius of curvature of the layers is the same as the radius of curvature of the top surface of the subgrade, under the center of the loaded area.

4.7. Energy Approach

4.7.1. Introduction

During the deflection of the highway body under loading, two types of deformations occur:

- Deformations due to the change of the volume;
- Deformations due to the change of the form.

The stresses and strains studied in the last three sections are connected with the change of the volume. The stresses and strains due to the change of the form are studied next.

During the deflection of the highway body, an energy phenomenon occurs: the exterior load transfers energy to the highway body and the highway body gains energy. When the exterior load is removed, the highway body (if loaded within elastic limits) loses the energy by recovering its previous form.

It is obvious that the phenomenon described implies that no plastic or viscoelastic strains occur in the highway body during its loading.

For this is the reason that additional stresses occur in the pavement during deflection and these also should be taken into account.

4.7.2. Bending Stresses

As it was demonstrated in some previous works (Ref. 7; Ref. 8; Ref. 9; Ref. 11) the highway layers, except the subgrade, usually behave as slabs of a low rigidity.

The explanation of this fact lies in the low friction stresses which can be mobilized at the interfaces of the layers and the prestressed state (compressive stresses) which occurs even in the granular or noncohesive materials during compaction and which disappears only when the pavement has completely failed.

Experiments reported in Ref. 11 have demonstrated that the friction factor at the interface of two layers (f_i) lies in the range of 0.3 to 0.665, the lower values (0.3-0.4) being reported for rolled granular materials, the medium values (0.4-0.5) for bituminous mixtures placed upon any kind of compacted material, and the higher values (0.5-0.665) for crushed stone, Macadam, or materials which penetrate into each another during compaction; for example, crushed stone on clay or clayey materials, bituminous mixtures spread upon an open textured crushed stone, etc.

Consider the region under the center of the loaded area. If one makes the assumption that, in this particular region, one can add radial stresses with shear stresses, and if one considers an average value for f_i , for example 0.5, one will get--for the particular depths where the interfaces of the layers lies (see Fig. 9)--the values shown in Table 3.

Certainly, the above computation does not observe the rules of the theory of elasticity and it was made only to get a better idea about the general state of stresses in that region.

It can be observed immediately that the friction stresses which can be mobilized at the interfaces of the layers are less than the global horizontal stresses which occur at these levels. This is the reason why slip is possible between the layers.

But there is neither perfect slip nor rough contact there but an intermediate situation which can be taken into account within computations if the friction factor is known.

The experiments reported in Ref. 11 have shown that the friction factor at the interface of two layers is equal to the smallest value of the $\tan \phi_i^*$ of the materials the layers are built with, except when materials penetrate into each another. In this case f_i would be the average of the two values of $\tan \phi_i$.

A more interesting problem is that involving the prestressed state of the layers.

The prestressed state has been taken into account by many authors. Among them are: Burmister (Ref. 1, page 444), Bonitzer

* See list of notations

and Leger (Ref. 2, page 783) and Livneh and Shklarsky (Ref. 1, page 345-353) with the mention that the latter used also cohesion characteristics in their developments.

The compressive stresses which occur at the bottom of the granular layers and which remain approximately at the same level even after the exterior loading ceases its action were studied in depth by Vasile Izdraila*. He has shown that a prestressed situation can occur even if the material of the layer is composed of steel balls of the same diameter. Also, that the remaining compressive stresses increase with the internal angle of friction and the nonuniformity of the grading of the material.

These are the reasons why even the granular layers can behave as slabs of low rigidity. Nevertheless it should be taken into account that the prestressed condition of the layers cannot be correctly estimated within a computation because the remaining compressive stresses at the bottom of the layers are functions of the characteristics of the means of compaction and the number of coverages, and not only of the characteristics of the materials in layers.

If the layers of the pavement behave as slabs, one can compute the stresses under the center of the load.

* Associate Professor at the Polytechnic Institute from Timisoara, Romania, Doctoral Thesis.

According to the theory of elasticity (Ref. 14, page 313) one can write:

$$\begin{aligned}\sigma_x &= -\frac{E}{1-\mu^2} \cdot \left(\frac{\partial^2 w}{\partial x^2} + \mu \cdot \frac{\partial^2 w}{\partial y^2} \right) \cdot z \\ \sigma_y &= -\frac{E}{1-\mu^2} \cdot \left(\frac{\partial^2 w}{\partial y^2} + \mu \cdot \frac{\partial^2 w}{\partial x^2} \right) \cdot z \\ \tau_{zy} &= -\frac{E}{1-\mu^2} \cdot \frac{\partial^2 w}{\partial x \cdot \partial y} \cdot z\end{aligned}\tag{89}$$

But one knows that the second partial derivative at a given point gives the curvature of the surface, along the considered axis at that point. Thus:

$$\frac{\partial^2 w}{\partial x^2} = -\frac{1}{R_x}; \quad \frac{\partial^2 w}{\partial y^2} = -\frac{1}{R_y}\tag{90}$$

Because of the axial symmetry of the load one can write:

$$\frac{\partial^2 w}{\partial x^2} = \frac{\partial^2 w}{\partial y^2} = -\frac{1}{R}\tag{91}$$

If one replaces the partial derivatives from (89) by the values in (91) and one considers:

$$z = \pm \frac{h}{2}\tag{92}$$

one can write:*

$$\sigma_i^m = \pm \frac{E_i \cdot h_i}{2 \cdot R_i (1 - \mu_i)} \quad (93)$$

$$\tau_i^m = \frac{E_i \cdot h_i}{2 \cdot R_i (1 + \mu_i)} \quad (94)$$

The bending moment M_i will be (Ref. 11, page 440):

$$M_i^m = \frac{E_i \cdot h_i^3}{12 \cdot R_i (1 - \mu_i)} \quad (95)$$

This bending moment will occur as a result of each layer following the subgrade during deformation.

But two other moments will occur in the layer:

- The moment due to the nonuniform distribution of the radial stress within the thickness of the layer;
- The moment due to the friction stresses which occur at the interfaces of the layers.

The moment due to the nonuniform distribution of the radial stress can be approximate as suggested in Fig. 18:

$$M_i^r = (\sigma_{i+1}^r - \sigma_i^r) \frac{h_i^2}{12.0} \quad (96)$$

* See the list of notations.

The moment due to the friction stresses which occur at the interfaces of the layers can also be approximate as suggested in Fig. 19:

$$M_i^f = \sigma_{i+1}^f \cdot \frac{h_i}{2} + \sigma_i^f \cdot \frac{h_i}{2} = \left(\sigma_i^f + \sigma_{i+1}^f \right) \frac{h_i}{2} \quad (97)$$

The total moment would be:

$$M_i^T = M_i^m + M_i^r + M_i^f \quad (98)$$

If one analyzes the variations of the radial and friction stresses within the thickness of the pavement, it will be observed that the bending moments due to the friction stresses always reduce the bending moment due to the following of the subgrade by each layer while the moment due to the radial stresses increases the bending moment.

In the writer's opinion the moment due to the nonuniformity of the distribution of the radial stresses should not be necessarily taken into account because the radial stresses and their influence were taken into consideration when the deformations due to the change of volume were studied. For this reason the moment as given in (96) will not be considered further.

Previous studies made in this particular area (Ref. 11, page 440) have shown that the smaller the radius of curvature of the surface the smaller the influence of radial and friction stresses. The relationship in (98) agrees with the previous results because if M_i^r and M_i^f are independent of the radius of curvature of the

layer, the bending moment M_i^m is directly related to the radius of curvature. Thus, one can check immediately the relationship in (95) and see that the smaller the radius of curvature, the greater the bending moment.

A logical inference of the fact mentioned above is that the greater the bending moment, the greater the horizontal stresses in the layers. Therefore, if the layers have to support higher stresses than was assumed when only the deformations due to the change of the volume were taken into account, it may be hypothesized that the participation of the layers in the load bearing energy is greater. For this reason, the deflection at the top level of the subgrade would be less than that computed before.

The above hypothesis agrees with the conclusions of the previous section and this shall be made use of in the next chapter.

4.8. Shear Stresses on the Contour of the Load

In Ref. 3, pages 823 to 843 it was demonstrated that important shear stresses can occur along the contour of the load. This fact fits one of the writer's previous ideas, that, for subgrades with a very low bearing capacity, the shear stresses along the contour of the loaded area, at each level of the pavement, should be taken into account.

According to these facts a model for computing these stresses was assumed as shown in Fig. 20.

The magnitude of these shear stresses should be less than that which can be supported by the layer ($\tau_i^{a\phi}$).

For this reason we can write (for a layer i):

$$\pi \cdot \frac{(\alpha_i \cdot D)^2}{4} \cdot (\sigma_i^V - \sigma_{i-1}^V) \leq \tau_i^{a\phi} \cdot \pi \cdot \alpha_i \cdot D \cdot h_i \quad (99)$$

If σ_i^V and σ_{i-1}^V are replaced respectively by p_i^{ad} and p_{i-1}^{ad} and one considers h_i as function of the other parameters, one can write:

$$h_i = \frac{\alpha_i \cdot D \cdot (p_i^{ad} - p_{i-1}^{ad})}{\tau_i^{a\phi}} \quad (100)$$

The relationship in (100) is obviously an approximation but it can help us with computing at least the degree of magnitude of these stresses (or the required thickness of the layer to support them).

But, the sum of all shear stresses along contours should be equal to the exterior load (as a limit). So one can write:

$$p \cdot \pi \cdot \frac{D^2}{4} \leq \sum_{k=2}^m \tau_k^{a\phi} \cdot \pi \cdot h_k \cdot \alpha \cdot D, \quad (101)$$

and after simplifications:

$$\frac{p \cdot D}{4} \leq \sum_{k=1}^m \tau_k^{a\phi} \cdot h_k \cdot \alpha_k \quad (102)$$

Equation (102) is to be used only to verify, at the level of the first layer (layer number 1), what the remaining h_i could be:

$$h_i \geq \frac{\frac{p \cdot D}{4} - \sum_{k=2}^m \tau_k^{a\phi} \cdot h_k \cdot \alpha_k}{\tau_1^{a\phi} \cdot \alpha_1} \quad (103)$$

If h_1 calculated with the relationship in (103) is less than h_1 calculated with equation (100), it means that the pavement will not be distressed under the load. If the assertion above is not true, one must increase the thickness of the layer number 1 at least up to the value computed from equation (103).

One must also take into account that all these computations must be made for the heaviest load which is expected to use the highway.

5. Deriving a New Design Method

5.1. Design Criteria

As a consequence of the developments presented in the previous part, the following criteria were considered:

1. The energy gained by the pavement system including subgrade must be equal to the exterior energy, transferred by the load during deflection.

2. Vertical stresses in the top of the layer (subgrade included) must be less than the allowable stresses.

3. Tensile stresses at the bottom of the layer must be lower than the allowable stresses.

4. Shear stresses (horizontal) in the center plane of the layer must be lower than the allowable stresses.

5. The maximum vertical stresses should be located in the surface course.

6. The location of maximum shear stresses should be in the base-course.

7. Vertical shear stresses along the circumference of the load must be lower than the allowable stresses.

8. The depth of frost penetration into the pavement must be less than the thickness of the pavement.

9. A minimum practical thickness must be assigned to each layer.

One could consider this list of design criteria as being too long.

In fact, previous studies (Ref. 7) have demonstrated that, for most subgrade, if the first design factor has been accounted for, the following three ones are also satisfied automatically. But all the design criteria are necessary for determining all the constraints which are to be observed for a structural or economical (optimal) design of the pavement.

5.2. Design Parameters

Many parameters are to be taken into account in the design procedure in order to solve all the problems raised by the design criteria.

Within the further developments the following design parameters will be taken into consideration (for each layer i):

- E_i - Young's modulus, units of force/unit of area;
- μ_i - Poisson's ratio, dimensionless;
- h_i - thickness of the layer, units of length;
- ϕ_i - angle of internal friction, degrees;
- σ_i^{av} - allowable vertical compressive stress at the top of the layer, units of force/unit of area ($= p_i^{ad}$);
- σ_i^{am} - allowable horizontal tensile stress at the bottom of the layer, units of force/unit of area;
- τ_i^{am} - permitted shear stress (horizontal), units of force/units of area;
- τ_i^a - permitted vertical shear stress along the circumference of the loaded area, units of force/unit of area;
- C_i^{fr} - coefficient of resistance to the frost penetration.

$$C_i^{fr} = \frac{1}{\zeta_i} \quad (104)$$

where ζ_i is the thermo conductivity of the material in layers i.

Many other parameters will be used for the exterior load characterization (environment included):

- D - diameter, units of length;
- P - total load, units of force;
- p - unit load on the loaded area, in units of force/unit of area;

- N - present annual traffic, in EWL;
- N_R - annual traffic growth rate, dimensionless;
- N_T - total estimated traffic, in EWL;
- K_W - wheel equivalence factor, dimensionless;
- K_S - season equivalence factor, dimensionless;
- S_ℓ - service life of the pavement, years;
- w_a - permitted deflection at the surface of the pavement, units of length;
- F_d - correction factor, as defined in the list of notations part 4;
- Z_f - frost penetration depth, in units of length.

The main problem is to define the parameters characterizing the behavior of the layers. Some of them are given in the Table 4, and they are a result of several statistical manipulations presented in Ref. 3, 8, 10, 11 and 20.

It should be noted that the Young's moduli are defined as being those found out within the plate test, at the second loading of the plate, on the "return" curve.

5.3. The Development of the New Method

5.3.1. Limit Thickness of the Layers

As a consequence of the results obtained within the previous part one can define both the minimum and maximum thickness of the layers.

The limit thicknesses of the layers can be determined by the aid of the design criteria, namely numbers 2, 3, 4, 5, 6, 7

and 9. Having been used once they will not be used again in this development.

It should be noted that number 3, 4 and 9 are common for all the layers, except the subgrade.

In order to make this development more systematic the equations will be determined for each layer separately. It will be assumed that the pavement is composed from four main layers: surface, base; subbase and drainage courses.

5.3.1.1. Surface Course

5.3.1.1.1. Minimum Thickness

a. According to the design criterium number 2 and equation (33) and after computations one can write:

$$h'_{\min_i} = D \cdot \frac{\sqrt{\frac{p}{P_i} - \alpha_i}}{a_1 \cdot \sqrt[3]{\frac{E_i}{E_o}}} \quad (105)$$

b. According to the design criterium number 5 the maximum vertical stresses has to lie in the surface course. The maximum vertical stresses are defined herein as being those whose range lies between 0.9 and 1.0 p.

For the lower limit, according to the curve shown in Fig. 9, the corresponding value Z/D is 0.3. So one can write:

$$h''_{\min_i} = 0.3 \cdot a_1 \cdot D \sqrt[3]{\frac{E_i}{E_o}} \quad (106)$$

or, after computations:

$$h'_{\min_i} = 0.252 \cdot D \cdot \sqrt[3]{\frac{E_i}{E_0}} \quad (107)$$

c. According to the design criterium number 7 and equation (100) we have:

$$h_{\min_i} = \frac{D \cdot (p_i^{\text{ad}} - p_{i-1}^{\text{ad}})}{\tau_i^{\text{a}\phi}} \quad (108)$$

d. According to the design criterium number 9, one can write:

$$h_{\min_i} = \text{Constant}_i \quad (109)$$

where Constant_i is a value chosen arbitrarily by the designing agency according to its experience. In Romania this value, for the surface course, is 5.0 cm (2.0 in).

5.3.1.1.2. Maximum Thickness

a. If one wants to limit the tensile stress at the bottom of the layer, according to the design criteria number 3 and equation (93), one can write:

$$h_i = \frac{2 \cdot \sigma_i^{\text{am}} (1 - \mu_i) R_i}{E_i} \quad (110)$$

But, at the beginning of the computations, one does not know what the value of R_i is.

If one takes into account the fact that R_i is a function of the E_1/E_0 ratio, the number of the layers and the value of the deflection (which is this case would be the permitted deflection) one can write:

$$R_i = f (E_1/E_0; N_\ell; w_a) \quad (111)$$

After a stochastic approach the function f in (111) was defined as follows:

$$R_i = \frac{500.0}{w_a} \sqrt[3]{\frac{E_1}{E_0}} \quad (112)$$

if R_i and w_a are given in the metric system of measure, and

$$R_i = \frac{200.0}{w_a} \sqrt[3]{\frac{E_1}{E_0}} = \frac{500.0}{F_d w_a} \sqrt[3]{\frac{E_1}{E_0}} \quad (112.a)$$

if R_i and w_a are given in the American system of measure.

If one computes the value of h_i by equation (110), the thicknesses found would be too conservative, namely too small. For this reason the value of h_i calculated is to be multiplied by the safety coefficient, F_s , used in the design method. As a first approximation one could use the value of 17 which was obtained after more than 2000 experiments reported in Ref. 7, this value being only a provisional one. Now one can write:

$$h_{\max_i} = \frac{2 \cdot \sigma_i^{\text{am}} \cdot (1 - \mu_i) R_i}{E_i} F_s \quad (113)$$

b. In order to limit the horizontal shear stresses in the center plane of the layer one must observe the design criteria number 4 and use equation (94).

If one uses the development presented above one obtains the following equation:

$$h_{\max_i} = \frac{2 \cdot \tau_i^{\text{am}} \cdot (1 + \mu_i) R_i}{E_i} F_s \quad (114)$$

But the value of τ_i^{am} in (114) is not a constant one and it can be calculated by Coulomb's equation:

$$\tau_i^{\text{am}} = Co_i + \sigma_i^v \cdot \tan \phi_i \quad (115)$$

where Co_i is the cohesion of the material i .

One can see immediately that the value of τ_i^{am} is a function of the vertical stress σ_i^v which cannot be calculated until one knows the thickness of the layer.

The most conservative approach is to consider that all layers above the layer i have their maximum thickness.

Then, the vertical stresses on the layer beneath will be the least ones and hence the value of τ_i^{am} will be the least possible. For this reason one will consider herein that σ_i^v is measured at the top of the layer and not at its middle. Therefore the values of τ_i^{am} will be a little higher than the least ones.

For the surface course one will have:

$$\tau_i^{am} = C_{o_i} + p \cdot \tan \phi_i \quad (116)$$

where the cohesion C_o can be measured in the laboratory before the design procedure is started.

By using equation (105), (107), (108) and (109) one gets four values for h_{\min_i} . It is obvious that the greatest one will be used in the computations.

Equations (113) and (114) give the maximum values for h_i . It is also obvious that the smallest one will be used in the further computation.

Because most of the developments are the same, in the presentation below only those which show some differences will be presented in detail.

5.3.1.2. Base Course

5.3.1.2.1. Minimum Thickness

a. Design criterium No. 2.

$$h_{\min_i} = D \cdot \frac{\sqrt{\frac{p}{a_d} - \alpha_i}}{a_1 \cdot \sqrt[3]{\frac{E_i}{E_o}}} \quad (105.a)$$

b. Design criterium No. 6. It requires that the maximum horizontal shear stresses lie in the base course. This means that the maximum shear stress should lie in the middle third of the thickness of the base course, in order to better use its resistance to shear failure.

According to Figure 12 and equation (46) the maximum shear stresses under the center of the load will occur at a relative depth $0.35 \frac{z}{D}$.

The relative depth of the surface course being:

$$h_{eg_m} = a_1 \cdot \frac{h_m}{D} \sqrt[3]{\frac{E_m}{E_o}} \quad (117)$$

one can determine immediately the minimum thickness of the base course:

$$h_{min_i} = \frac{3D}{2} \left[0.35 - a_1 \cdot \frac{h_m}{D} \sqrt[3]{\frac{E_m}{E_o}} \right] \cdot \frac{1}{a_1} \quad (118)$$

After computation and reduction of the constants, equation (118) becomes:

$$h_{min_i} = 0.63 \cdot D - 1.5 \cdot h_m \cdot \sqrt[3]{\frac{E_m}{E_o}} \quad (119)$$

c. Design criterium No. 7.

$$h_{min_i} = D \frac{(p_i^{ad} - p_{i-1}^{ad})}{\tau_i^{a\phi}} \quad (108.a)$$

d. Design criterium No. 9.

$$h_{\min_i} = \text{constant } i \quad (109.a)$$

In Romania the minimum thickness of the base course is 8.0 cm (3.0 in).

5.3.1.2.2. Maximum Thickness

The equations are the same as those in (113) and (114) and nothing is to be gained by repeating them again.

5.3.1.3. Subbase Course

5.3.1.3.1. Minimum Thickness

The same equations are used as for the previous layers except for (106) or (119). Therefore, one uses equations (105), (108) and (109) only.

In Romania the minimum thickness for the subbase is 15 cm (6.0 in).

5.3.1.3.2. Maximum Thickness

One uses equations (113) and (114).

5.3.1.4. Drainage Course

The drainage course has only minimum thickness and no maximum thickness. Previous experiments and theoretical developments report in Ref. 7 and 9 revealed the fact that if the thickness of a layer is greater than $2.5 \cdot D$, then it behaves as having an infinite thickness. It can be considered as an actual subgrade if the real subgrade is not too weak and can support the highway body without appreciable deformations ($E \geq 100.0 \text{ kgf/cm}^2$ or $E \geq 1380 \text{ psi}$).

It is not the purpose of this work to study this phenomenon but the previous findings reported in Ref. 7 and 9 will be used in the optimal design of the pavements.

The minimum thickness can be either a calculated or an evaluated one.

The calculated minimum thickness is related to the frost penetration. In Romania it is required that the thickness of the drainage course be such that the thermo-conductivity of the pavement will be the same as that of the natural subgrade with a depth that is equal to the frost penetration depth.

It should be noted that this requirement is applicable only to subgrades which are frost susceptible.

If the coefficients of resistance to the frost penetration, C_i^{fr} , are known, one can write the equation which will allow the determination of the computed minimum thickness of the drainage course:

$$h_{\min_i} = \frac{z_f - \sum_{i=2}^m h_i \cdot c_i^{fr}}{c_1^{fr}} \cdot c_o^{fr} \quad (120)$$

One can observe immediately that the thickness of the drainage course is related to the thicknesses of the other layers.

If one accepts the bearing capacity of this layer is not taken into consideration, one can compute its thickness after the thicknesses of the other layers are found. If not, an alternative calculation will be necessary.

According to Ref. 7 and 9, if the thickness of the drainage course is less than $0.4 \cdot D$ it is not worth taking it into account. If the thickness of this layer lies between $0.4 \cdot D$ and $0.8 \cdot D$ it is taken into account as a common layer. Between $0.8 \cdot D$ and $2.5 \cdot D$ a correction function ϕ is used:

$$\phi = 0.51 / (h_i / \alpha_i \cdot D)^3 \quad (121)$$

Finally, if $h_1 \geq 2.5 D$ it is considered as being an actual subgrade and all computations are done over again.

The evaluated minimum thickness of the drainage course varies from one design agency to another. In Romania this value is 5.0 cm (2.0 in) but it will not remain at this value as many proposals have been made to increase it up to 15.0 cm (6.0 in).

5.3.2. Actual Development of the New Method

The fundamental principle of the new method is the principle of the conservation of the energy. This requires that the exterior energy, transferred by the load during the deflection of the pavement, will be equal to the interior energy gained by the highway body during its deflection. This principle can be presented as follows:

$$W_e = W_i \quad (122)$$

The interior energy is formed by the subgrade energy W_t and the pavement energy W_{sr} defined as presented in the list of notations at the beginning of the fourth part.

So, one can write:

$$W_e = W_t + W_{sr} \quad (123)$$

Now, the main problem is to find the equations whereby these energies can be computed. Each energy will be considered separately.

5.3.2.1. Exterior Energy

At first sight this energy seems to be easy to compute: one multiplies the load by the deflection and is done.

For rigid pavements or for flexible pavements with high bearing capacity, the error could be less than 3%. But for flexible pavements with medium or low bearing capacity the error can increase to 10 and 30% respectively, which cannot be accepted in a design method.

It was demonstrated in Ref. 7 that the load being flexible follows the pavement in its deformation and the average displacement of the load is less than the deflection under the center of the load. This is shown in Fig. 21.

The problem is to calculate the value of the deflection reduction factor F_r .

In Ref. 7 a geometric approach is presented and the following formula is given:

$$F_r = 1.0 - \frac{1.0}{3 \cdot \alpha_o^2} \quad (124)$$

In order to have a more accurate definition of the value of F_r a new development was done as follows.

The deflection at the distance r from the center of the load is given by equation (21):

$$w_r = \frac{w_o}{1 + a \cdot r^2} \quad (21)$$

where:

$$a = \frac{4.0}{\alpha_o^2 \cdot D^2} \quad (20.a)$$

For more convenience in further computations one will consider:

$$a = \frac{2.0}{\alpha_o \cdot D} \quad (125)$$

and:

$$w_r = \frac{w_o}{1 + a^2 \cdot r^2} \quad (126)$$

The load pressure is assumed to be constant throughout the loaded area and equal to p.

Now, one can compute the exterior energy as follows:

$$W_e = \int_0^{D/2} p \frac{w_o}{1 + a^2 \cdot r^2} 2 \cdot \Pi \cdot r \cdot d_r \quad (127)$$

Equation (127) can be presented as follows:

$$W_e = 2 \cdot p \cdot \Pi \cdot w_o \cdot \int_0^{D/2} \frac{r}{1 + a^2 \cdot r^2} d_r \quad (128)$$

then:

$$\int_0^{D/2} \frac{r}{1 + a^2 \cdot r^2} d_r = \left| \frac{1}{2 \cdot a^2} \ln (1 + a^2 \cdot r^2) + C_1 \right|_0^{D/2} \quad (129)$$

By boundary conditions $C_1 = 0$. Then, after replacing "a" with its value from (125) one gets:

$$W_e = 2 \cdot p \cdot \Pi \cdot w_o \frac{\alpha_o^2 \cdot D^2}{8} \ln \left(1.0 + \frac{1.0}{\alpha_o^2} \right) \quad (130)$$

The factor F_r is then:

$$F_r = \frac{W_e}{2 \cdot \Pi \cdot \frac{D^2}{4} \cdot p \cdot w_o} = \alpha_o^2 \cdot \ln \left(1.0 + \frac{1.0}{\alpha_o^2} \right) \quad (131)$$

Equation (131) is very different from (124).

In order to verify the validity of equations (124) and (131) their results were compared with measured values of F_r as shown in Fig. 22.

Equation (124) better fits the data than equation (131). Nevertheless, neither of them is satisfactory and an experimental correction factor is added to get a better agreement between calculated and measured values of F_r .

The reason of this lack of fit may be explained by the non-uniform pressure of the tire and by the fact that the real F_r factors were measured under a dual wheel area whereas the calculated values of F_r were computed under a unique circular area.

So, for the further developments one may use one of the following equations:

$$F_r = 1.0 - \frac{1.0}{3 \cdot \alpha_o^2} + 0.03 \quad (132)$$

$$F_r = \alpha_o^2 \cdot 1_n \left(1.0 + \frac{1.0}{\alpha_o^2} \right) + 0.046 \quad (133)$$

and then:

$$W_e = F_r \cdot P \cdot w_s \quad (134)$$

In order to get a more consistent theory the relationship in (131) will be used.

5.3.2.2. Subgrade Energy

There are two ways to compute the subgrade energy:

- By using equation (15) given by the theory of elasticity (Bezuhov variant) or
- By using equation (21) which is an empirical approach (Empirical variant)

Both of them will be discussed.

Bezuhov Variant

The equation which gives the distribution of the load on

the subgrade (and which is not given in Bezuhov's developments) is:

$$\zeta_r = \frac{p}{\alpha_o} \left[1.0 - \frac{r}{b} \right]^2 \quad (135)$$

where:

$$b = \frac{\alpha_o \cdot D}{2} = \frac{1}{a} \quad (135.a)$$

One can demonstrate easily that if equation (135) is integrated throughout the loaded area one obtains the actual exterior load, so there exists a real equality between actions and reactions.

In order to simplify the further computations equation (135) will be presented as follows:

$$\zeta_r = c_1 \cdot (b^2 - r^2) \quad (136)$$

where:

$$c_1 = \frac{p}{b^2 \cdot \alpha_o} \quad (137)$$

Equation (15) can be presented as follows if required computations are made:

$$w_r = \frac{1}{4} \cdot \frac{p}{\alpha_o} \cdot \frac{1 - \mu_o^2}{E_o} \cdot \frac{\pi}{b} (2 \cdot b^2 - r^2) \quad (138)$$

or, in a more convenient form:

$$w_r = C_2 (2 \cdot b^2 - r^2) \quad (139)$$

where:

$$C_2 = \frac{1}{4} \cdot \frac{p}{\alpha_o} \cdot \frac{1 - \mu^2}{E_o} \cdot \frac{\Pi}{b} \quad (140)$$

The subgrade energy is:

$$W_t = \int_0^b 2 \cdot \Pi \cdot b \cdot \zeta_r \cdot w_r \cdot dr \quad (141)$$

or:

$$W_t = 2 \cdot \Pi \cdot b \int_0^b \zeta_r \cdot w_r \cdot dr \quad (142)$$

and, after replacing ζ_r and w_r with their respective expressions from (136) and 139) one gets:

$$W_t = 2 \cdot \Pi \cdot b \cdot C_1 \cdot C_2 \int_0^b (b^2 - r^2) (2 \cdot b^2 - r^2) dr \quad (143)$$

Equation (143) can be written as follows:

$$W_t = C_3 \int_0^b (2 \cdot b^4 - 3 \cdot b^2 \cdot r^2 + r^4) dr \quad (144)$$

where:

$$C_3 = 2 \cdot \Pi \cdot b \cdot C_1 \cdot C_2 \quad (145)$$

After integration one obtains:

$$W_t = C_3 \left| 2 \cdot b^4 \cdot r - 3 \cdot b^2 \cdot \frac{r^3}{3} + \frac{r^5}{5} + C_4 \right|_0^b \quad (146)$$

By boundary conditions $C_4 = 0$ and after computations:

$$W_t = C_3 \cdot \frac{6}{5} \cdot b^5 \quad (147)$$

If one replaces C_3 by its expression in (145) and all required computations are made one obtains:

$$W_t = \frac{18 \cdot \Pi^2}{160} \cdot \frac{1 - \alpha_o^2}{E_o} \cdot \frac{p^2 \cdot D^3}{\alpha_o} \quad (148)$$

or, in a more compact form:

$$W_t = 0.45 \frac{1 - \mu_o^2}{E_o} \cdot \frac{p^2}{\alpha_o \cdot D} \quad (149)$$

Empirical Variant

The equation for ζ_r is the same as in Bezuhov variant.

The equation of the subgrade deflection is the same as in (126).

Using the same approach as for the Bezuhov variant,

$$W_t = 2 \cdot \Pi \cdot b \int_0^b \zeta_r \cdot w_r \cdot dr \quad (150)$$

$$W_t = 2 \cdot \Pi \cdot b \cdot w_0 \cdot C_1 \int_0^b (b^2 - r^2) \frac{1}{1 + a^2 \cdot r^2} dr \quad (151)$$

$$C_2 = 2 \cdot \pi \cdot b \cdot w_0 \cdot C_1 \quad (152)$$

$$W_t = C_2 \int_0^b \left(\frac{b^2}{1 + a^2 \cdot r^2} - \frac{r^2}{1 + a^2 \cdot r^2} \right) dr \quad (153)$$

After integration one obtains:

$$W_t = C_2 \left| \frac{b^2}{a} \arctan(a \cdot r) - \frac{r}{a^2} + \frac{1}{a^3} \arctan(a \cdot r) + C_3 \right|_0^b \quad (154)$$

After replacing C_2 , a and b by their expressions and after making all required computations one gets:

$$W_r = \frac{3 \cdot \Pi^2 (\Pi - 2)}{32} \cdot \frac{1 - \mu_0^2}{E_0} \frac{P^2}{\alpha_0 \cdot D} \quad (155)$$

and, in a more compact form:

$$W_t = 0.43 \frac{1 - \mu_o^2}{E_o} \cdot \frac{p^2 \cdot D^3}{\alpha_o \cdot D} \quad (156)$$

The difference between equations (149) and (156) is about 5% which means that the empirical approach used to define the equation of the deformed surface in (21) is very good.

5.3.2.3. Pavement Energy

According to Ref. 7, the energy of a layer can be computed by using the following equation:

$$W_s = \frac{1}{2} \cdot \frac{E \cdot h^3}{12 (1 - \mu^2)} \iint_A \left[\left(\frac{\partial^2 w}{\partial x^2} \right)^2 + \left(\frac{\partial^2 w}{\partial y^2} \right)^2 + 2 \cdot \frac{\partial^2 w}{\partial x^2} \cdot \frac{\partial^2 w}{\partial y^2} + 2 (1 - \mu) \left(\frac{\partial^2 w}{\partial x \partial y} \right)^2 \right] d_x \cdot d_y \quad (157)$$

where the domain A is the area of the deformed surface.

Equation (157) can be simplified by assuming that the loaded area and hence the deformed area are circular.

Recognizing that:

$$x = y = r \quad (158)$$

equation (157) becomes:

$$W_s = \frac{1}{2} \cdot \frac{E \cdot h^3}{12 (1 - \mu^2)} \iint_A \left[2 \cdot \left(\frac{\partial^2 w}{\partial r^2} \right)^2 + 2 \cdot \mu \cdot \left(\frac{\partial^2 w}{\partial r^2} \right)^2 + 2 (1 - \mu) \cdot \left(\frac{\partial^2 w}{\partial r^2} \right)^2 \right] dr \cdot dr \quad (159)$$

But, since the deformed area is a circular one and it is assumed that, at the same distance r from the center of the loaded area, the same deflection w occurs, the last term under the integral is equal to zero (Ref. 7, page 20).

Therefore equation (159) can be simplified as follows:

$$W_s = \frac{1}{2} \cdot \frac{E \cdot h^3}{12 (1 - \mu^2)} \iint_A \left[\left(\frac{\partial^2 w}{\partial r^2} \right)^2 + \mu \cdot \left(\frac{\partial^2 w}{\partial r^2} \right)^2 \right] dr \cdot dr \quad (160)$$

and finally

$$W_s = \frac{E \cdot h^3}{12 (1 - \mu^2)} \iint_A \left(\frac{\partial^2 w}{\partial r^2} \right)^2 dr \cdot dr \quad (161)$$

Although equation (161) seems to be easy to integrate, in reality it is very difficult. For this reason some simplifications were made as follows.

First of all it is known that the curvature of the surface at a given point can be computed by equation (90). This is the reason why one can write:

$$W_s = \frac{E \cdot h^3}{12 (1 - \mu)} \iint \left(-\frac{1}{R_r} \right)^2 dr \cdot dr \quad (162)$$

where R_r is the radius of curvature of the deformed surface at the distance r from the center of the load.

It it can be assumed that the radius of curvature is constant along the deformed surface, the integration of equation (162) will no longer be difficult.

Experiments made by Brown and Pell (Ref. 2, pages 487-504) and which were analyzed in Ref. 7 (page 14) have demonstrated that there is not too great a difference between an "ideal" radius of curvature (constant) and the real radius of curvature, as shown in Fig. 23.

For this reason R_r is replaced by the radius of curvature at the top surface of the subgrade, calculated by equation (26).

Then one can write:

$$W_e = \frac{E \cdot h^3}{12 (1 - \mu) R} \iint_A dr \cdot dr \quad (163)$$

But:

$$\iint_A dr \cdot dr = \frac{\Pi (\alpha_o \cdot D \cdot 2)^2}{4} \quad (164)$$

because the deformed surface is a circle with a diameter equal to $2.06 \cdot D$.

$$W_s = \frac{E \cdot h^3}{12 (1 - \mu) R} \cdot \frac{\Pi (2 \cdot \alpha_o \cdot D)^2}{4} \quad (165)$$

or

$$W_s = \frac{\Pi \cdot \alpha_o^2 \cdot D^2}{12 \cdot R} \cdot \frac{E \cdot h^3}{1 - \mu} \quad (166)$$

If W_s is the energy accumulated by a layer during deflection, the energy of the pavement would be:

$$W_{sr} = \sum_{i=1}^m W_{si} \quad (167)$$

and, after replacing W_{si} by equation (166):

$$W_{sr} = \frac{\Pi \cdot \alpha_o^2 \cdot D^2}{12 \cdot R} \sum_{i=1}^m \frac{E_i \cdot h_i^3}{1 - \mu_i} \quad (168)$$

But W_{sr} does not represent the whole energy of the pavement because the effect of the friction stresses is to be added.

If one compares equations (95) and (166) it will be immediately observed that the energy of a layer is a direct function of the bending moment:

$$\frac{W_{si}}{M_i} = \frac{\Pi \cdot \alpha_o^2 \cdot D^2}{R} \quad (169)$$

The moment due to the friction stresses is given by equation (97).

So, one can write:

$$W_{sr} = \frac{\Pi \cdot \alpha_o^2 \cdot D^2}{R} \left[\frac{E_i \cdot h_i^3}{12 (1 - \mu_i)} + (\sigma_i^f + \sigma_{i+1}^f) \frac{h_i}{2} \right] \quad (170)$$

and:

$$W_{sr} = \frac{\Pi \cdot \alpha_o^2 \cdot D^2}{R} \sum_{i=1}^m \left[\frac{E_i \cdot h_i^3}{12(1 - \mu_i)} (\sigma_i^f + \sigma_{i+1}^f) \frac{h_i}{2} \right] \quad (171)$$

5.3.2.4. Equality of Interior and Exterior Energies

After the above developments one can write the equality between the exterior and interior energy:

$$F_r \cdot P \left(w_o + \sum_{i=1}^m w_i^{pj}, (j=m+1) \right) = 0.43 \frac{1 - \mu_o^2}{E_o} \cdot \frac{P^2}{\alpha_o \cdot D} \quad (172)$$

$$+ \frac{\Pi \cdot \alpha_o^2 \cdot D^2}{R} \sum_{i=1}^m \left[\frac{E_i \cdot h_i^3}{12(1 - \mu_i)} + (\sigma_i^f + \sigma_{i+1}^f) \frac{h_i}{2} \right]$$

If one replaces R by equation (26) one will get:

$$F_r \cdot P \left(w_o + \sum_{i=1}^m w_i^{pj}, (j=m+1) \right) = 0.43 \frac{1 - \mu_o^2}{E_o} \frac{P^2}{\alpha_o \cdot D}$$

$$+ \frac{16}{3} \cdot \Pi \cdot \frac{w_o^2}{\alpha_o^2 \cdot D^2} \sum_{i=1}^m \frac{E_i \cdot h_i^3}{1 - \mu_i} + 8 \cdot \Pi \cdot w_o \quad (173)$$

$$\sum_{i=1}^m \left[\frac{h_i}{2} (\sigma_i^f + \sigma_{i+1}^f) \right]$$

If one considers that:

$$w_o = 1.5 \frac{1 + \mu_o^2}{E_o} \cdot \frac{P}{\alpha_o \cdot D} \quad (174)$$

which agrees with the theory of elasticity (Ref. 14, page 260) and one replaces in (173):

$$\frac{1 - \mu_o^2}{E_o} \cdot \frac{P}{\alpha_o \cdot D} = \frac{w_o}{1.5} \quad (175)$$

it follows that:

$$\begin{aligned} F_r \cdot P \left(w_o + \sum_{i=1}^m w_i^{pj}, (j=m+1) \right) &= 0.286 \cdot w_o \cdot P \\ + \frac{16}{3} \cdot \Pi \cdot \frac{w_o^2}{\alpha_o^2 \cdot D^2} \sum_{i=1}^m \frac{E_i \cdot h_i^3}{1 - \mu_i} + 4 \cdot \Pi \cdot w_o \cdot \\ &\sum_{i=1}^m h_i \cdot (\sigma_i^f + \sigma_{i+1}^f) \end{aligned} \quad (176)$$

After grouping terms one can write:

$$\begin{aligned} A &= \frac{16 \cdot \Pi}{3 \cdot \alpha_o^2 \cdot D^2} \sum_{i=1}^m \frac{E_i \cdot h_i^3}{1 - \mu_i}, \\ B &= -F_r \cdot P + 0.286 \cdot P + 4 \cdot \Pi \sum_{i=1}^m h_i (\sigma_i^f + \sigma_{i+1}^f), \\ C &= -F_r \cdot P \cdot \sum_{i=1}^m w_i^{pj}, (j=m+1) \end{aligned} \quad (177)$$

and finally,

$$A \cdot w_o^2 + B \cdot w_o + C = 0 \quad (178)$$

In order to verify equation (178) a computer program shown in Appendix 6 was written.

The results are presented in Fig. 24 and 25.

In Fig. 24 a comparison between calculated and measured deflections (regardless of the layer on which they were measured) was done.

Several observations are to be made.

The correlation between computed and measured deflections is much better using the energy approach.

The computed deflections show a definite trend to be higher than those measured ($\approx 34\%$) which is explained by the following reasons:

- As was demonstrated* several years ago, for the same pavement structures the deflections measured under real wheels are about 8% higher than those measured under flexible plates. In the plot only measures under plates are given.

Thus, the real difference between calculated and measured deflections is about 26%.

It should be noted here that in the definition of F_r a very flexible load was taken into account, so the difference mentioned above is justified.

* Between 1968-1971 a research group formed by: Assist. Prof. Horia Zarojanu; B. Cososchi and N. Vlad from the Polytechnic Institute of Iassy Romania, lead by Emm. Prof. D. Atanasiu, worked in this area.

- Two important simplifications were made for these computations. First, load is distributed upon a limited surface at the top level of the subgrade (which leads to a concentration of the load in the central part of the loaded area and hence a higher computed deflection). Second, the radius of curvature of the layers was considered as being a little greater than the real one as one can see in Fig. 23 (and hence the energy of the layers was underestimated).

It is hoped that further studies will allow the discarding of these simplifications, after these studies have been done, better correlations can be expected.

In Fig. 25 a comparison between computed and measured tensile stresses at the bottom of the layers is presented.

It can be seen immediately that actual tensile stresses show a definite tendency to be greater than the computed ones.

The average ratio between calculated and measured stresses is 0.79.

It should be pointed out that the average values mentioned above (either for deflections or for tensile stresses) were determined statistically and they differ from the means (arithmetic means) which were computed within the computer-program in Appendix 6. The latter are greater than the statistical values used.

One can assume that the magnitude of tensile stresses is proportional to the energy accumulated in the layers. If this energy is underestimated the tensile stresses are also underestimated.

If there exists some proportionality, the product of deflection ratio (1.26) and the stress ratio (0.79) should be close to 1. In fact, $1.26 \cdot 0.79 \approx 1.0$.

This means that further studies have to start with a better approach to evaluate the energy of the layers.

At this time a coefficient of lack of fit will be introduced.

This coefficient can be calculated as follows:

If the tensile stresses computed at the bottom of the layers represent, as an average, 0.79 of the actual tensile stresses, the average computed radius of curvature is about $1/0.79$ greater than the actual one.

As a consequence the formula in (26) becomes:

$$R = 0.79 \frac{\alpha_o^2 \cdot D^2}{8 \cdot w_o} \quad (179)$$

Then, by replacing R from equation (172) by equation (179) one obtains:

$$\begin{aligned} F_r \cdot P \left(w_o + \sum_{i=1}^m w_i^{pj}, (j=m+1) \right) &= 0.286 w_o \cdot P \\ &+ \frac{16.0}{1.84} \cdot \Pi \cdot \frac{w_o^2}{\alpha_o^2 D^2} \sum_{i=1}^m \frac{E_i \cdot h_i^3}{1 - \mu_i} \\ &+ 6.5 \cdot \Pi \cdot w_o \sum_{i=1}^m h_i (\sigma_i^f + \sigma_{i+1}^f) \end{aligned} \quad (180)$$

Then one gets:

$$\begin{aligned}
 A &= \frac{16.0 \cdot \Pi}{1.84 \cdot \alpha_o^2 \cdot D^2} \sum_{i=1}^m \frac{E_i \cdot h_i^3}{1 - \mu_i} \\
 B &= -P (F_r - 0.286) + 6.5 \cdot \pi \cdot \sum_{i=1}^m h_i (\sigma_i^f + \sigma_{i+1}^f) \\
 C &= -F_r \cdot P \sum_{i=1}^m w_i^{pj}, \quad (j=m+1)
 \end{aligned} \tag{181}$$

But now a new problem occurs.

As can be seen in Fig. 24 and 25 the ratios between calculated and measured values have a stochastic distribution which is natural.

This stochastic distribution is caused by the fact that all values chosen for the parameters characterizing the quality of the materials in the layers are not constants, but they have normal distributions as shown in Ref. 10.

For this reason a safety coefficient is to be introduced.

The computation of the safety factor is a stochastic problem and will be amply discussed in the next report.

However some considerations will be made in this report.

It can be required that the actual deflections measured upon a new road be less than or equal to a given value, for instance

the permitted or the computed deflection. Although it is possible to have this requirement for all the surface of the road, it would be too expensive to build such strong pavement structures. For this reason, in Romania for instance, only 85% of the surface of the road has to have deflections less than or equal to the permitted deflection.

Using this rule, which was provisionally accepted in this work, the value of the safety factor is determined in Fig. 24. This value is 1.5 which means that the permitted deflection is to be reduced in computations by 1.5.

It is interesting to observe that the new value obtained for the safety coefficient is less than that mentioned before. But, as shall be seen in the next report, the value 1.5 for the safety coefficient "covers" only the variations due to the nonuniformity of the materials characteristics. The influence of the variation of the thicknesses of the layers will be also taken into account. And it is to be expected that the latter will lead to an increase of the value of the safety coefficient.

The calculation of the permitted deflection may be done by different means. One of them is the formula offered in Ref. 7 page 26:

$$W_a = F_d (0.280 - 0.031 \log N_t) \quad (182)$$

where F_d is a correction factor defined in the list of notations Chapter 4. The result of the computation by using formula in (182) is given in cm, if $F_d = 1$ or in inches, if $F_d = 0.3937$.

N_t is, as one knows, the total estimated traffic for the service life of the pavement and it can be easily computed by means of the present annual traffic (N), the annual traffic increase rate (N_R), and the service life of the pavement (S_ℓ):

$$N_t = N \sum_{i=1}^{S_\ell} (1 + N_R)^i \quad (183)$$

But, the total estimated traffic has to be affected by a coefficient taking into account the seasonal influence (K_s). This coefficient may be calculated, and in Ref. 7 page 33 a way to do this computation is presented but this computation is a little too difficult to do through a structural design computation. For this reason a more simple and convenient formula can be used:

$$K_s \approx 1 + 0.30 \frac{F}{1000} \quad (184)$$

where F represents days \times $^{\circ}\text{C}$ below 0°C during one year.

If F calculated in degrees (below $+32^{\circ}\text{F}$), equation (184) becomes:

$$K_s \approx 0.968 + 0.166 \frac{F}{1000} \quad (185)$$

and finally,

$$N_t = K_s \cdot N \sum_{i=1}^{S_\ell} (1 + N_R)^i \quad (186)$$

It should be said that the formula in (184) fits both with data in Ref. 7 and data reported several years ago by Kucera (Czechoslovakia).

Another problem is to derive a formula for the equivalence wheel load factor computation.

Many methods are given in the literature, the most of them resulting from correlations based on experience.

The writer would like to present here the results reported in Ref. 7, because these results were based on a theoretical development which fitted rather well the AASHO road test findings.

The formula presented in Ref. 7, page 30 is the following"

$$\log N_e = (9 - \log N_B) (\eta - 1) + \eta \cdot \log N_i \quad (187)$$

where:

- N_B - the basic traffic evaluated for the service life of the pavement. It can be evaluated at first by the equivalent wheel load traffic expected over the highway and then it can be corrected by an iterative procedure. Finally N_B is to be equal to N_t ;
- N_i - number of load repetitions over a lane estimated for the vehicle type i ;
- N_e - number of load repetitions over a lane calculated for the equivalent vehicle;
- η - factor, dimensionless, that is computed by using the formula in (188) or in (188.a):

$$\eta = \sqrt{\frac{D_e}{D_i}} \quad (188)$$

$$\eta = \sqrt[4]{\frac{P_i \cdot p_e}{P_e \cdot p_i}} \quad (188.a)$$

where all terms are known.

The equivalence load factor will be:

$$K_w = \frac{N_i}{N_e} \quad (189)$$

For $N_B = 10^6$ (which corresponds to the traffic applied in AASHO Road Test) and for three different types of equivalent vehicles, comparisons between the results given by the above procedure and AASHO test results are given in Fig. 26, 27 and 28.

If the permitted deflection under the standard wheel is known (w_a reduced by the safety coefficient) one can develop the design formula.

In order to make the appropriate development to obtain the design formula one has to observe that:

$$w_a = w_o + \sum_{i=1}^m w_i^{p_j}, (j=m+1) \quad (190)$$

and then to go back to equation (173) which is written in another form:

$$\begin{aligned}
 F_r \cdot P \cdot w_a &= 0.43 \frac{1 - \mu_o^2}{E_o} \frac{P^2}{\alpha_o \cdot D} \\
 &+ \frac{16}{3} \Pi \frac{\left[w_a - \sum_{i=1}^m w_i^{pj}, (j=m+1) \right]^2}{\alpha_o^2 D^2} \cdot \sum_{i=1}^m \frac{E_i \cdot h_i^3}{1 - \mu_i} \\
 &+ 8 \cdot \Pi \left[w_a - \sum_{i=1}^m w_i^{pj}, (j=m+1) \right] \cdot \sum_{i=1}^m \frac{h_i}{2} (\sigma_i^f + \sigma_{i+1}^f)
 \end{aligned} \tag{191}$$

Now introduce the lack of fit factor ($F_\ell = 0.79$) and equation (191) becomes:

$$\begin{aligned}
 F_r \cdot P \cdot w_a &= 0.286 \left[w_a - \sum_{i=1}^m w_i^{pj}, (j=m+1) \right] \cdot P \\
 &+ \frac{16.0}{1.84} \frac{\left[w_a - \sum_{i=1}^m w_i^{pj}, (j=m+1) \right]^2}{\alpha_o^2 D^2} \cdot \sum_{i=1}^m \frac{E_i \cdot h_i^3}{1 - \mu_i} \\
 &+ 6.5 \cdot \Pi \left[w_a - \sum_{i=1}^m w_i^{pj}, (j=m+1) \right] \cdot \sum_{i=1}^m h_i (\sigma_i^f + \sigma_{i+1}^f)
 \end{aligned} \tag{192}$$

It can immediately be observed that there is a common term on the right side of equation (192). This will allow us to simplify the form of the design formula as follows:

$$\begin{aligned}
 F_r \cdot P \cdot w_a &= \left[w_a - \sum_{i=1}^m w_i^{p_j}, (j=m+1) \right] \cdot \left[0.286 \cdot P \right. \\
 &+ 8.7 \cdot \Pi \sum_{i=1}^m \frac{E_i \cdot h_i^3}{1 - \mu_i} + 6.5 \cdot \pi \cdot \\
 &\left. \sum_{i=1}^m h_i (\sigma_i^f + \sigma_{i+1}^f) \right]
 \end{aligned} \tag{193}$$

The ultimate form of the design formula will be:

$$\begin{aligned}
 F_r \cdot P \cdot w_a &= \left[w_a - \sum_{i=1}^m w_i^{p_j}, (j=m+1) \right] \cdot \left\{ 0.286 \cdot P \right. \\
 &+ 6.5 \cdot \Pi \cdot \left[1.34 \sum_{i=1}^m \frac{E_i \cdot h_i^3}{1 - \mu_i} + \right. \\
 &\left. \left. \sum_{i=1}^m h_i (\sigma_i^f + \sigma_{i+1}^f) \right] \right\}
 \end{aligned} \tag{194}$$

A discussion of this equation follows:

- There is no direct way to determine the thicknesses of the layers from the formula even if all exterior data (exterior load and its characteristics; subgrade and its characteristics; Young's moduli of the layers and their Poisson's ratios) are given.

- The stress and strains state within the pavement structure varies with the absolute and relative thickness of the layers, their position in the pavement structure, and their relative rigidity.

- The design process must be an iterative one. A set of thicknesses is to be defined by the designer and then the iterative computation can be continued until limit differences between "initial" and "final" thicknesses are obtained. These limit differences should differ from layer to layer according to some practical rules. In Romania, for instance, the thickness of the surface course varies by 1/2 cm and the thickness of the other layers by 1 cm.

- Any set of thicknesses must observe the constraints concerning the minimum and maximum thicknesses as it was discussed in the previous section of this report.

For all these reasons no "manual" procedure can be used for the structural design of asphalt pavements and only computers are able to do this job with a real efficiency.

If only computers can be used it is natural to try to optimize the design, namely the minimization of the construction costs, all technical requirements or constraints being observed. This will be the subject of the next report.

6. Conclusions

Although partial conclusions were presented throughout the previous parts, several main conclusions are to be summarized here.

a) There exists empirical formulas, developed through a consistent theory, which can predict with a high accuracy (under the center of the load):

- the vertical stresses at the top of the layers (equation 33),

- the radial stresses at the bottom of the layers (equation 42), and

- the shear stresses at the bottom of the layers (equation 45).

b) The integration of these equations has demonstrated that the stress function which could solve the equations of the theory of elasticity (equation 1), if only one, could be a transcendental function as shown in equation (72). This means that the functions which are usually introduced in equation (1), for instance Airy, Bessel or polynomials types, are suspect and could lead to wrong conclusions.

c) The basic equation proposed by Leger, presented in equation (18), describes rather well the top surface of the pavement when distorted. This equation may also be used to predict the strains (deflections) at the top surface of each layer of the pavement.

d) The study of the distorted state of the highway body, under load, taking into account only the energy necessary for

the change of volume is not sufficient for describing the real state of the stresses and strains. This is because the layers slip with respect to each other and the energy for the change of form must be taken into account.

e) The layers can actually be considered as slabs of a low rigidity even if they are built with noncohesive materials.

f) In order to eliminate any factor which could lead to the distress of the pavement, the following design criteria are to be taken into account:

- The energy gained by the highway body during deflection must be equal to the exterior energy, transferred by the load.

- Vertical stress at the top of each layer must be lower than the allowable stress.

- Tensile stress at the bottom of each layer, except subgrade, must be lower than the allowable stress.

- Shear stress in the center plane of each layer, except subgrade, must be lower than the allowable stress.

- The maximum vertical stresses should be located in the surface course.

- The location of maximum shear stress should be in the base-course.

- Vertical shear stresses along the circumference of the loaded area at the top of each layer, except subgrade, must be lower than the allowable stress.

- The depth of frost penetration must be less than the thickness of the pavement.

g) The design process is an iterative calculation under technical constraints and cannot be done except with the use of a computer with a large memory (3 million bits or more) and with a high speed of execution. This is because of the large quantity of information that is to be processed and the length of the computer-programs.

h) The method described in the previous part is subject to important improvements that will result from replacing a number of simplifying assumptions with more realistic ones. Nevertheless this method predicts correctly (at least from a stochastic point of view) the vertical stresses at the top of the layers, deflections at the top of the layers and tensile stresses at the bottom of the layers.

i) Although the deflections permitted at the top surface of the pavement appear to be the principal design criterium, it should be pointed out that this is as a consequence of using the radius of curvature as a parameter (see equations 171 to 176).

Acknowledgments

The material in this paper was developed in a research project sponsored by the National Academy of Sciences of the U.S.A., The Ministry of Education of Romania and The University of Michigan, Department of Civil Engineering.

The opinions, findings and conclusions expressed herein are those of the author and not necessarily those of the sponsors.

The author would like to express his appreciation to Professor Robert Goetz for his marvelous lectures, full of common sense, which helped the author with his not forgetting the true reality of the structural design of asphalt pavements.

The author would also like to express his particular acknowledgments to his adviser, Professor Egons Tons, who helped him in many different ways with his improving the knowledge in the area.

References

1. International Conference on the Structural Design of Asphalt Pavements, Proceedings, Ed., Braun-Brumfield Inc., Ann Arbor, Michigan, 1963.
2. Second International Conference on the Structural Design of Asphalt Pavements, Proceedings, Ed., Braun-Brumfield Inc., Ann Arbor, Michigan, 1968.
3. Third International Conference on the Structural Design of Asphalt Pavements, Vol. I Proceedings, Ed., Cushing-Malloy Inc., Ann Arbor, Michigan, 1972.
4. Yoder, E. J., Principles of Pavement Design, Ed., John Wiley & Sons, Inc., New York, 1959.
5. Carnahan, B., Wilkes, O. J., Digital Computing, FORTRAN IV, WATFIV, and MTS, Ann Arbor, Michigan, 1972.
6. McLeod, N.W., The Asphalt Institute's Layer Equivalency Program, RS-15, March, 1967.
7. Rafiroiu, M., Contributii la studiul problemei dimensionarii sistemelor rutiere nerigide (Resumé of the doctoral thesis), Iasi, 1971.
8. Rafiroiu, M., Une nouvelle méthode pour le dimensionnement des chaussées souples, Revue Générale des Routes et des Aérodrômes Paris, Nr. 431, Apr., 1968, page 49-74.
9. Rafiroiu, M., Quelques considerations sur les chaussées bicouches, Revue Générale des Routes et des Aérodrômes, Paris, Nr. 452, March, 1970, page 85-92.
10. Rafiroiu, M., Essai d'étude statistique des constantes élastiques des matériaux routiers, Revue Générale des Routes et des Aérodrômes, Paris, Nr. 467, July-Aug. 1971, page 51-56.
11. Rafiroiu M., Sur le frottement a l'interface des couches des chaussées, Strasse und Verkehr, Zurich, Nr. 9, Sept., 1971, page 438-440.

12. Rafiroiu M., Le dimensionnement aux bords des chaussées souples, Strasse und Verkehr, Zurich, Nr. 2, Feb. 1971, page 61-65.
13. Dimensionierung der Strassenoberbaues, Strasse und Verkehr, Zurich, Nr. 8, Aug., 1972, page 373-415.
14. Bezuhov, N. I., Teoria elasticitatii si plasticitatii, Transl. from Russian, Ed. Tehnica, Bucuresti, 1957.
15. Hilton, P. J. Partial Derivatives, Dover Publications Inc., New York, 1965.
16. Smoleanski, M. L., Tabele de integrale nedefinite, Ed. Technica, Bucuresti, 1972.
17. Ahlvin, R. G., et al., The Principle of Superposition in Pavement Analysis, HRB, 52nd Annual Meeting, Report No. 5 in Session 32, Washington, Jan. 22 - 26, 1973.
18. Barksdale, R. D. and Hicks, R. G., Material Characterization and Layered Theory for Use in Fatigue Analyses, HRB, 52nd Annual Meeting, Report No. 2 in Session 22, Washington, Jan. 22-26, 1973.
19. Timoshenko, S. and Goodier, Y. N., Theory of Elasticity, Ed. McGraw-Hill Book Company, Inc., New York, 1951.
20. Rafiroiu, M., O INCERCARE DE REZOLVARE A PROBLEMEI DIMENSIONARII ECONOMICE A SISTEMELOR RUTIERE NERIGIDE, Transporturi, Bucuresti, 2 (19), Nr. 5, Mai 1972, page 259-264.

List of Figures

Figure

1. Element of stress.
2. Element of strain.
3. Stresses acting on an element.
4. Uniform loaded plate.
5. Semispherical loaded plate.
6. Model for flexible pavements analysis.
7. Stresses under the center of the loaded area for an m-layered system.
8. Stresses in the i-th layer.
9. Vertical stresses under a uniform loaded flexible circular plate.
10. Average vertical stresses under a uniformly loaded circular plate.
11. Radial stresses under a uniformly loaded circular plate.
12. Shear stresses under a uniformly loaded circular plate.
13. Comparison between measured and calculated vertical compressive stresses under the center of the loaded area.
14. Comparison between measured and computed tensile stresses at the bottom of the layers under the center of the loaded area.
15. Comparison between measured and computed deflections at the surface of the pavement under the center of the loaded area.
16. Comparison between deflections calculated without taking into account the energy necessary to change the form of the layers (w , computed) and those which take it into account (w , LMD).

17. $R \cdot w$ values for various structures of asphalt pavements.
18. Bending moment due to the radial stresses.
19. Bending moment due to the friction stresses.
20. Shear stresses along the contour of the loaded area, at different levels.
21. Average deflection under load.
22. Computed versus measured values for the factor F_r .
23. Theoretical versus actual deflection profile.
24. Computed versus measured deflections.
25. Computed versus measured tensile stresses at the bottom of the layers.
26. Theoretical versus AASHO Road Test results for the wheel equivalency factor, for EWL = 8.1 metric tons (18000 pounds) standard axle.
27. Theoretical versus AASHO Road Test results for 10.4 metric tons (22500 pounds) standard axle.
28. Theoretical versus AASHO Road Test results for 13.6 metric tons (30000 pounds) standard axle.

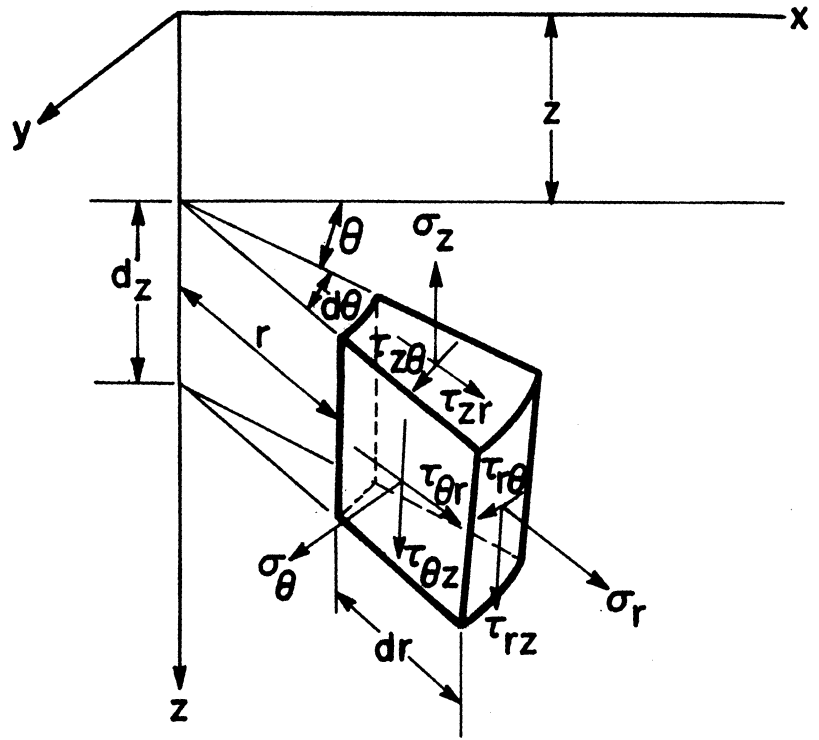


Figure 1. Element of stress.

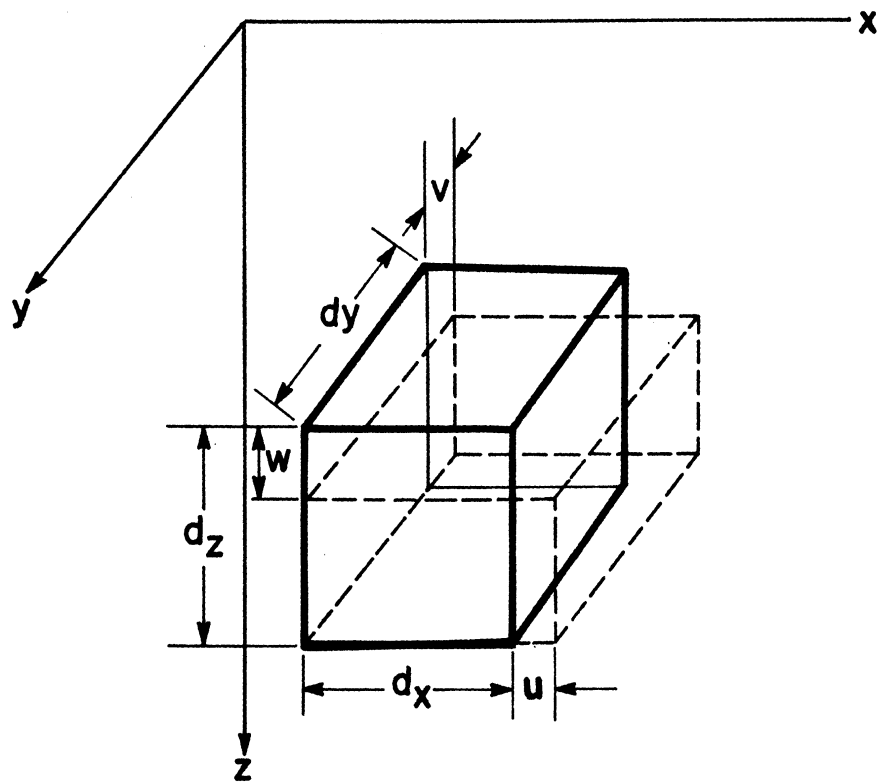


Figure 2. Element of strain.

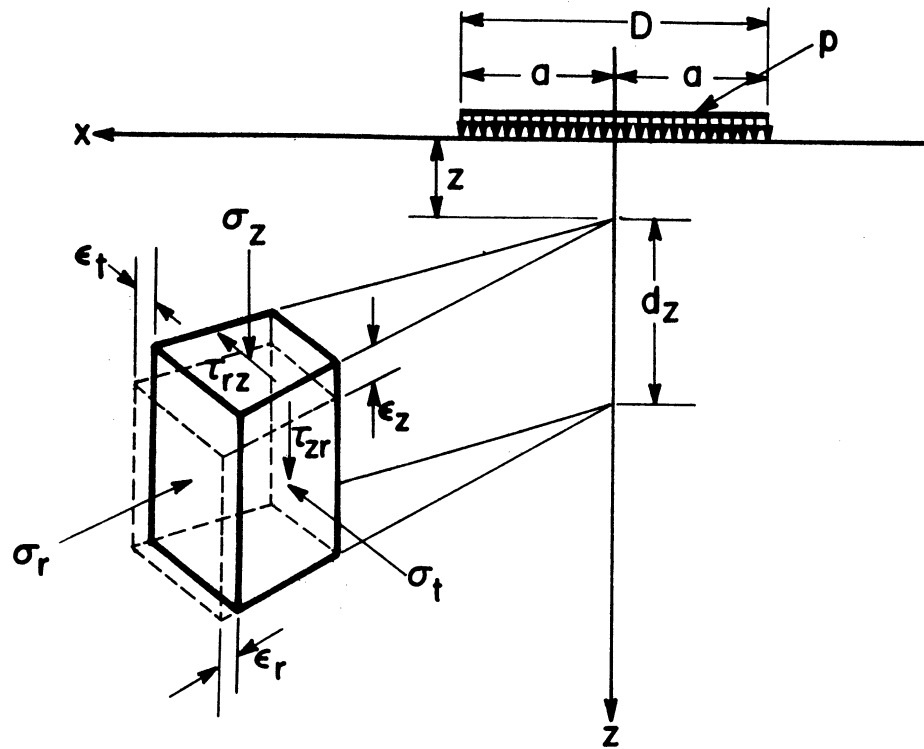


Figure 3. Stresses acting on an element.

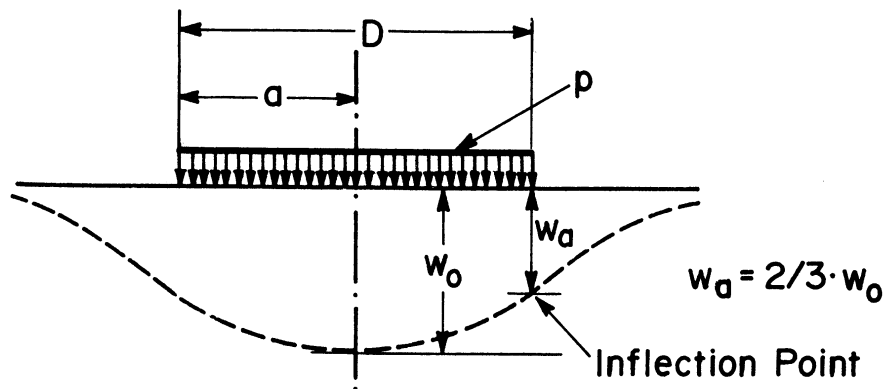


Figure 4. Uniform loaded plate.

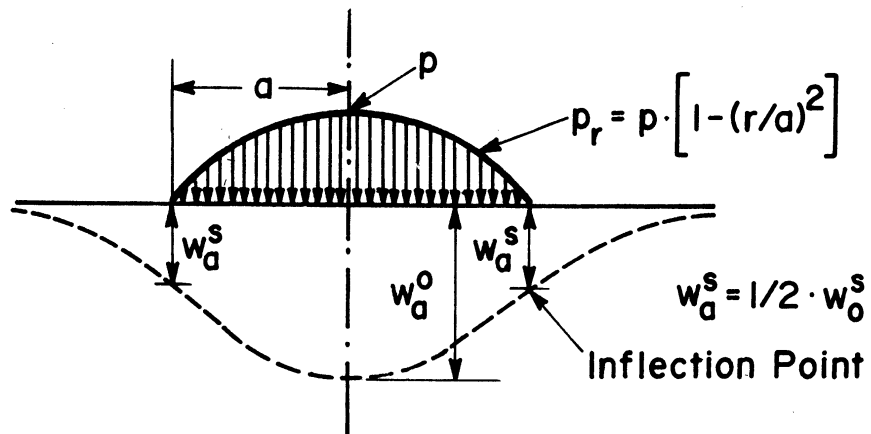


Figure 5. Semispherical loaded plate.

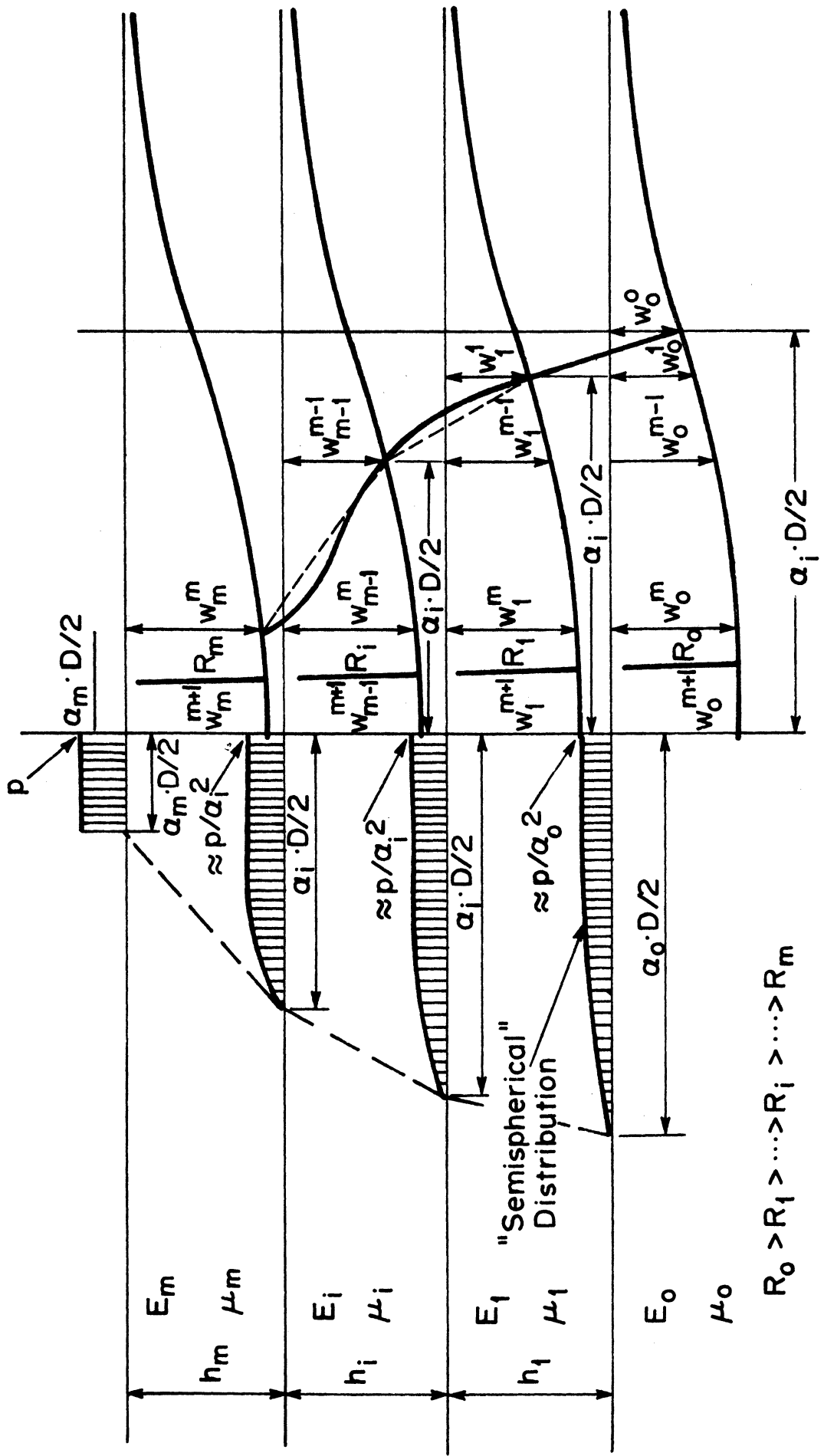


Figure 6. Model for flexible pavements analysis.

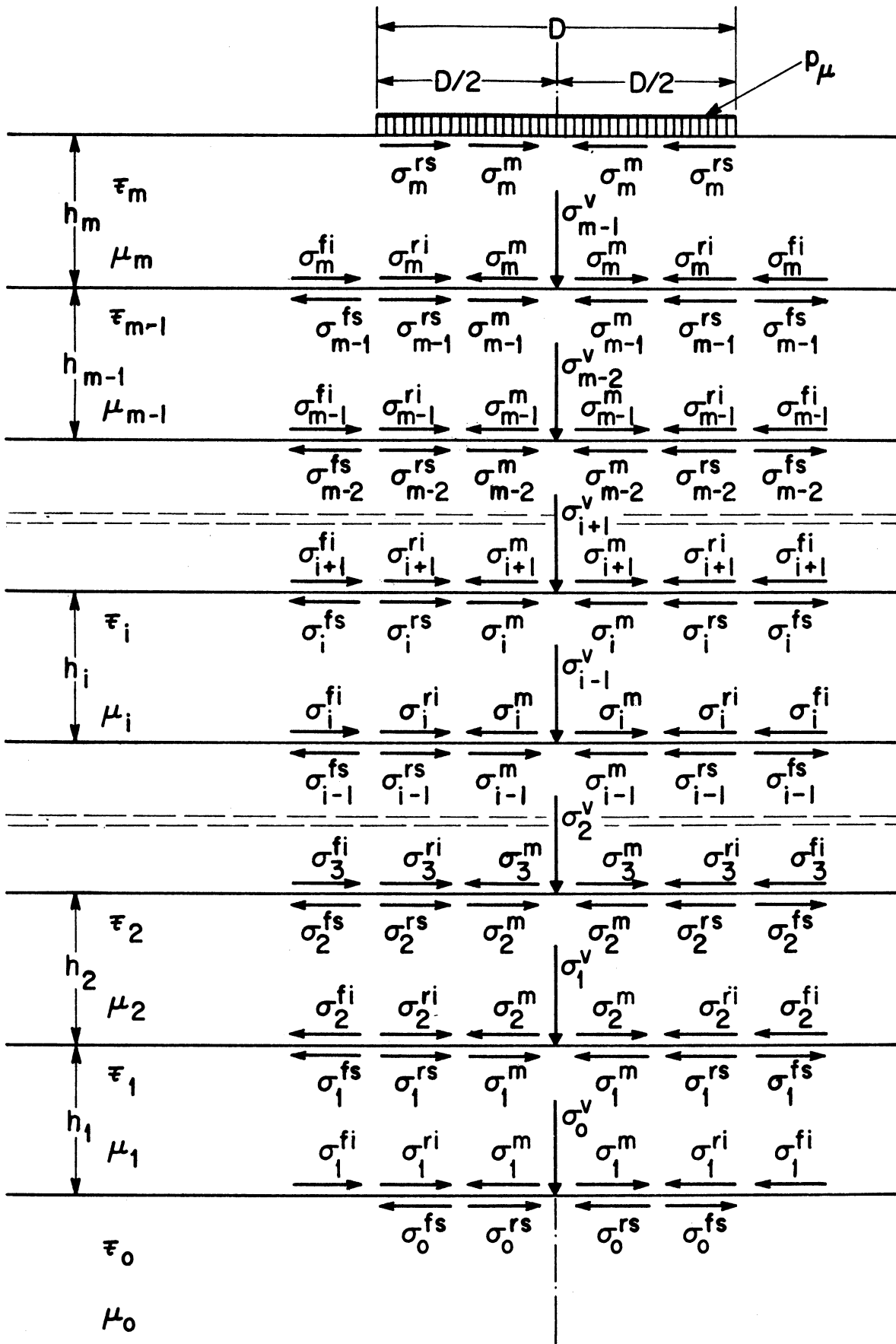


Figure 7. Stresses under the center of the loaded area for an m -layered system.

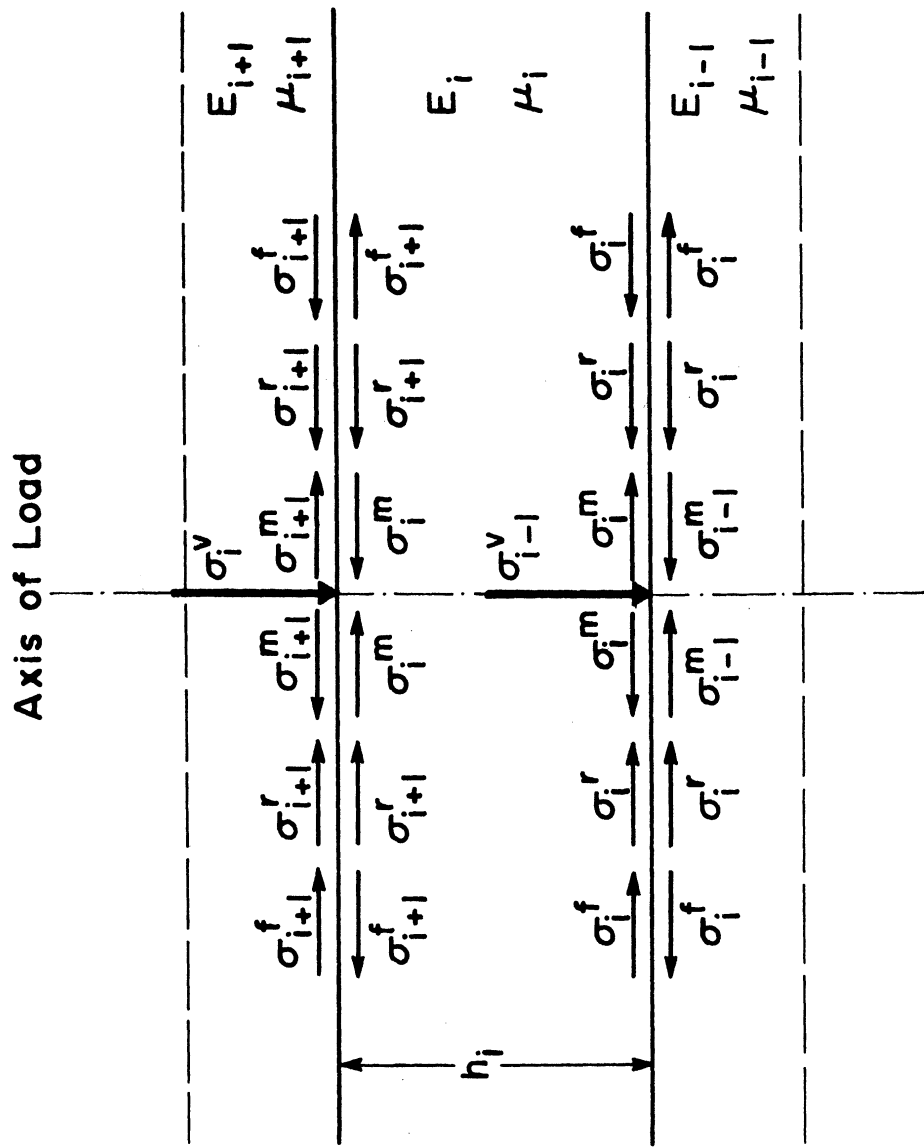


Figure 8. Stresses in the i -th layer.

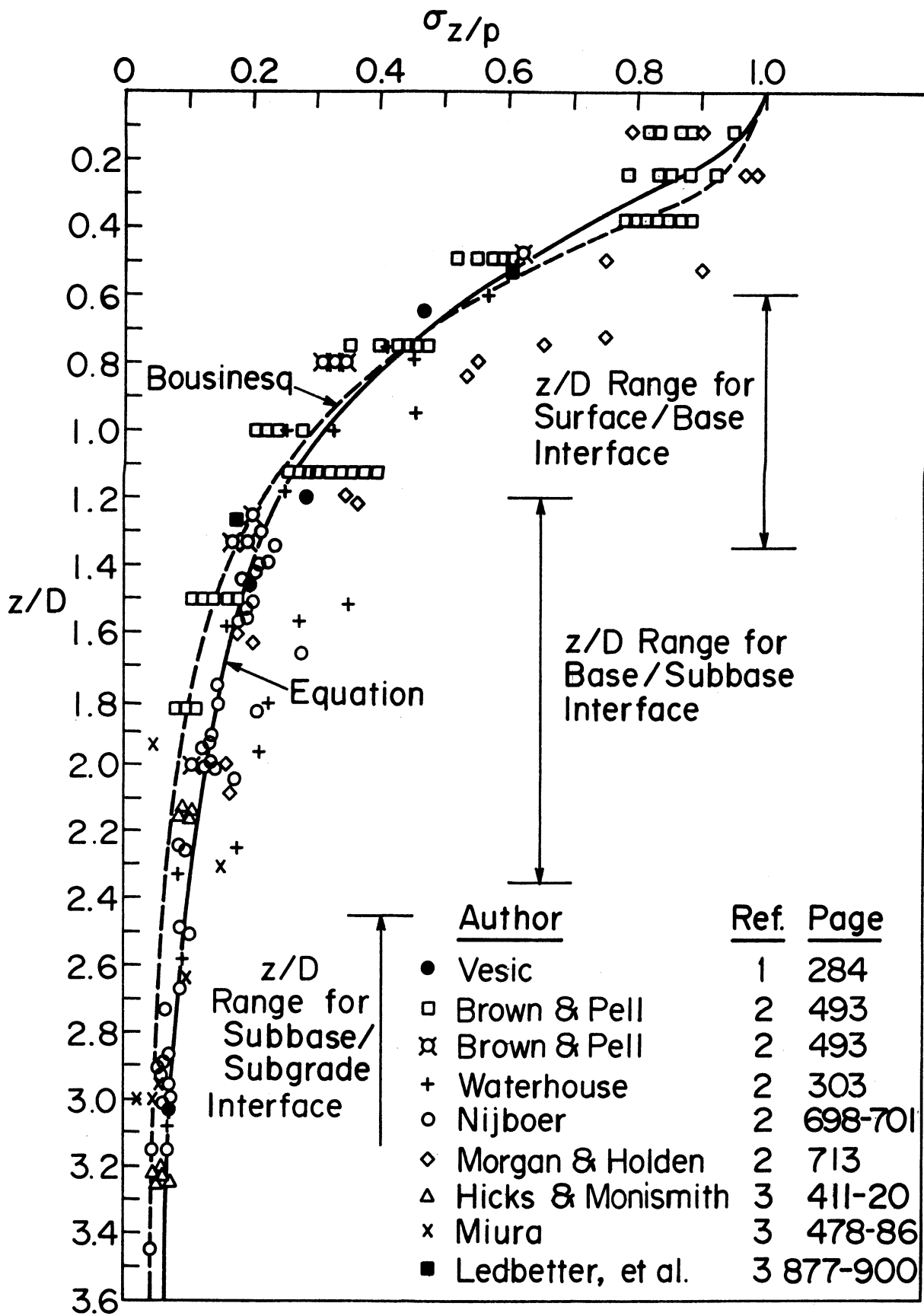


Figure 9. Vertical stresses under a uniform loaded flexible circular plate.

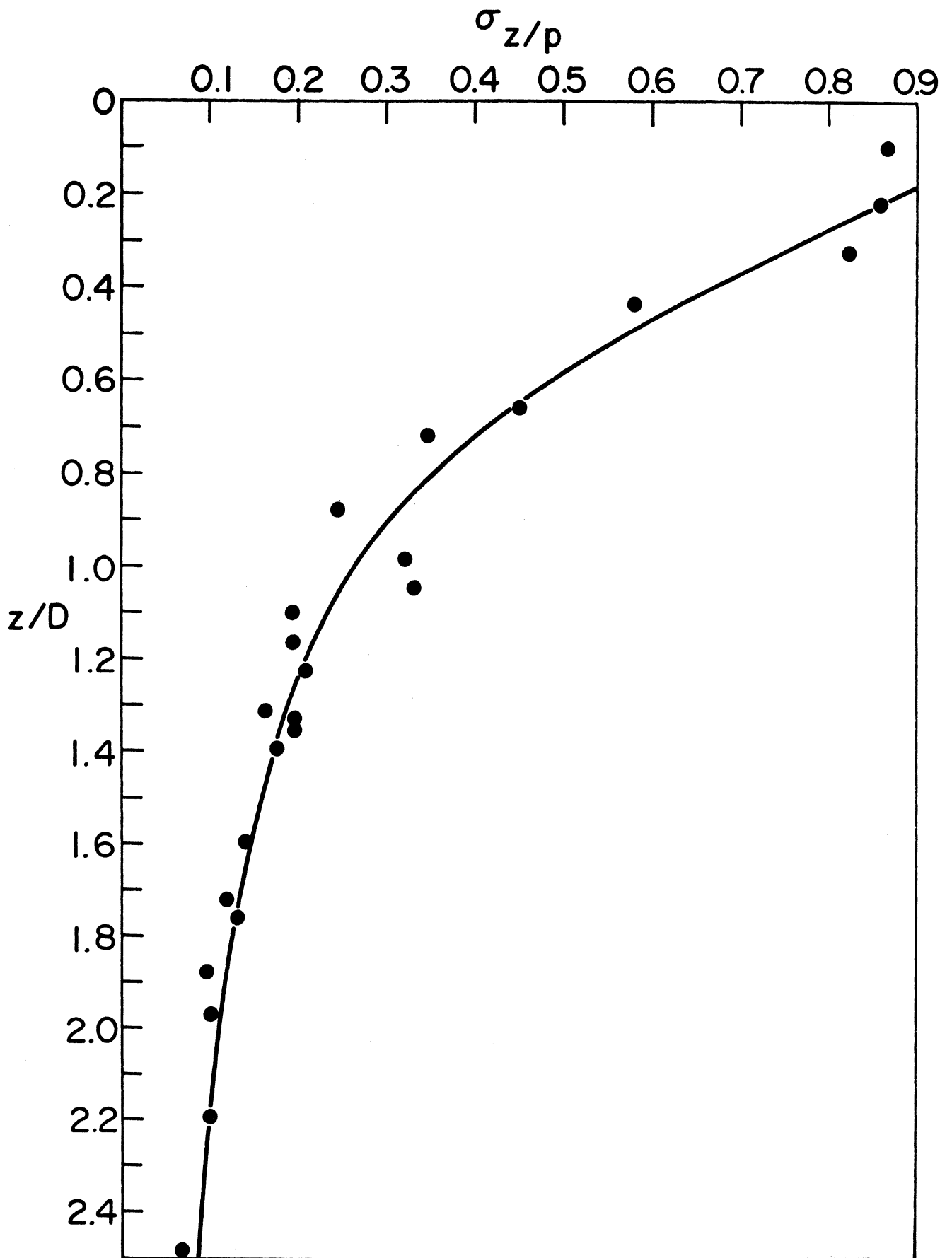


Figure 10. Average vertical stresses under a uniformly loaded circular plate.

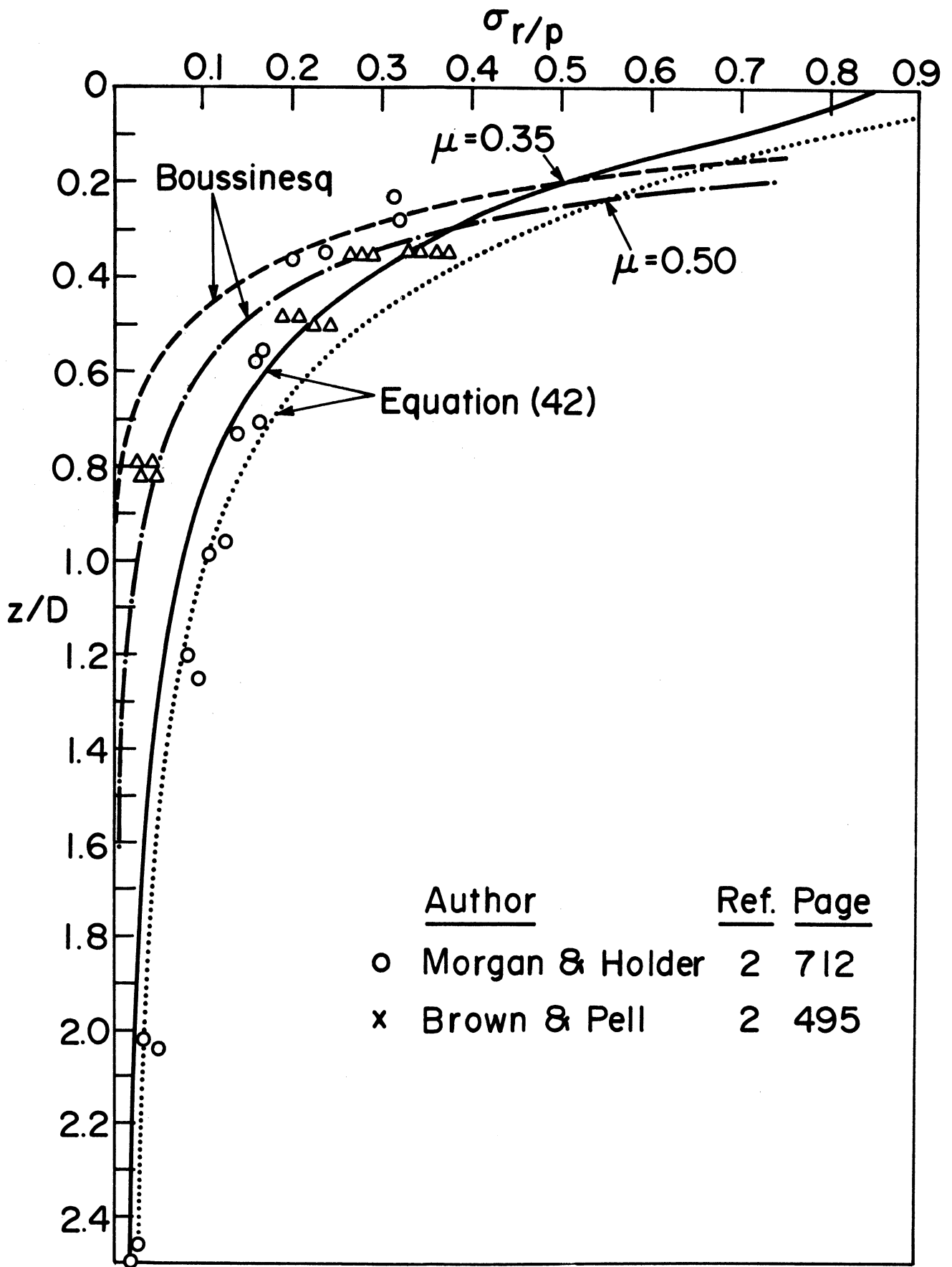


Figure 11. Radial stresses under a uniformly loaded circular plate.

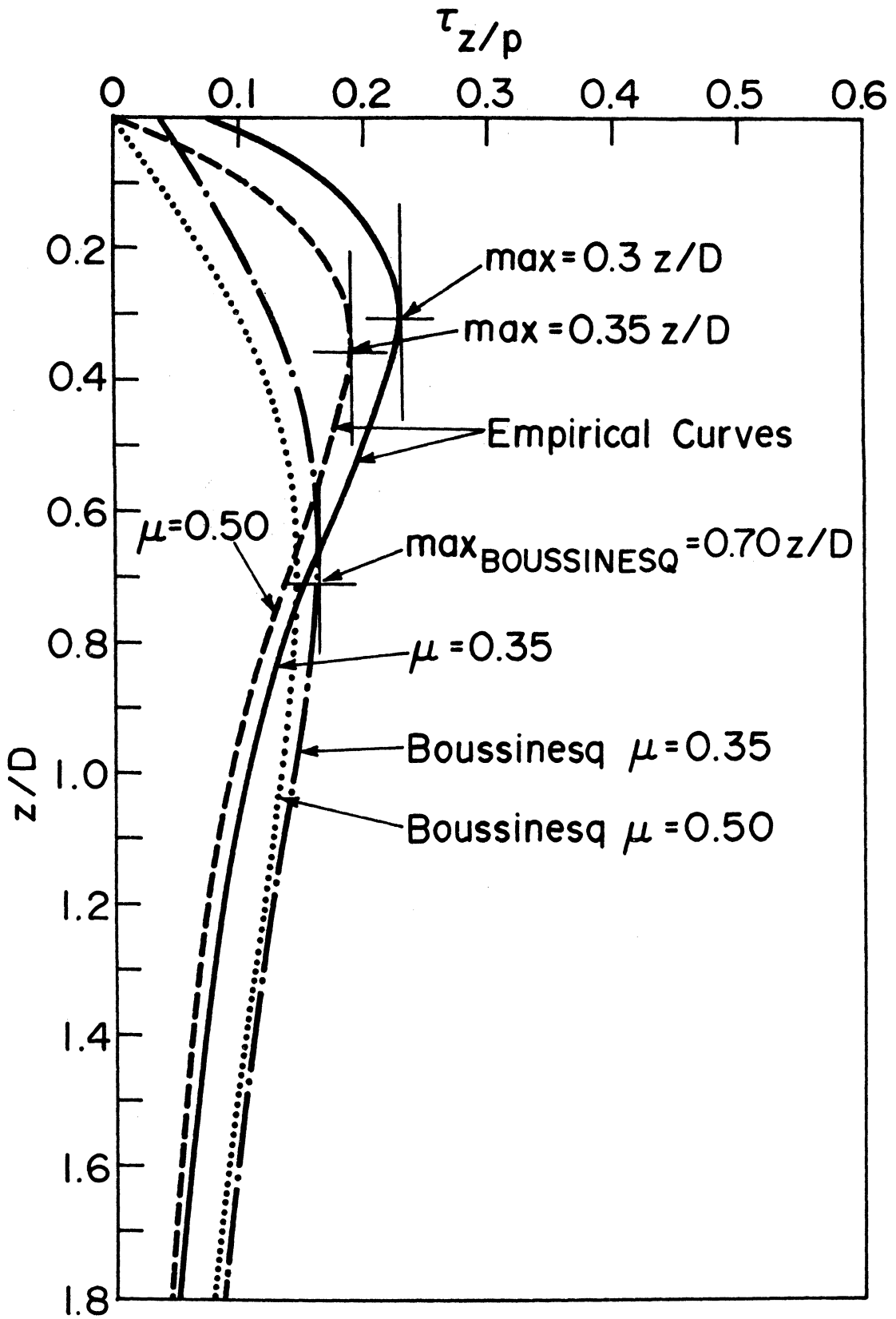


Figure 12. Shear stresses under a uniformly loaded circular plate.

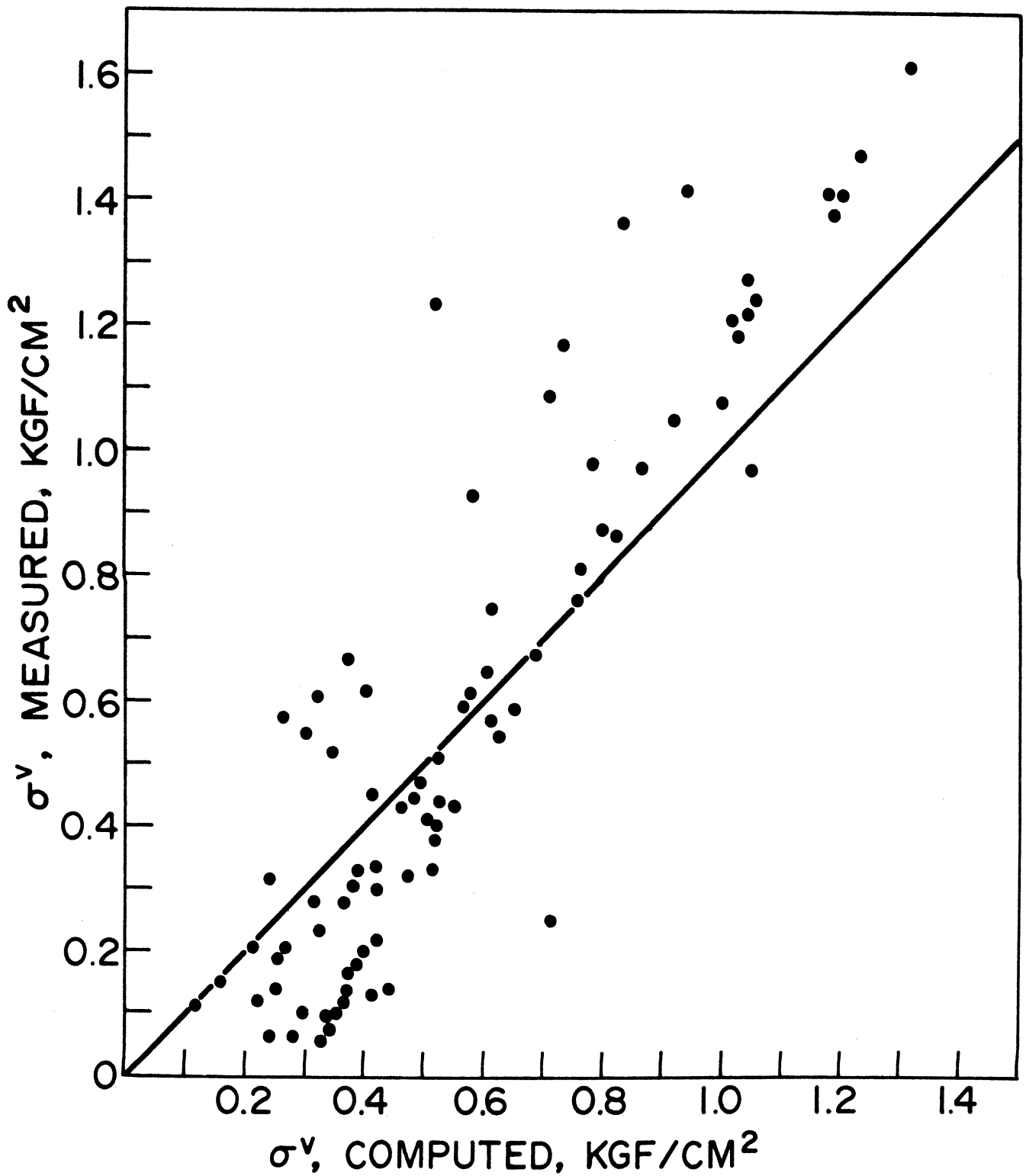


Figure 13. Comparison between measured and calculated vertical compressive stresses under the center of the loaded area.

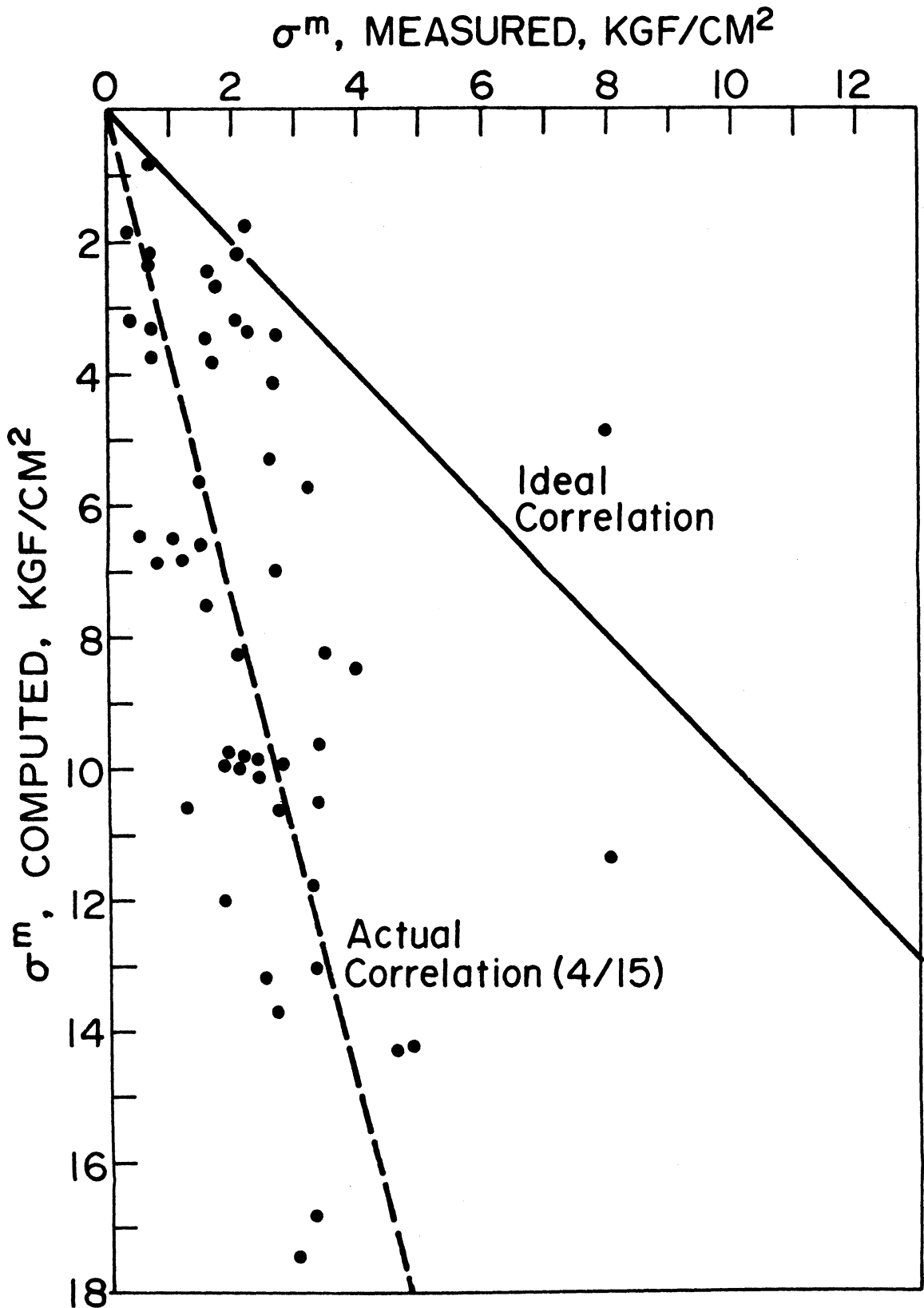


Figure 14. Comparison between measured and computed tensile stresses at the bottom of the layers under the center of the loaded area.

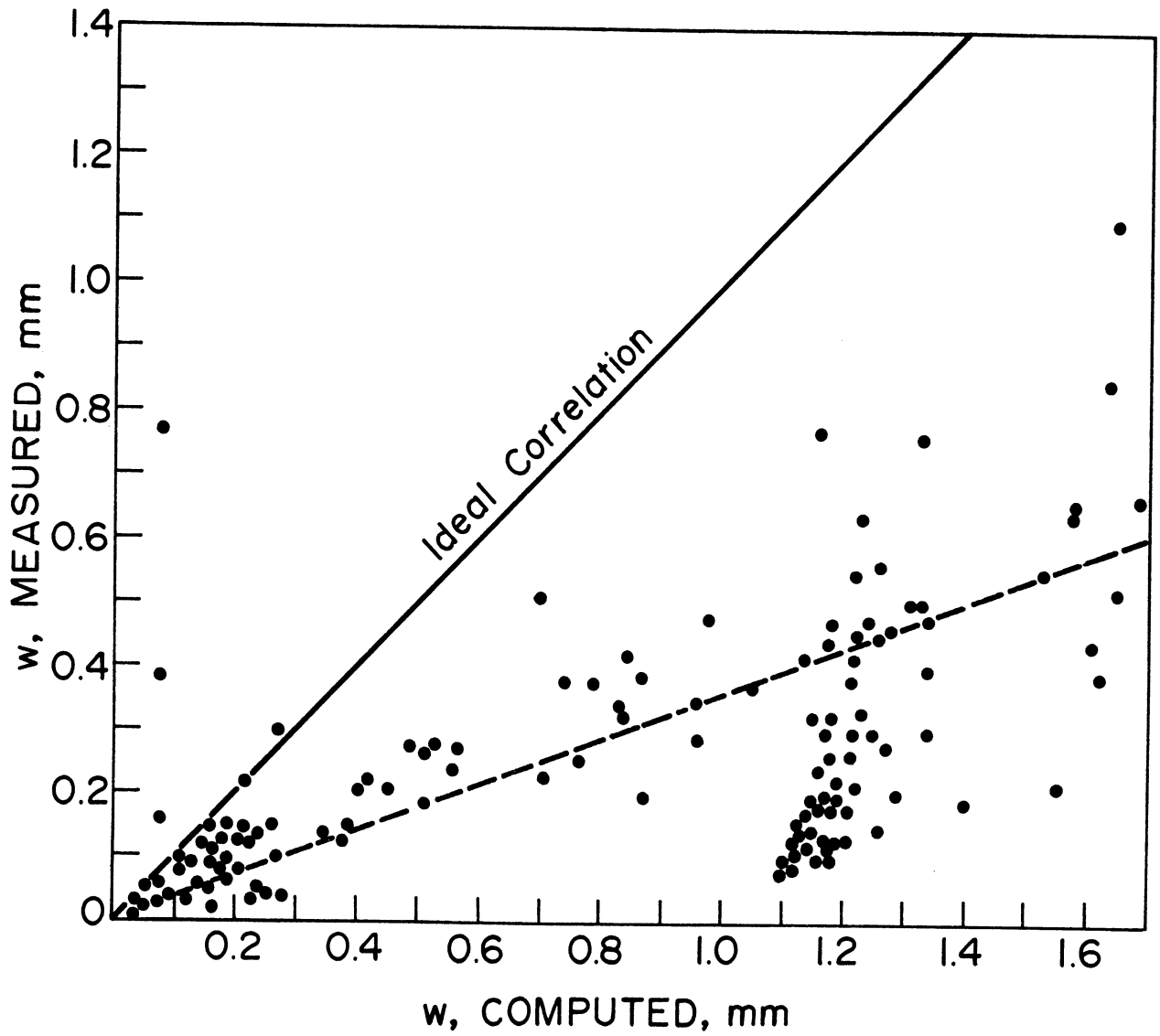


Figure 15. Comparison between measured and computed deflections at the surface of the pavement under the center of the loaded area.

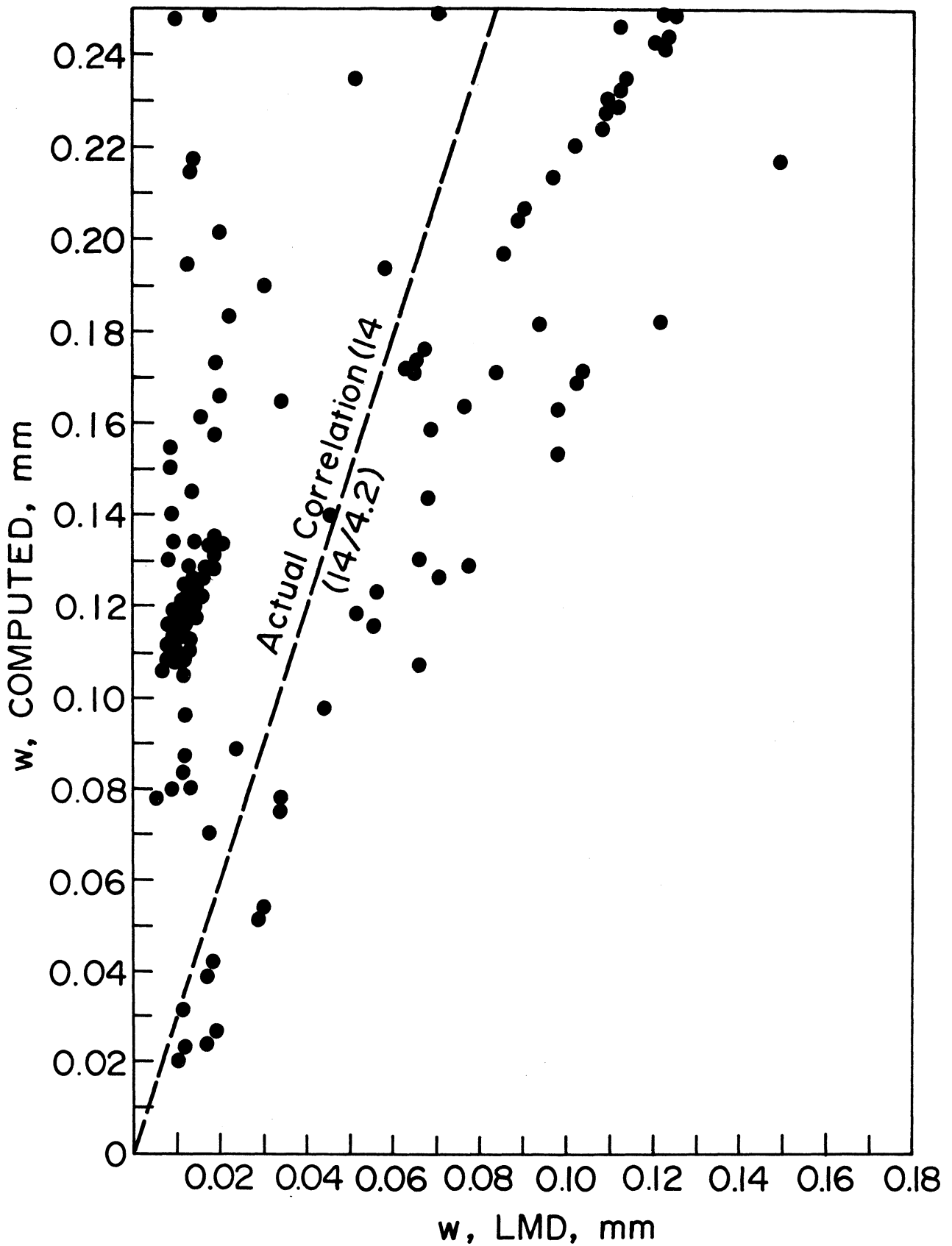


Figure 16. Comparison between deflections calculated without taking into account the energy necessary to change the form of the layers (w , computed) and those which take it into account (w , LMD).

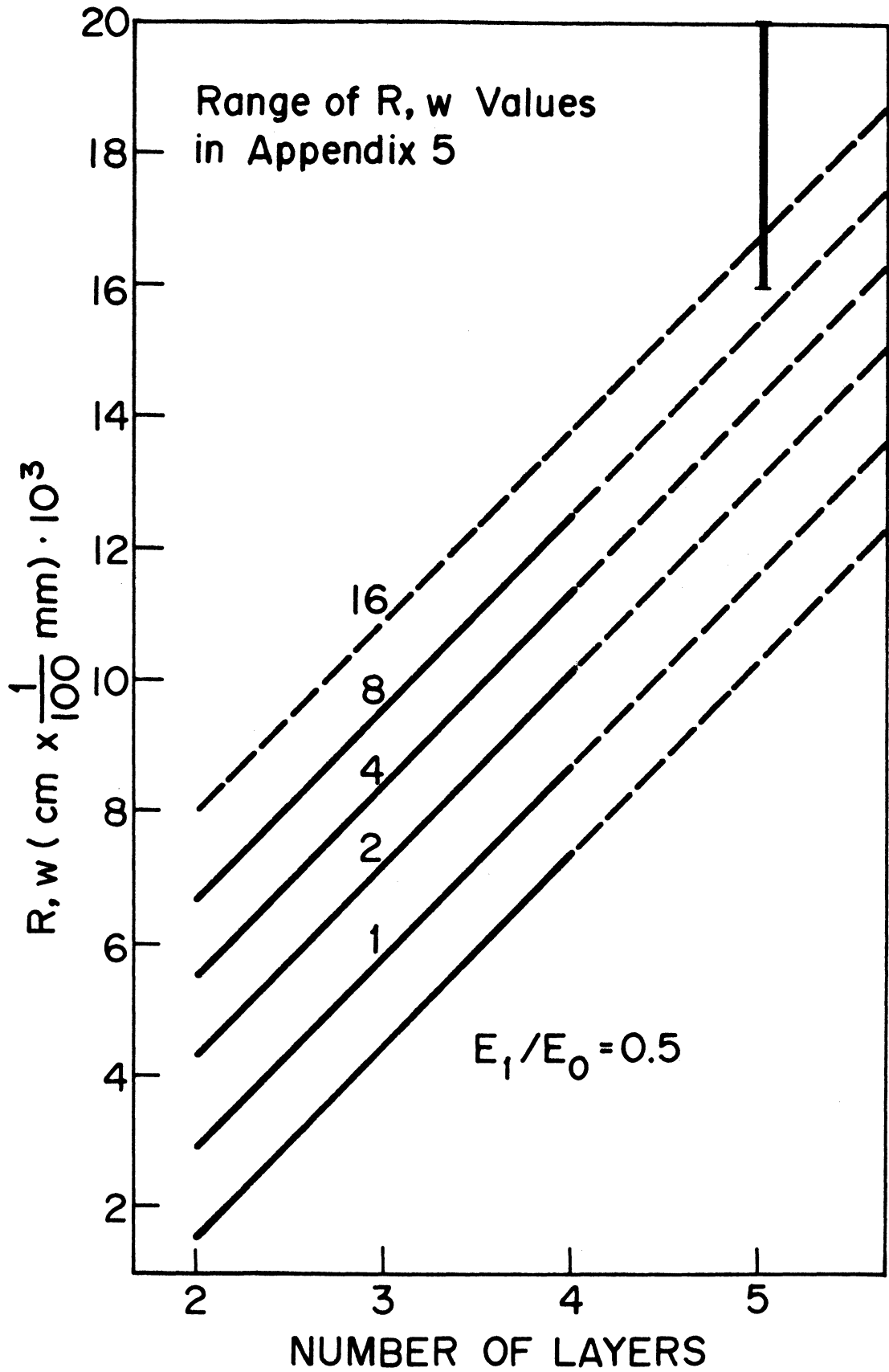


Figure 17. R·w values for various structures of asphalt pavements.

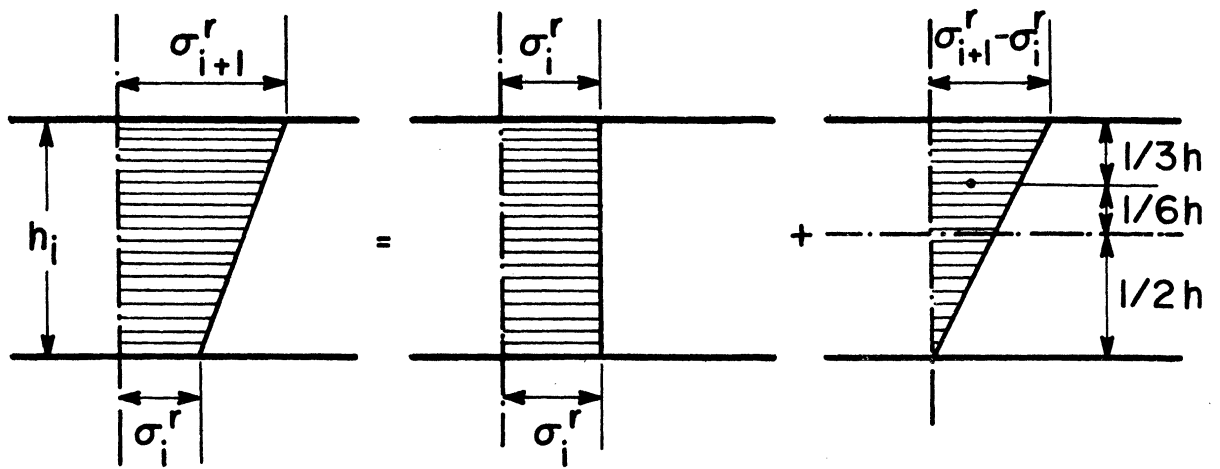


Figure 18. Bending moment due to the radial stresses.

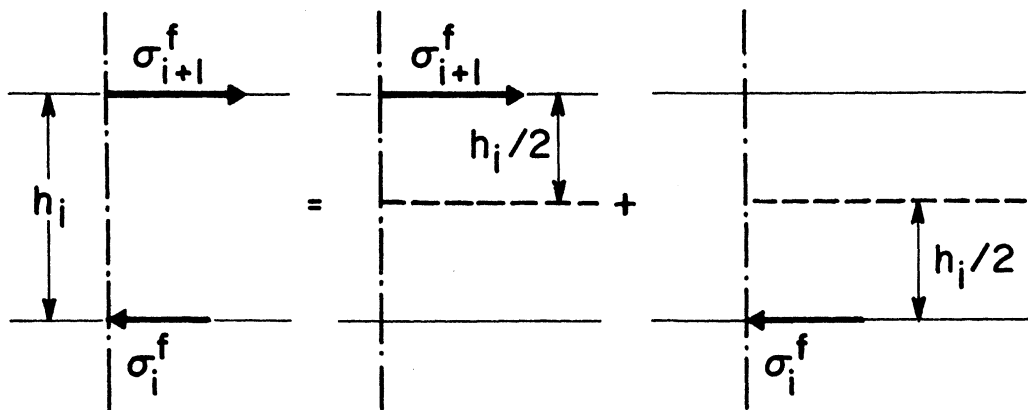


Figure 19. Bending moment due to the friction stress.

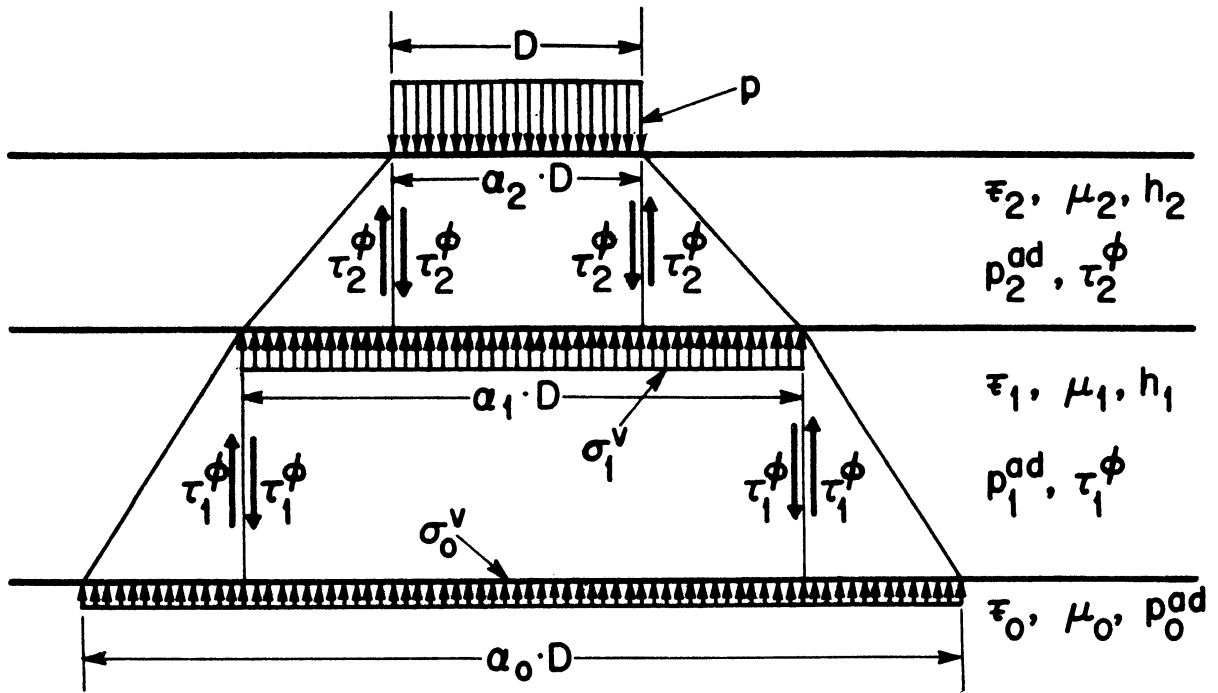


Figure 20. Shear stresses along the contour of the loaded area, at different levels.

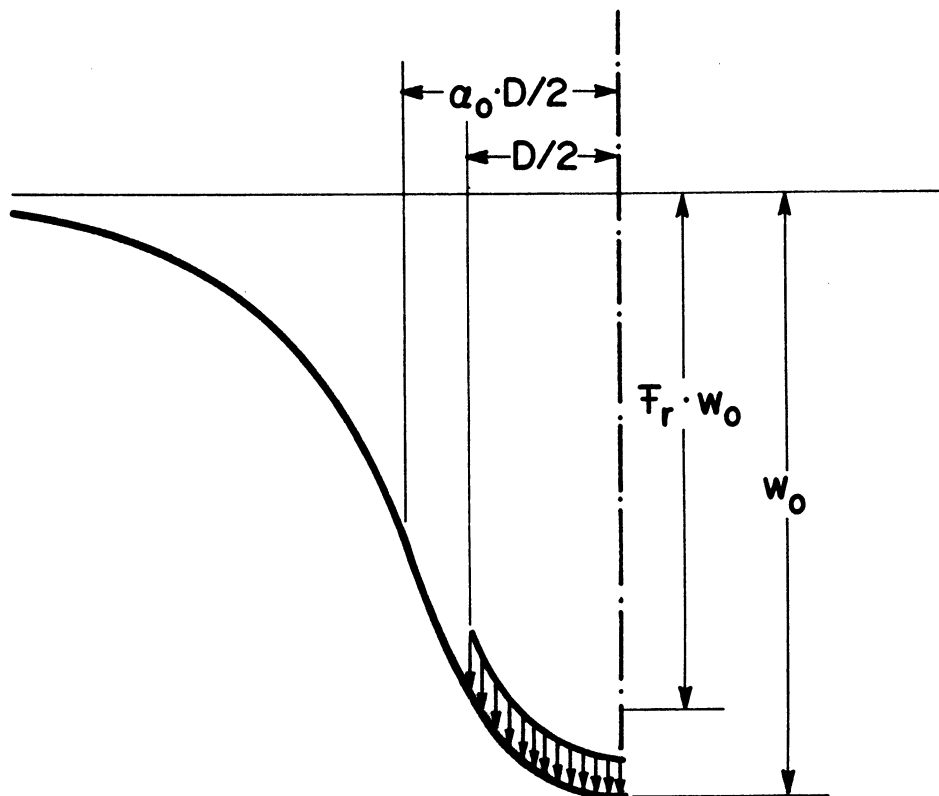


Figure 21. Average deflection under load.

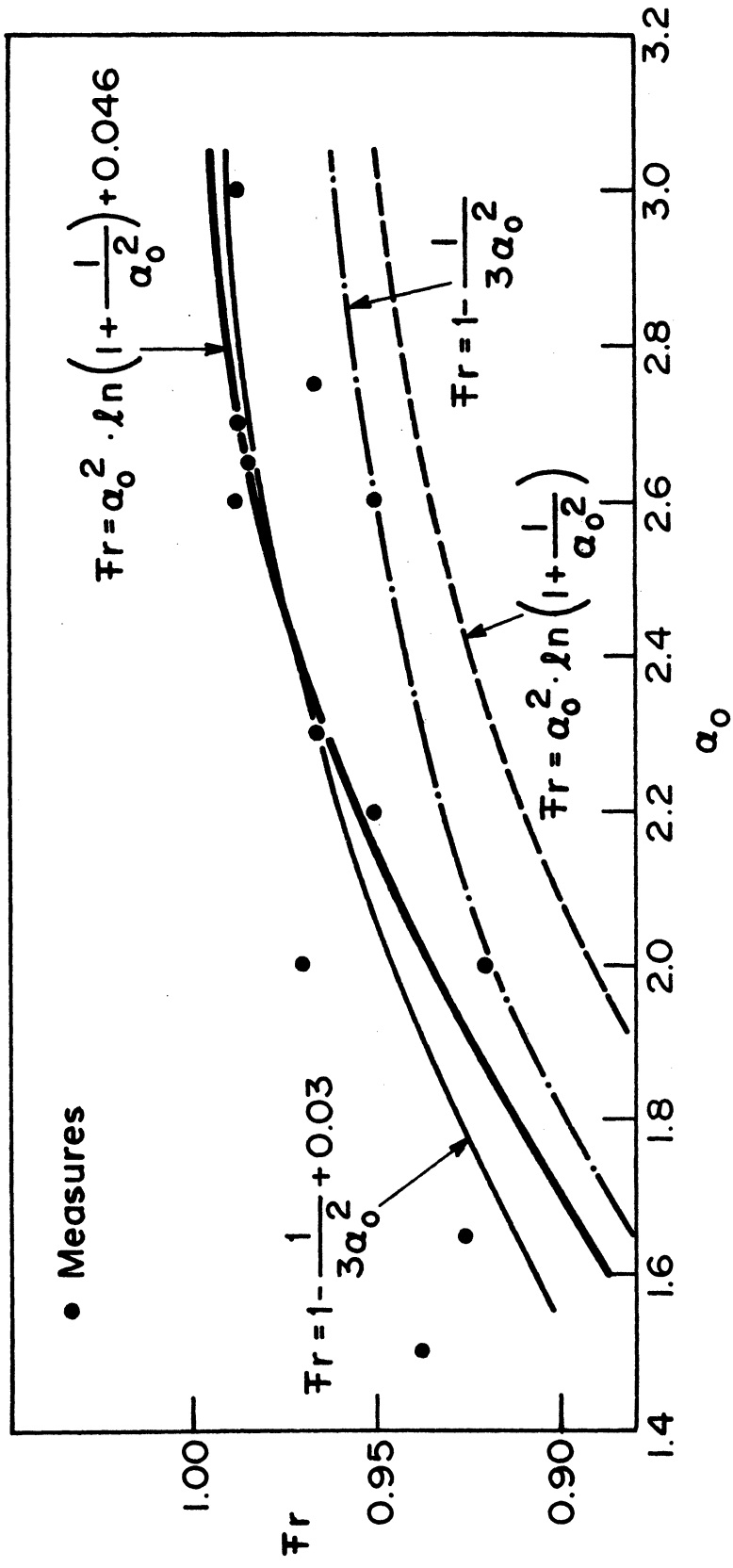


Figure 22. Computed versus measured values for the factor Fr.

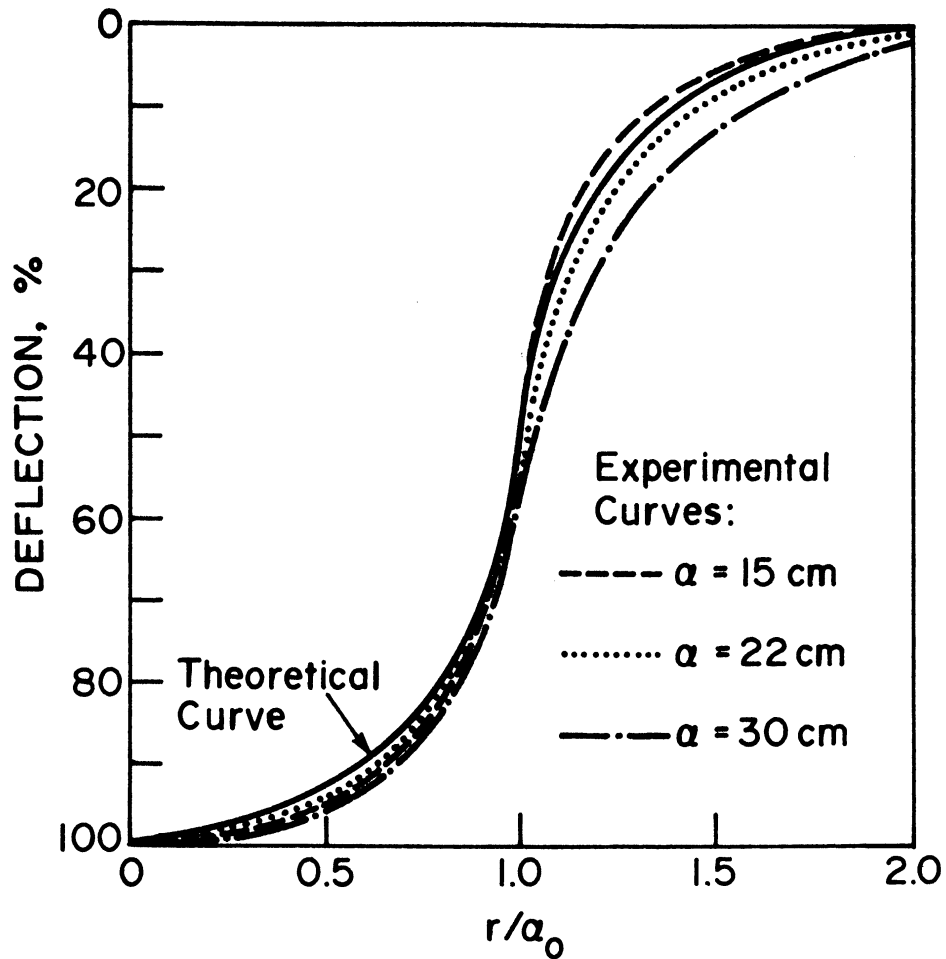


Figure 23. Theoretical versus actual deflection profile.

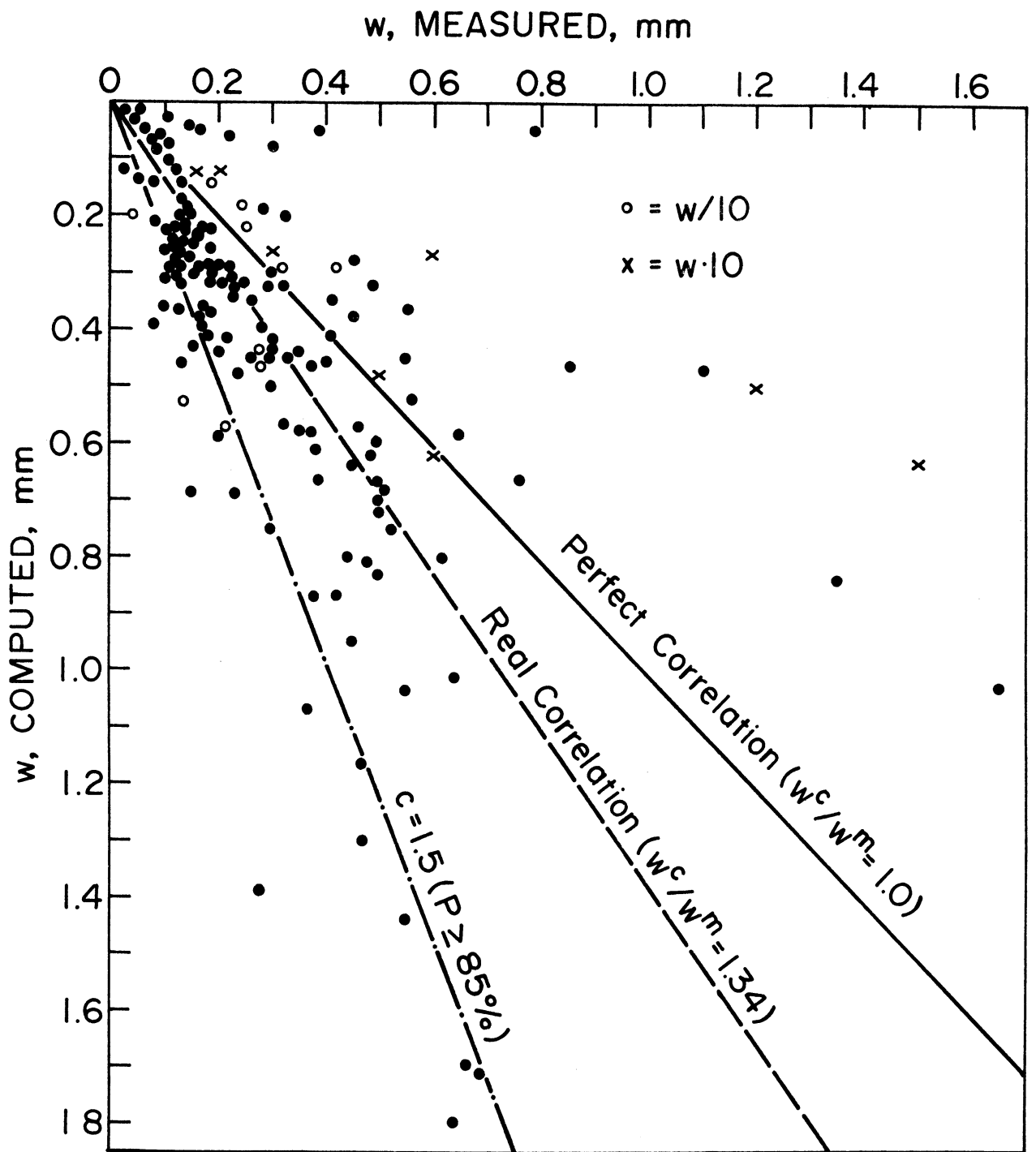


Figure 24. Computed versus measured deflections.

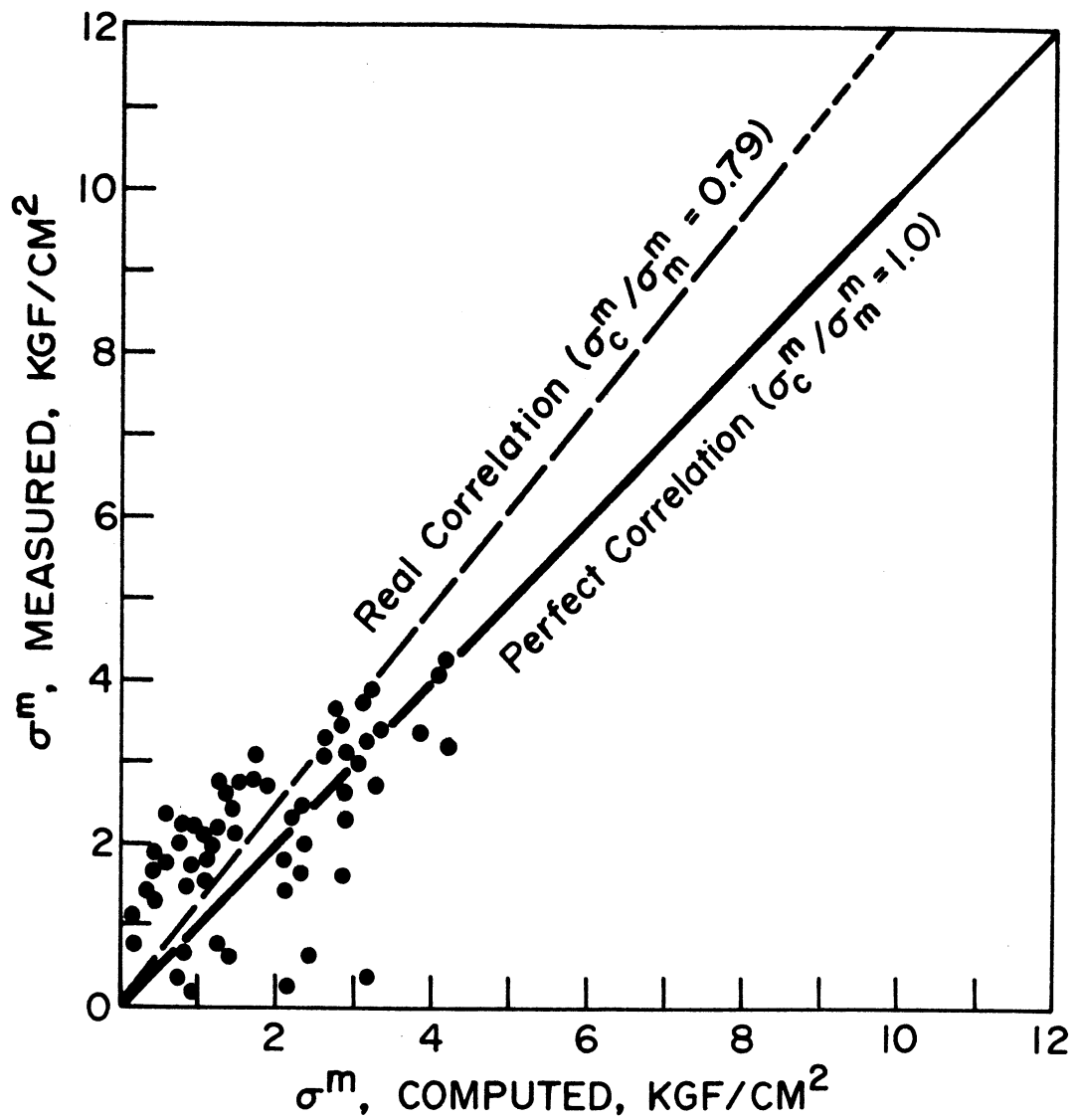


Figure 25. Computed versus measured tensile stresses at the bottom of the layers.

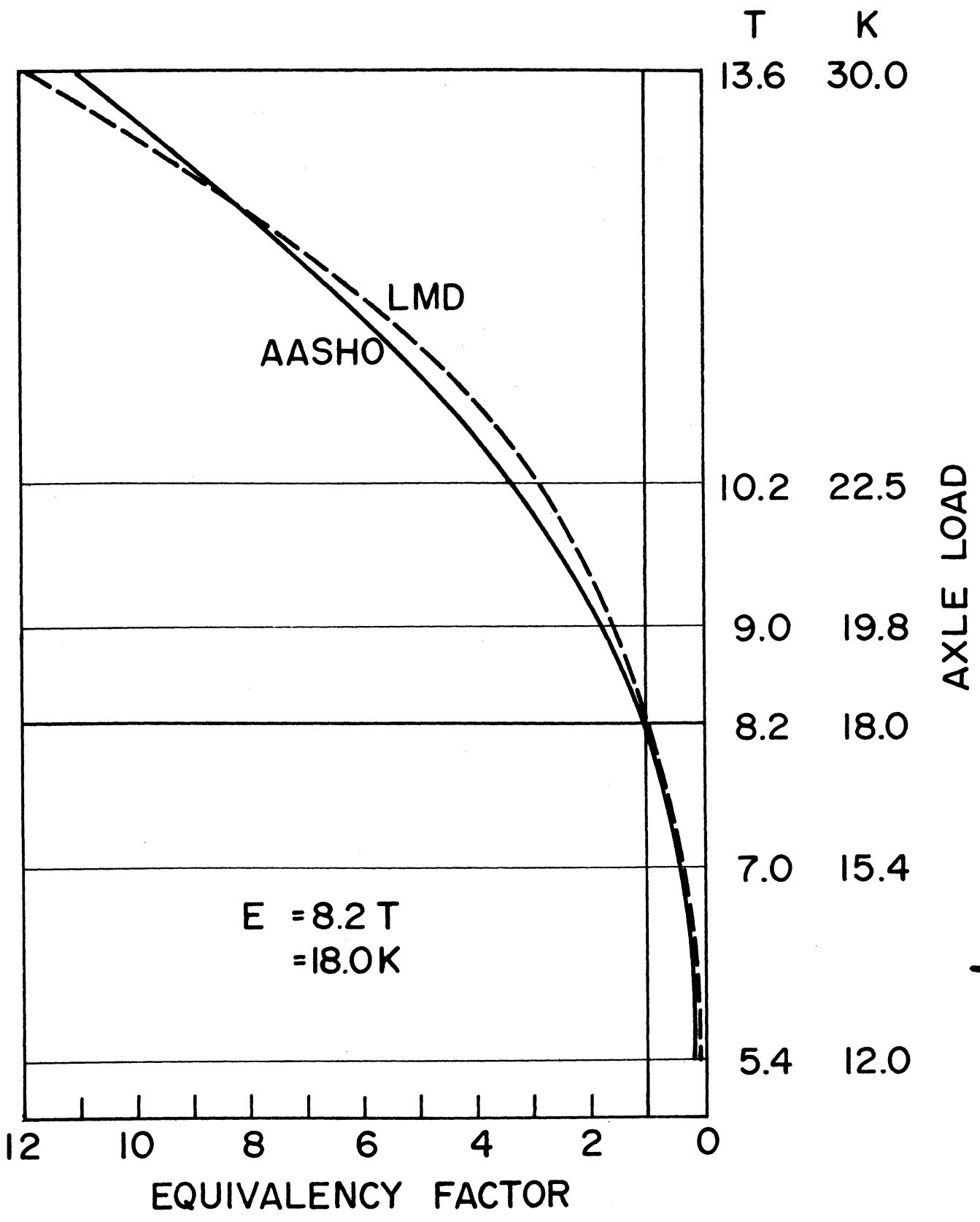


Figure 26. Theoretical versus AASHO road test results for the wheel equivalency factor, for EWL = 8.1 metric tons (18,000 pounds) standard axle.

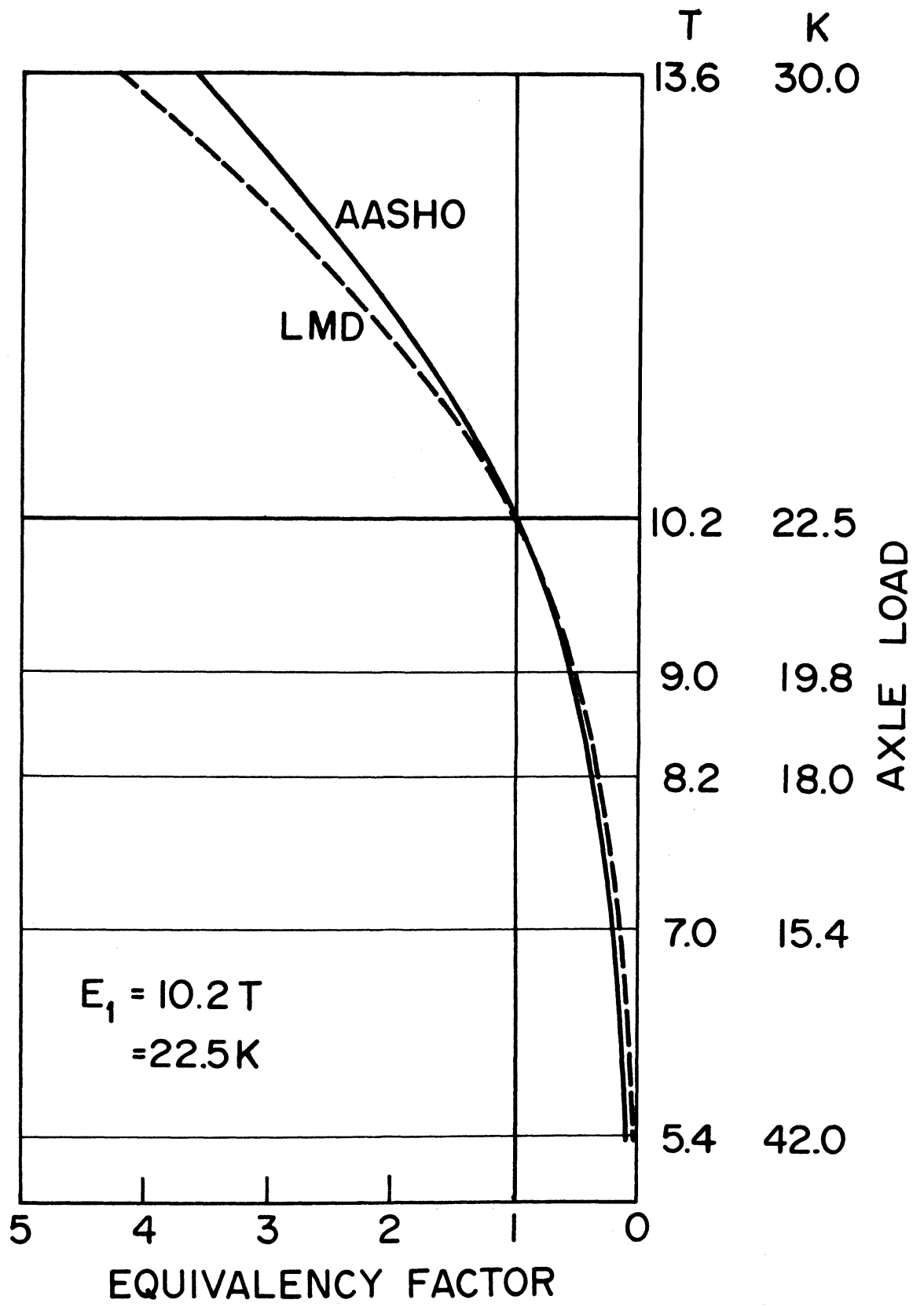


Figure 27. Theoretical versus AASHO road test results for 10.4 metric tons (22,000 pounds) standard axle.

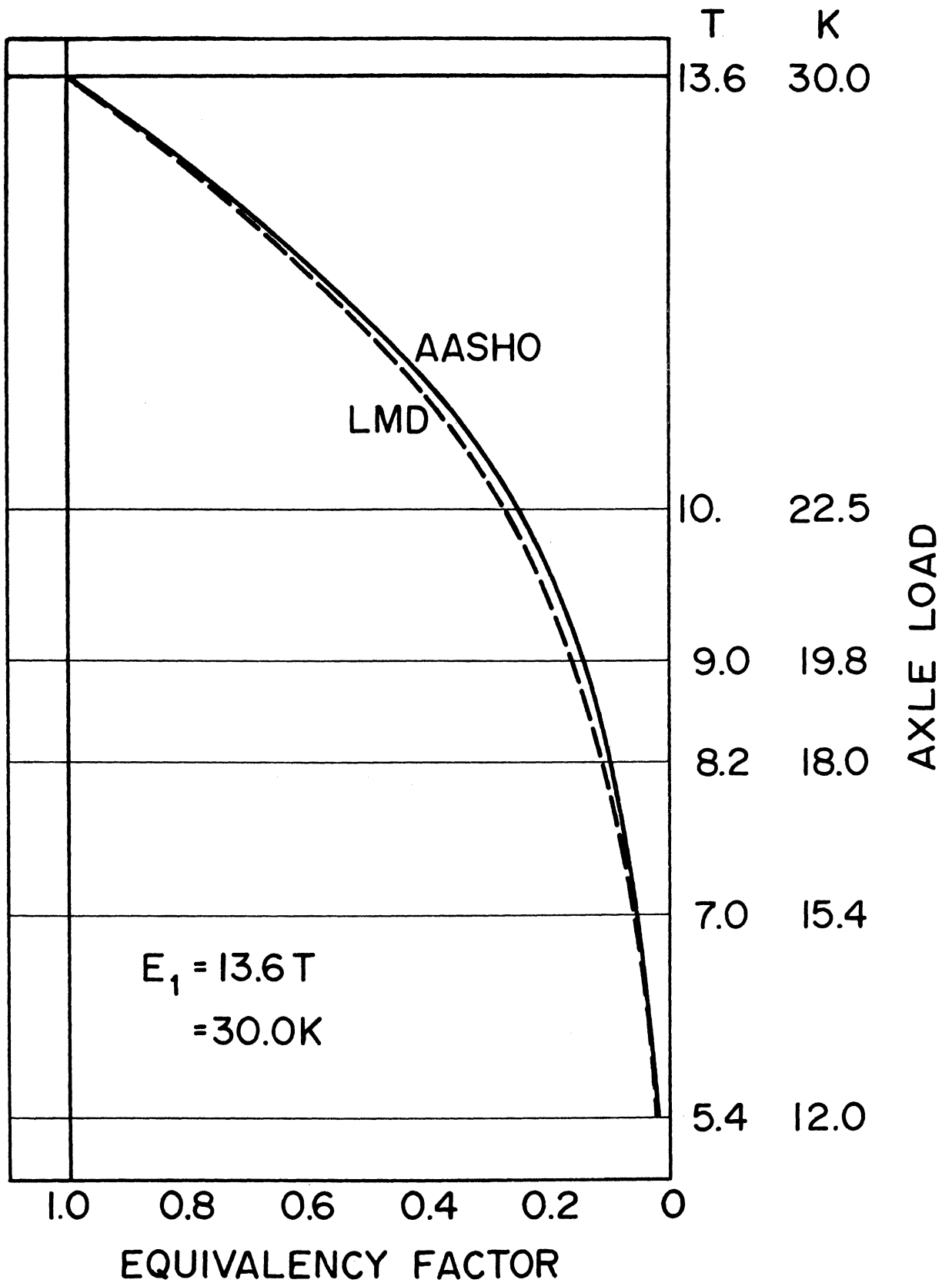


Figure 28. Theoretical versus AASHO road test results for 13.6 metric tons (30,000 pounds) standard axle.

List of Tables

Table

1. External conditions to define Leger's equation.
2. $R \cdot w_0$ values.
3. Stresses at the interfaces of the layers.
4. Design parameters for some materials.

Table 1

External Conditions to
Define Léger's Equation

| Condition | | |
|-----------|------------------------------|-----------------|
| m | r | w |
| 1 | 0 | w_0 |
| 2 | $\frac{\alpha_0 \cdot D}{2}$ | $\frac{w_0}{2}$ |
| 3 | ∞ | 0 |

Table 2

R · w₀ Values

| E ₁ /E ₀ | Type of the Pavement | | | | Average | After Grant and Walker |
|--------------------------------|----------------------|---------------|--------------|--|---------|------------------------|
| | Two-layered | Three-layered | Four-layered | | | |
| 0.5 | 1,540 | 4,330 | 7,500 | | 4,450 | 3,670 |
| 1 | 3,250 | 5,370 | 9,100 | | 5,900 | 5,200 |
| 2 | 4,560 | 6,280 | 10,100 | | 7,000 | 7,350 |
| 4 | 6,100 | 7,600 | 11,100 | | 8,300 | 10,400 |
| 8 | 7,300 | 9,600 | 11,400 | | 9,500 | 14,700 |
| Average | ~4,550 | ~6,650 | ~9,650 | | ~7,000 | ~8,450 |

Table 3

Stresses at the Interfaces of the Layers

$\mu = 0.35; f_i = 0.5$

| Z/D | σ_v | σ_r | τ_{zr} | $\sigma_r + \tau_{zr}$ | $\sigma_r f_i$ |
|-----|------------|------------|-------------|------------------------|----------------|
| 0.0 | 1.000 | 0.850 | 0.075 | 0.925 | 0.500 |
| 1.0 | 0.271 | 0.063 | 0.106 | 0.169 | 0.136 |
| 1.7 | 0.133 | 0.027 | 0.055 | 0.082 | 0.066 |
| 2.6 | 0.079 | 0.016 | 0.035 | 0.051 | 0.040 |

TABLE 4
DESIGN PARAMETERS FOR SOME MATERIALS

| Material | Temperature | | Young's Modulus | | | μ | ϕ Degrees | $r^{\alpha\phi}$ | | C_i^{fr} | Observations |
|-----------------------------------|---|-------------|---------------------|--------|----------------------------------|-------|-------------------|---------------------|--------|------------|---|
| | $^{\circ}C$ | $^{\circ}F$ | kgf/cm ² | p.s.i. | Coefficient of Variation % | | | kgf/cm ² | p.s.i. | | |
| Loess | - | - | 300 | 4200 | 26.5 | 0.4 | 20 | - | - | 1.5 | Loess = 40% porosity. All materials at the optimum moisture content and 100% standard AASHO compaction. |
| Clay | - | - | 240 | 3300 | 40.5 | 0.4 | 20 | - | - | 0.8 | |
| Silt | - | - | 320 | 4400 | 28.5 | 0.4 | 20 | - | - | 0.65 | |
| Silty Clay | - | - | 230 | 3200 | 38.0 | 0.4 | 20 | - | - | 0.7 | |
| Sandy Clay | - | - | 410 | 5700 | 48.5 | 0.4 | 21 | - | - | 0.8 | |
| Clayey Sand | - | - | 340 | 4700 | 42.5 | 0.35 | 20 | - | - | 0.9 | |
| Silty Sand | - | - | 360 | 5000 | 41.0 | 0.35 | 20 | - | - | 0.8 | |
| Fine Sand | - | - | 740 | 10200 | 42.1 | 0.30 | 22 | - | - | 1.0 | |
| Medium Sand | - | - | 830 | 11400 | 34.4 | 0.30 | 24 | - | - | 1.0 | |
| Coarse Sand | - | - | 930 | 12800 | 26.9 | 0.30 | 25 | - | - | 1.0 | |
| Clayey Gravel | - | - | 1450 | 20000 | 28.8 | 0.30 | 26 | - | - | 0.8 | |
| Sandy Gravel | - | - | 1340 | 18500 | 19.8 | 0.30 | 32 | - | - | 1.0 | |
| Common Gravel | - | - | 2200 | 30500 | 12.1 | 0.30 | 30 | - | - | 1.2 | |
| Well Graded Gravel | - | - | 3650 | 50000 | 34.8 | 0.30 | 52 | - | - | 1.45 | |
| Crushed Stone | Soft and Medium Rocks | - | 2040 | 28200 | 33.1 | 0.25 | 28 | - | - | 0.75 | |
| | Tough Rocks | - | 4950 | 68500 | 20.0 | 0.25 | 36 | - | - | 0.75 | |
| Macadam | Medium Rocks | - | 4000 | 55300 | - | 0.25 | 40 | 4.65 | 64.0 | 0.75 | |
| | Tough Rocks | - | 4680 | 64800 | 11.1 | 0.25 | 35 | - | - | 0.75 | |
| Bituminous Concrete | 0 | 32 | 66000 | 915000 | 33.3 | 0.35 | 84 | - | - | 0.50 | |
| | 15 | 59 | 32000 | 445000 | 2.6 | 0.45 | 61 | 7.40 | 102.0 | 0.50 | |
| | 30 | 86 | 10900 | 150000 | 2.6 | 0.49 | 45 | - | - | 0.50 | |
| | 40 | 104 | 7450 | 103000 | 25.5 | 0.50 | 40 | - | - | 0.50 | |
| Coarse Graded Bituminous Concrete | 0 | 32 | 15000 | 207000 | - | 0.35 | 49 | - | - | 0.50 | |
| | 20 | 68 | 9250 | 128000 | 16.4 | 0.48 | 42 | - | - | 0.50 | |
| | 40 | 104 | 5000 | 69000 | - | 0.50 | 36 | - | - | 0.50 | |
| Sand Asphalt | 0 | 32 | 19000 | 263000 | - | 0.35 | 53 | - | - | 0.80 | |
| | 20 | 68 | 10600 | 146000 | 4.3 | 0.48 | 45 | - | - | 0.80 | |
| | 40 | 104 | 8000 | 110000 | 6.7 | 0.50 | 41 | - | - | 0.80 | |
| Bituminous Binder | 0 | 32 | 15000 | 207000 | - | 0.35 | 49 | - | - | 0.60 | |
| | 20 | 68 | 5200 | 72000 | - | 0.48 | 36 | - | - | 0.60 | |
| | 40 | 104 | 4150 | 57000 | - | 0.50 | 34 | - | - | 0.60 | |
| Mastic Bituminous Concrete | 10 | 50 | 20800 | 288000 | 28.5 | 0.42 | 55 | - | - | 0.85 | |
| Bituminous Penetrated Macadam | 20 | 68 | 7250 | 100000 | 31.0 | 0.48 | 40 | - | - | 0.75 | |
| Bitumen Stabilized Gravel | 20 | 68 | 8920 | 124000 | 35.0 | 0.48 | 44 | - | - | 0.85 | |
| Bitumen Stabilized Sand | 20 | 68 | 1200 | 16600 | 42.3 | 0.48 | 25 | - | - | 0.65 | |
| Cement Stabilized Gravel | - | - | 12500 | 172000 | - | 0.16 | 47 | - | - | 0.65 | |
| Cement Stabilized Sand | - | - | 5000 | 69000 | - | 0.20 | 36 | - | - | 0.55 | |
| Pavements with | Rectangular ⁽¹⁾ Stone Blocks | - | 4780 | 66000 | 30.0 | 0.25 | - | - | - | 0.55 | |
| | Irregular Stones ⁽²⁾ | - | 3350 | 46500 | 31.8 | 0.25 | - | - | - | 0.55 | |
| | Cobblestones ⁽³⁾ | - | 3200 | 44300 | 33.2 | 0.25 | - | - | - | 0.55 | |

¹⁾Cubes 15 x 15 x 15 cm³ (6 x 6 x 6 in.³); ²⁾Stones obtained by crushing large blocks in quarries. Irregular blocks with average dimensions between 12 and 20 cm (5 to 8 in.); ³⁾Cobblestones size range 6 to 10 in.

List of Appendices

Appendix

1. Computer program for the values of coefficients a , and b_1 (in equation 31) determination.
2. Computer program for the computation of the radial stresses under a uniform loaded circular plate.
3. Computer program for the computation of the shear stresses under a uniform loaded circular plate (multilayered systems).
4. Computer program for the computation of the shear stresses in homogeneous mass under a uniform loaded circular plate.
5. Computer program for equations in (75) through (88) checking.
6. Computer program for equation in (178) checking.

```

0001      WRITE(6,10)
0002 10 FORMAT('1','ODEMARK')
0003      B = 0.94
0004      A = 0.84
0005      EXPR = 0.0
0006      C = (A**2)*(EXPR**2)
0007      T = 1.0-B*C/(0.25+C)
0008      WRITE(6,1) A,B,EXPR,T
0009 1 FORMAT('1','A=',F5.2,5X,'B=',F5.2,
15X,'EXPR=',F5.3,5X,'T=',F5.3)
0010      EXPR = EXPR+0.2
0011      IF(EXPR.GT.3.6)GO TO 2
0012      GO TO 3
0013      A = A+0.01
0014      IF(A.GT.0.94) GO TO 4
0015      GO TO 5
0016      B = B+0.01
0017      IF(B.GT.1.00) GO TO 6
0018      GO TO 7
0019      WRITE(6,11)
0020 11 FORMAT('1','BUSSINESQ')
0021      D = 0.96
0022      A = 0.88
0023      EXPR = 0.0
0024      B = (D*EXPR)**2
0025      C = (A**3)*(EXPR**3)
0026      CC = (A**2)*(EXPR**2)
0027      T = 1.0-B*C/(0.25+CC)**3/2
0028      WRITE(6,21) A,B,EXPR,T
0029 21 FORMAT('1','A=',F5.2,5X,'B=',F5.2,
15X,'EXPR=',F5.3,5X,'T=',F5.3)
0030      EXPR = EXPR+0.2
0031      IF(EXPR.GT.3.0) GO TO 12
0032      GO TO 13
0033      A = A+0.010
0034      IF(A.GT.0.92) GO TO 14
0035      GO TO 15
0036      D = D+0.01
0037      IF(D.GT.0.92) GO TO 16
0038      GO TO 17
0039      16 STOP
0040      END

```

APPENDIX 2

```

0001 COE1A = 0.89
0002 COE2P = 0.96
0003 AMTU = 0.25
0004 PAR1 = 1.0+2.0*AMTU
0005 PAR2 = 2.0*(1.0+AMTU)
0006 EXPR = 0.0
0007 ALFA = COE1A*EXPR
0008 ALFPA = ALFA**2
0009 COE1A = COE1A***(1.0/2.0)*ALFA/(0.25+ALFPA)**(1.0/2.0)
0010 COE1A = BETA**2
0011 S = (1.0/2.0)*(0.01-PAR2**3BETA+GAMA)
0012 WRITE(5,1) AMTU,EXPR,S
0013 I EFORMAT('1.1M') = ,F7.4,5X,'H/D=',F7.4,5X,'S=',F7.4)
0014 EXPR = EXPR+0.1
0015 IF (EXPR.GT.3.6) GO TO 2
0016 GO TO 3
0017 2 AMTU = AMTU+0.15
0018 IF (AMTU.GT.0.50) GO TO 4
0019 GO TO 5
0020 4 STOP
0021 END
*OPTIONS IN EFFECT* ID,ERRDIG,SOURCE,NOLIST,NORECK,LOAD,NOMAP
*OPTIONS IN EFFECT* NAME = RADJAI , LINECNT = 57
*STATISTICS* SOURCE STATEMENTS = 21, PROGRAM SIZE = 766
*STATISTICS* AND DIAGNOSTICS GENERATED
NO ERRORS IN RADJAI
NO STATEMENTS FLAGGED IN THE ABOVE COMPILE STATEMENT.

```

MICHIGAN TERMINAL SYSTEM FURTRAN G(41336)

```

0001 COF1A = 0.88
0002 COF23 = 0.96
0003 AMIU = 0.35
0004 5 PAR1 = 1.0-2.0*AMIU
0005 PAR2 = 2.0*(1.0+AMIU)
0006 EXPR = 0.0
0007 3 ALFA = COF1A*EXPR
0008 ALFPAT = ALFA**2
0009 BETA = (COF28**{(1.0/2.0)}*ALFA/(0.25+ALFPAT)**{(1.0/2.0)}
0010 GAMA = BETA**2
0011 TAU = (1.0/4.0)*(PAR1+PAK2*BETA-3.0*GAMA)
0012 WRITE(6,1) AMIU,EXPR,TAU
0013 1 FORMAT(' ',MIU=,F7.4,5X,'H/D=,F7.4,5X,'TAU=,F7.4)
0014 EXPR = EXPR+0.05
0015 IF(EXPR.GT.2.5) GO TO 2
0016 GO TO 3
0017 2 AMIU = AMIU+0.15
0018 IF(AMIU.GT.0.50) GO TO 4
0019 GO TO 5
0020 4 STOP
0021 END
*OPTIONS IN EFFECT* ID,EBCDIC,SOURCE,NOLIST,NODECK,LOAD,NOMAP
*OPTIONS IN EFFECT* NAME = TANGEN , LINECNT = 57
*STATISTICS* SOURCE STATEMENTS = 21,PROGRAM SIZE = 782
*STATISTICS* NO DIAGNOSTICS GENERATED
NO ERRORS IN TANGEN

```

NO STATEMENTS FLAGGED IN THE ABOVE COMPILATIONS.

MICHIGAN TERMINAL SYSTEM FORTRAN S(41536)

BUSTAN

02-15-73

08:18.35

PAGE 001

```

0001      AMIU = 0.35
0002      WRITE(6,1) AMIU
0003      1  FORMAT('1', 'MIU=', F10.3)
0004      A = (1.0-2.0*AMIU)/2.0
0005      D = 1.0+AMIU
0006      X = 0.0
0007      4  B = SQRT(1.0+X**2)
0008      C = X/B
0009      TAU = 0.5*(A+D*C-1.5*C**3)
0010      WRITE(6,2) X,TAU
0011      2  FORMAT(' ', 'ZECH=', F5.2, 'X', 'TAU=', F5.3)
0012      X = X+0.05
0013      IF(X.GT.3.0) GO TO 3
0014      GO TO 4
0015      3  AMIU = AMIU+0.15
0016      IF(AMIU.GT.0.50) GO TO 5
0017      GO TO 6
0018      5  STOP
0019      END
*OPTIONS IN EFFECT* ID,EBCDIC,SOURCE,NOLIST,NODECK,LOAD,NOMAP
*OPTIONS IN EFFECT* NAME = BUSTAN , LINECNT = 57
*STATISTICS* SOURCE STATEMENTS = 19,PROGRAM SIZE = 662
*STATISTICS* NO DIAGNOSTICS GENERATED
NO ERRORS IN BUSTAN

```

```

C
C SIGVER(I),SIGRF(I),SIGRAD(I),ARE GIVEN
C IN KGF/CM2 AND THEY ARE MEASURED AT THE TOP
C OF THE LAYER.
C
C DEFL(I,J) AND DEFPAR(I,J) ARE GIVEN
C IN CM AND THEY ARE MEASURED AT THE TOP
C OF THE LAYER.
C
C R(I) IS GIVEN IN CM AND IT IS MEASURED
C AT THE TOP OF THE LAYER.
C
C STGMM(I) IS GIVEN IN KGF/CM2 AND IT IS
C MEASURED WITH SIGN - AT THE TOP OF
C THE LAYER AND WITH SIGN + AT THE BOTTOM
C OF THE LAYER.
C
C SIGSUP(I) IS THE HORIZONTAL STRESS AT THE
C TOP OF THE LAYER , SIGINF(I)
C IS THE HORIZONTAL STRESS AT THE BOTTOM OF THE LAYER.
C BOTH OF THEM ARE MEASURED IN KGF/CM2.
C
C EXPR(I),A(I),ALFPAT(I),ZECH(I),B(I) ARE CALCULATED AT
C THE TOP OF THE LAYER(I)
C
C Y(L,I),PREVE(L,I),ORIZ(L,I) ARE GIVEN AT THE
C TOP OF THE LAYER (I).
C
C F(I), IS GIVEN AT THE BOTTOM OF LAYER (I).
C
C DEPL(L,I) IS THE COMPUTED DEFLECTION
C AT THE TOP OF THE LAYER I , AND IT IS
C MEASURED IN MM.
C
C DIMENSION F(200,10),AMTH(200,10),F(200,10),H(200,10)
C DIMENSION Y(200,10),PREVE(200,10),ORIZ(200,10)
C DIMENSION WL(200),D(200),PU(200),ZFCH(10)
C DIMENSION A(10),EXPR(10),R(10),SIGVER(10),ALFPAT(10)
C DIMENSION SIGRF(10),SIGRAD(10),DEFL(10,10),DEFPAR(10,10)
C DIMENSION R(10),STGMM(10),SIGSUP(200,10),SIGINF(200,10)
C DIMENSION DEPL(200,10),P(200,10),I(200,10),ALF(10)
C DIMENSION RAZA(10),SIGRAZ(10),SIGSUP1(10),SIGSUP2(10)
C DIMENSION DEBF(10,10),SIMAR1(10),SIMAR2(10)
C DIMENSION SINFL(10),SINF2(10)
C DIMENSION H3(10),F3H3(10),RAFR(10)
C DIMENSION Q(10),DEFBR(10,10),DEFB0(10,10)
C
C L = 1
6 READ(5,1) WL(L),D(L),PU(L),KAY
1 FORMAT(3F8.2,I6)
5 IF(KAY.GT.0) GO TO 8
5 READ(5,2) (F(L,I),I=1,7)
READ(5,2) (AMTU(L,I),I=1,7)
READ(5,2) (F(L,I),I=1,7)
READ(5,3) (H(L,I),I=2,7),IND1
0001 DIMENSION F(200,10),AMTH(200,10),F(200,10),H(200,10)
0002 DIMENSION Y(200,10),PREVE(200,10),ORIZ(200,10)
0003 DIMENSION WL(200),D(200),PU(200),ZFCH(10)
0004 DIMENSION A(10),EXPR(10),R(10),SIGVER(10),ALFPAT(10)
0005 DIMENSION SIGRF(10),SIGRAD(10),DEFL(10,10),DEFPAR(10,10)
0006 DIMENSION R(10),STGMM(10),SIGSUP(200,10),SIGINF(200,10)
0007 DIMENSION DEPL(200,10),P(200,10),I(200,10),ALF(10)
0008 DIMENSION RAZA(10),SIGRAZ(10),SIGSUP1(10),SIGSUP2(10)
0009 DIMENSION DEBF(10,10),SIMAR1(10),SIMAR2(10)
0010 DIMENSION SINFL(10),SINF2(10)
0011 DIMENSION H3(10),F3H3(10),RAFR(10)
0012 DIMENSION Q(10),DEFBR(10,10),DEFB0(10,10)
C
0013 L = 1
0014 6 READ(5,1) WL(L),D(L),PU(L),KAY
0015 1 FORMAT(3F8.2,I6)
0016 5 IF(KAY.GT.0) GO TO 8
0017 5 READ(5,2) (F(L,I),I=1,7)
0018 READ(5,2) (AMTU(L,I),I=1,7)
0019 READ(5,2) (F(L,I),I=1,7)
0020 READ(5,3) (H(L,I),I=2,7),IND1

```

```

0021 2 FORMAT(7F8.2)
0022 3 FORMAT(6F8.2,1I2)
0023 IF(IND1.EQ.1) GO TO 10
0024 IF(IND1.EQ.2) GO TO 20
0025 IF(IND1.EQ.3) GO TO 30
0026 IF(IND1.EQ.12) GO TO 120
0027 IF(IND1.EQ.13) GO TO 130
0028 IF(IND1.EQ.23) GO TO 230
0029 IF(IND1.EQ.123) GO TO 123

0030 10 READ(5,4) (Y(L,I),I=1,7),IND2
0031 4 FORMAT(7F8.2,14)
0032 7 L = L+1
0033 IF(IND2.EQ.0) GO TO 15
0034 GO TO 5
0035 L = L-1
0036 FORTA = WL(L)
0037 DIAM = D(L)
0038 PREST = PU(L)
0039 L = L+1
0040 WL(L) = FORTA
0041 D(L) = DIAM
0042 PU(L) = PREST
0043 GO TO 5
0044 20 READ(5,4) (PREVE(L,I),I=1,7),IND2
0045 GO TO 7
0046 30 READ(5,4) (CRIZ(L,I),I=1,7),IND2
0047 GO TO 7
0048 120 READ(5,4) (Y(L,I),I=1,7)
0049 READ(5,4) (PREVE(L,I),I=1,7),IND2
0050 GO TO 7
0051 130 READ(5,4) (Y(L,I),I=1,7)
0052 READ(5,4) (CRIZ(L,I),I=1,7),IND2
0053 GO TO 7
0054 230 READ(5,4) (PREVE(L,I),I=1,7)
0055 READ(5,4) (CRIZ(L,I),I=1,7),IND2
0056 GO TO 7
0057 123 READ(5,4) (Y(L,I),I=1,7)
0058 READ(5,4) (PREVE(L,I),I=1,7)
0059 READ(5,4) (CRIZ(L,I),I=1,7),IND2
0060 GO TO 7
0061 8 LIMITA = L-1
0062 CCFIA = 0.88
0063 CCF2R = 0.96
0064 DO 1000 L=L,LIMITA
0065 WRITE(6,3001) L
0066 3001 FORMAT('1',5X,'L=',I3)
0067 WRITE(6,8001)
0068 8001 FORMAT('1',5X,'CONTROL WRITINGS',/,5X,'*****')
0069 WRITE(6,8002) WL(L),D(L),PU(L)
0070 8002 FORMAT('1',5X,'WL=',F9.2,5X,'D=',F5.2,5X,'PU=',F5.2)
0071 DO 1001 I=1,10
0072 IF(F(L,I).EQ.0.0) GO TO 1002
0073 M = I
0074 1001 CONTINUE

```



```

0075 I = I
0076 ARFC = F(L,I)
0077 I = M
0078 EXPR(I) = 0.0
0079 A(I) = 0.0
0080 I = I-1
0081 IF(I.LT.1) GO TO 1003
0082 K = I+1
0083 EXPR(I) = (H(L,K)*(E(L,K)/A3EC)**(1.0/3.0))**2
0084 GO TO 1004
0085 I = M
0086 SPA = 0.0
0087 I = I-1
0088 IF(I.LT.1) GO TO 1006
0089 ZECH(I) = SPA+C3FIA*(EXPR(I)**(1.0/2.0))/D(L)
0090 SPA = ZECH(I)
0091 GO TO 5001
0092 I = M
0093 B(I) = 0.0
0094 I = I-1
0095 IF(I.LT.1) GO TO 1005
0096 A(I) = ZECH(I)**2
0097 B(I) = C3F2R*A(I)/(0.25+A(I))
0098 GO TO 1106
0099 I = I
0100 SIGVER(I) = PU(L)*(1.0-B(I))
0101 ALFPAT(I) = PU(L)/SIGVER(I)
0102 ALF(I) = ALFPAT(I)**(1.0/2.0)
0103 I = I+1
0104 IF(I.GT.M) GO TO 6100
0105 GO TO 1208
0106 I = M
0107 SIGFRE(I) = 0.0
0108 SIGRAD(I) = (PU(L)/2.0)**(1.0+2.0*AMIU(L,I))
0109 N = M-1
0110 WRITE(6,3002) N,SIGVER(I),N,ALFPAT(I),N,SIGFRE(I),
1 N,SIGRAD(I),N,ZECH(I),N,ALF(I)
0111 6200 I = I-1
0112 K = I+1
0113 IF(I.LT.1) GO TO 6300
0114 SIGFRE(I) = SIGVER(I)*F(L,K)
0115 SIGRAD(I) = PU(L)/2.0*(1.0+2.0*AMIU(L,I)-2.0*(
1 1.0+AMIU(L,I))*R(I)**(1.0/2.0))+R(I)
0116 N = I-1
0117 WRITE(5,3002) N,SIGVER(I),N,ALFPAT(I),N,SIGFRE(I),N,SIGRAD(I)
1 N,ZECH(I),N,ALF(I)
0118 3002 FORMAT(' ',SIGVER(' ,I,')=' ,F6.3,5X,'ALFPAT(' ,I,')=' ,
1F6.3,5X,'SIGFRE(' ,I,')=' ,F6.3,5X,'SIGRAD(' ,I,')=' ,F5.3,
25X,'ZECH(' ,I,')=' ,F5.2,5X,'ALF(' ,I,')=' ,F5.2)
GO TO 6200
0119 5300 I = I
0120 J = M+1
0121 DEF1(I,J) = (3.0**2.1415/9.0)*(1.0-AMIU(L,I)**2)/E(L,I)
0122 I*(PU(L)*D(L)/ALF(I))
0123 ALFA = DEF1(I,J)

```

```

0124      J = 1
0125      DEFL(I,J) = ALFA/2.0
0126      K = M+1
0127      DO 1009 J=2,M
0128      DEFL(I,J) = DEFL(I,K)/(ALFPAT(J)/ALFPAT(I)+1.0)
0129      DEBE(I,J) = ALFA*(1.0-0.5*(ALF(J)/ALF(I))**2)
0130      CONTINUE
0131      J = M+1
0132      DO 1012 I=2,M
0133      K = I-1
0134      SI = (SIGVER(I)+SIGVER(K))/2.0
0135      BI = (BI(I)+BI(K))/2.0
0136      DEFPAR(I,J) = H(L,I)*(1.0+AMIU(L,I))/F(L,I)*
1 (SI-2.0*AMIU(L,I)*PIU(L,I)*(1.0-3I**2*(1.0/2.0)))
1012 CONTINUE
MM = M+1
DO 1010 I=2,4
DO 1011 J = I,M
DEFPAR(I,J) = DEFPAR(I,MM)
1011 CONTINUE
1010 CONTINUE
K = M+1
KKK = M-1
DO 1013 I=2,KKK
J = 1
DEFPAR(I,J) = 0.0
N = I-1
DO 1014 J=2,N
DEFPAR(I,J) = DEFPAR(I,K)*((ALF(I)-ALF(J))/ALF(I))**2
DEFPAR(I,J) = DEFPAR(I,MM)*EXP(-(SIGVER(I)/O(L))*{ALF(J)/ALF(I)})
1014 CONTINUE
1013 CONTINUE
DO 1015 I=2,M
K=M+1
N = I-1
J = 1
1016 DEFL(I,J) = DEFL(N,J)+DEFPAR(I,J)
DEFB0(I,J) = DEFL(N,J)+DEFB7R(I,J)
J = J+1
IF(J.GT.K) GO TO 1015
GO TO 1016
1015 CONTINUE
K = M+1
MM = M+1
WRITE(6,3500) (ALF(I),I=1,MM)
3500 FORMAT(' ',5X,'ALF',5X,8(F10.4,2X))
I = 1
WRITE(6,3751) (DEBE(I,J),J=1,MM)
3751 FORMAT(' ',5X,'DEBE',5X,8(F10.9,2X))
WRITE(6,3700)
3700 FORMAT(' ',5X,'DEFL')
DO 3701 I=1,M
N = I-1
WRITE(6,3702) N,(DEFL(I,J),J=1,MM)
3702 FORMAT(' ',5X,I1,7X,8(F10.4,2X))

```



```

0227 SINFL(I) = SIMAR2(I)-SIGRAD(N)-SIGFRE(N)
0228 I = I+1
0229 IF(I.GT.M) GO TO 4400
0230 GO TO 4300
0231
0232
4400 WRITE(5,4500)
4500 FORMAT(' ',/,4X,'5X,4X,'SISUP1',17X,'SINFL',19X
1,'SISUP2',17X,'SINF2',/,16X,'R',20X,'R',22X
2,'RAZA',19X,'RAZA',/,7X,4('MEASURED',3X,'COMPUTED',
3,3X))
C
0233 DO 4600 I=2,M
0234 N = I-1
0235 WRITE(6,4700) ORIZ(L,I),SISUP1(I),ORIZ(L,I),SINFL(I)
1,ORIZ(L,I),SISUP2(I),ORIZ(L,I),SINF2(I)
4700 FORMAT(' ',5X,8(F9.4,2X))
4600 CONTINUE
C
I = M
P3001 = DEPL(L,I)*RAZI
P3002 = DEPL(L,I)*RAZ2
WRITE(6,4800) P3001,P3002
4800 FORMAT(' ',/,5X,'PROD1(R)=' ,F10.2,5X,'PROD2(RAZA)=' ,F10.2)
I = M
P3003 = R(I)*DEPL(L,I)
WRITE(6,4850) P3003
4850 FORMAT(' ',/,5X,'PROD3(R(I))=' ,F10.2)
VAL = 0.0
I = 2
301 Q(I) = E(L,I)*(H(L,I)**3)/(1.0-AMIU(L,I))
VAL = VAL+Q(I)
I = I+1
IF(I.GT.M) GO TO 300
GO TO 301
300 I = 1
ANUMER = 0.05*(1.0-AMIU(L,I)**2)*
1.4*(L)**2*ALF(I)*D(L)
ANUMIT = F(L,I)*VAL
DEFLMD = SQRT(ANUMER/ANUMIT)*1.2
WRITE(6,302) DEFLMD
302 FORMAT(' ',/,5X,'DEFLMD=' ,F10.6)
DEPLAS = DEPL(L,I)
I = M
DEPLOR = DEPL(L,I)
DEFCOR = DEFLMD+DEPLOR-DEPLAS
WRITE(5,303) DEFCOR
303 FORMAT(' ',5X,'DEFCOR=' ,F10.6)
SUME = 0.0
SUMH = 0.0
DO 9000 I=2,M
H3(I) = H(L,I)**3
SUMH = SUMH+H3(I)
E3H3(I) = E(L,I)*H3(I)
SUME = SUME+E3H3(I)
9000 CONTINUE

```

```

0275      RAPMOD = EMED/AREC
0276      WRITE(5,9001) EMED,RAPMOD
0277      FORMAT(' ',/,5X,'EMED=',F10.2,5X,'RAPMOD=',F10.3)
0278      DO 1100 I=1,7
0279          A(I) = 0.0
0280          EXPR(I) = 0.0
0281          ZECH(I) = 0.0
0282          R(I) = 0.0
0283          SIGVFR(I) = 0.0
0284          ALFPAT(I) = 0.0
0285          ALF(I) = 0.0
0286          SIGFRE(I) = 0.0
0287          STGRAD(I) = 0.0
0288          R(I) = 0.0
0289          SIGMM(I) = 0.0
0290          H3(I) = 0.0
0291          E3H3(I) = 0.0
0292      DO 1101 J=1,7
0293          DEF(I,J) = 0.0
0294          DEFPAR(I,J) = 0.0
0295      1101 CONTINUE
0296      1100 CONTINUE
0297      1000 CONTINUE
0298      STOP
0299      END
*OPTIONS IN EFFECT*  ID,FRCDIC,SOURCE,NOLIST,NODECK,LOAD,NOMAP
*OPTIONS IN EFFECT*  NAME = VERTER , LINECNT = 57
*STATISTICS*  SOURCE STATEMENTS = 299,PROGRAM SIZE = 111452
*STATISTICS*  NO DIAGNOSTICS GENERATED
NO ERRORS IN VERTER

```

NO STATEMENTS FLAGGED IN THE ABOVE COMPILATIONS.

APPENDIX 6

MICHIGAN TERMINAL SYSTEM FORTRAN G(41336)

VELMED

03-23-73

09:19.56

PAGE POOL

```

C
C SIGVER(I), SIGFRE(I), SIGRAD(I), ARE GIVEN
C IN KGF/CM2 AND THEY ARE MEASURED AT THE TOP
C OF THE LAYER.
C
C DEFL(I,J) AND DEFPAR(I,J) ARE GIVEN
C IN CM AND THEY ARE MEASURED AT THE TOP
C OF THE LAYER.
C
C R(I) IS GIVEN IN CM AND IT IS MEASURED
C AT THE TOP OF THE LAYER.
C
C SIGMOM(I) IS GIVEN IN KGF/CM2 AND IT IS
C MEASURED WITH SIGN - AT THE TOP OF
C THE LAYER AND WITH SIGN + AT THE BOTTOM
C OF THE LAYER.
C
C SIGSUP(I) IS THE HORIZONTAL STRESS AT THE
C TOP OF THE LAYER , SIGINF(I)
C IS THE HORIZONTAL STRESS AT THE BOTTOM OF THE LAYER.
C BOTH OF THEM ARE MEASURED IN KGF/CM2.
C
C EXPR(I), A(I), ALFPAT(I), ZECH(I), B(I) ARE CALCULATED AT
C THE TOP OF THE LAYER(I)
C
C Y(L,I), PREVE(L,I), DRIZ(L,I) ARE GIVEN AT THE
C TOP OF THE LAYER (I).
C
C F(I), IS GIVEN AT THE BOTTOM OF LAYER (I).
C
C DEPL(L,I) IS THE COMPUTED DEFLECTION
C AT THE TOP OF THE LAYER I , AND IT IS
C MEASURED IN MM.
C
C DIMENSION E(200,10), AMIU(200,10), F(200,10), H(200,10)
C DIMENSION Y(200,10), PREVE(200,10), DRIZ(200,10)
C DIMENSION WL(200), D(200), PUT(200), ZECH(10)
C DIMENSION A(10), EXPR(10), B(10), SIGVER(10), ALFPAT(10)
C DIMENSION SIGFRE(10), SIGRAD(10), DEFL(10,10), DEFPAR(10,10)
C DIMENSION R(10), SIGMOM(10), SIGSUP(200,10), SIGINF(200,10)
C DIMENSION DEPL(200,10), P(200,10), D(200,10), ALF(10)
C DIMENSION AMR(10), AMF(10), AMSUPL(10)
C DIMENSION ANTPTAT(10), ANT(10), RAPDEF(200,10)
C DIMENSION RAPREV(200,10), RAPORS(200), KAPORI(200)
C DIMENSION LIST(200)
C
C L = 1
6 READ(5,1) WL(L), D(L), PU(L), KAY
1 FORMAT(JF8.2,I6)
IF(KAY.GT.0) GO TO 8
5 READ(5,2) (E(L,I), I=1,7)
READ(5,2) (AMIU(L,I), I=1,7)
READ(5,2) (F(L,I), I=1,7)
(READ(5,3) (H(L,I), I=2,7), INDI

```

```

0021 3 FORMAT(6F8.2,I12)
0022 IF(INDL.EQ.1) GO TO 10
0023 IF(INDL.EQ.2) GO TO 20
0024 IF(INDL.EQ.3) GO TO 30
0025 IF(INDL.EQ.12) GO TO 120
0026 IF(INDL.EQ.13) GO TO 130
0027 IF(INDL.EQ.23) GO TO 230
0028 IF(INDL.EQ.123) GO TO 123
0029 10 READ(5,4) (V(L,I),I=1,7),IND2
0030 4 FORMAT(7F8.2,I3)
0031 L = L+1
0032 IF(IND2.EQ.0) GO TO 15
0033 GO TO 6
0034 L = L-1
0035 FORTA = WL(L)
0036 DIAM = D(L)
0037 PREST = PULL
0038 L = L+1
0039 WL(L) = FORTA
0040 DI(L) = DIAM
0041 PULL = PREST
0042 GO TO 5
0043 20 READ(5,4) (PREVE(L,I),I=1,7),IND2
0044 GO TO 7
0045 50 READ(5,4) (ORIZ(L,I),I=1,7),IND2
0046 GO TO 7
0047 120 READ(5,4) (V(L,I),I=1,7)
0048 READ(5,4) (PREVE(L,I),I=1,7),IND2
0049 GO TO 7
0050 130 READ(5,4) (V(L,I),I=1,7)
0051 READ(5,4) (ORIZ(L,I),I=1,7),IND2
0052 GO TO 7
0053 230 READ(5,4) (PREVE(L,I),I=1,7)
0054 READ(5,4) (ORIZ(L,I),I=1,7),IND2
0055 GO TO 7
0056 100 READ(5,4) (V(L,I),I=1,7)
0057 READ(5,4) (PREVE(L,I),I=1,7)
0058 READ(5,4) (ORIZ(L,I),I=1,7),IND2
0059 GO TO 7
0060 LIMITA = L-1
0061 CUF13 = 0.0+
0062 CUF28 = 0.97
0063 DO 1000 L=L,LIMITA
0064 WRITE(5,3001) L
0065 FORMAT(2,F5X,'L=',I3)
0066 WRITE(5,8001)
0067 FORTA(1,5X,'CONTROL WRITINGS',/,5X,'*****')
0068 WRITE(6,8002) WL(L),DI(L),PULL
0069 FORMAT(1,F5X,'WL=',F8.2,5X,'D=',F5.2,5X,'PU=',F5.2)
0070 DO 1001 I=1,10
0071 IF(L(I).EQ.0) GO TO 1002
0072 4 = I
0073 1001 CONTINUE
0074 1002 I = I
0075

```

```

0075 LIST(L) = M
0076 ABEC = E(L,I)
0077 I = M
0078 EXPR(I) = 0.0
0079 A(I) = 0.0
0080 I = I-1
0081 IF(I.LT.1) GO TO 1003
0082 K = I+1
0083 EXPR(I) = {H(L,K)*(E(L,K)/ABEC)**(1.0/3.0)**2
0084 GO TO 1004
0085 I = M
1003 SPA = 0.0
5001 I = I-1
IF(I.LT.1) GO TO 1006
ZECH(I) = SPA+COF1A*(EXPR(I)**(1.0/2.0))/D(L)
SPA = ZECH(I)
GO TO 5001
1006 I = M
B(I) = 0.0
ALF(I) = 1.0
1106 I = I-1
IF(I.LT.1) GO TO 1005
A(I) = ZECH(I)**2
B(I) = COF2B*A(I)/(0.25*A(I))
GO TO 1106
1005 I = 1
1008 SIGVER(I) = PU(L)*(1.0-B(I))
ALF(I) = SQR(SIGVER(I)/(SIGVER(I)**2.0/3.0))
ALFPAT(I) = ALF(I)**2
I = I+1
IF(I.GT.M) GO TO 6100
GO TO 1008
6100 I = M
SIGFRE(I) = 0.0
SIGRAD(I) = (PU(L)/2.0)*(1.0+2.0*AMIU(L,I))
N = M-1
6200 I = I-1
K = I+1
IF(I.LT.1) GO TO 6300
SIGFRE(I) = SIGVER(I)*F(L,K)
SIGRAD(I) = PU(L)/2.0*(1.0+2.0*AMIU(L,I)-2.0*(
1 1.0+AMIU(L,I))*B(I)**(1.0/2.0)+B(I))
N = I-1
GO TO 6200
6300 SUMDEF = 0.0
DO 1012 I=2,M
K = I-1
SI = (SIGVER(I)+SIGVER(K))/2.0
BI = (B(I)+B(K))/2.0
DEFPAR(I,J) = H(L,I)*{1.0+AMIU(L,I)}/E(L,I)*
1 (SI-2.0*AMIU(L,I))*PU(L)*(1.0-BI**(1.0/2.0))
SUMDEF = SUMDEF+DEFPAR(I,J)
1012 CONTINUE
C
0125
0126

```



```

0127 C
0128 C METHOD 1 CONSISTS OF :
0129 C XI = SORT((B*XO-C)/A)
0130 C
0131 C METHOD 2 CONSISTS OF :
0132 C XI = -C/(A*XO-B)
0133 C
0134 C METHOD 3 CONSISTS OF :
0135 C XI = (A*XO**2+C)/B
0136 C
0137 C METHOD 4 CONSISTS OF :
0138 C XI = (B*XO-C)/(A*XO)
0139 C
0140 C SUME = 0.0
0141 C DO 1300 I=2,M
0142 C SUME = SUME+E(L,I)*H(L,I)**5/(1.0-AMIG(L,I))
0143 C 1300 CONTINUE
0144 C I = I + 1
0145 C AL = 4.0*3.1416/(3.0*ALFPAT(I)*D(L)**2)*SUME**4.0
0146 C FR = ALFPAT(I)*ALOG(1.0+1.0/ALFPAT(I))
0147 C IF (FR.GT.1.0) FR=1.0
0148 C DO 1200 I=2,M
0149 C K = I-1
0150 C AMR(I) = 0.0
0151 C AMF(I) = -H(L,I)/2.0*(SIGFRE(I)*SIGFRE(K))
0152 C AMSOPL(I) = AMR(I)+AMF(I)
0153 C 1200 CONTINUE
0154 C JALE = 0
0155 C SUNOM = 0.0
0156 C DO 1201 I=2,M
0157 C SUNOM = SUNOM+AMSOPL(I)
0158 C 1201 CONTINUE
0159 C BIC = -(0.45-FR)*NL(L)+2.0*3.1416*SUNOM
0160 C C = -FR*NL(L)*SUMDEF
0161 C DEFLC = 0.0
0162 C INIT = 0
0163 C EQUA = (BIC*DEFLC-C)/AL
0164 C IF (EQUA.GT.0.0) GO TO 1202
0165 C WRITE(6,1257)
0166 C 1207 FORMAT(' ,5X, 'EQUA IS NEGATIVE')
0167 C GO TO 1203
0168 C DEFLAT = SQRT(EQUA)
0169 C MIMT = 1
0170 C IF (ABS(DEFLAT-DEFLC).LT.0.0001) GO TO 1204
0171 C IF (ABS(DEFLAT-DEFLC).GT.107.0) GO TO 1206
0172 C IF (ABS(DEFLAT).LT.0.00001) GO TO 1250
0173 C GO TO 1251
0174 C 1250 WRITE(6,1252)
0175 C 1252 FORMAT(' ,5X, 'WARNING COMPUTED DEFLECTION IS TOO SMALL ')
0176 C GO TO 1200
0177 C 1251 DEFLC = DEFLAT
0178 C GO TO 1205
0179 C 1206 WRITE(6,1207) MIMT
0180 C 1207 FORMAT(' ,10X, 'THE PROPOSED ',I4,' FOR THE ',I4,
0181 C ' COMPUTATION OF DEFLEC IS DIVERGENT')
0182 C GO TO 1250
    
```

```

0169 1203 DEFLAT = -C/(AI*DEFLEC-BIC)
0170     JALE = JALE+1
0171     IF(JALE.GT.30) GO TO 1290
0172     GO TO 1291
0173 1290 WRITE(6,1292)
0174 1292 FORMAT(' ',5X,'WARNING METHOD NO 2 IS NOT CONVERGENT ')
0175     GO TO 1293
0176 1291 MIMI = 2
0177     IF(ABS(DEFLAT-DEFLEC).LT.0.0001) GO TO 1204
0178     IF(ABS(DEFLAT-DEFLEC).GT.100.0) GO TO 1206
0179     DEFLEC = DEFLAT
0180     GO TO 1203
0181 1293 JALE = 0
0182 1295 DEFLAT = (AI*DEFLEC**2+C)/BIC
0183     MIMI = 3
0184     IF(ABS(DEFLAT-DEFLEC).LT.0.0001) GO TO 1204
0185     IF(ABS(DEFLAT-DEFLEC).GT.100.0) GO TO 1206
0186     DEFLEC = DEFLAT
0187     JALE = JALE+1
0188     IF(JALE.GT.30) GO TO 1294
0189     GO TO 1295
0190 1294 WRITE(6,1296)
0191 1296 FORMAT(' ',5X,'WARNING METHOD NO 3 IS NOT CONVERGENT ')
0192 1360 DEFLEC = 1.0
0193     JALE = 0
0194 1351 DEFLAT = (BIC*DEFLEC-G)/(AI*DEFLEC)
0195     MIMI = 4
0196     IF(ABS(DEFLAT-DEFLEC).LT.0.0001) GO TO 1204
0197     IF(ABS(DEFLAT-DEFLEC).GT.100.00) GO TO 1206
0198     DEFLEC = DEFLAT
0199     JALE = JALE+1
0200     IF(JALE.GT.30) GO TO 1350
0201     GO TO 1351
0202 1350 WRITE(6,1352)
0203 1352 FORMAT(' ',5X,'WARNING METHOD NO 4 IS NOT CONVERGENT ')
0204     GO TO 1000
0205 1204 K = M+1
0206     I = 1
0207     DEPL(L,I) = DEFLAT
0208     DO 1501 I=2,M
0209     N = I-1
0210     DEPL(L,I) = DEPL(L,N) + DEFPAR(I,K)
0211     CONTINUE
0212     I = 1
0213     R(I) = (ALFPAT(I)*D(I)**2)/(8.0*DEFLAT)
0214     PRUD = DEFLAT*R(I)*10.0
0215     WRITE(6,4800) PRUD,R(I)
0216 4800 FORMAT(' ',/5X,'PRUD = ',F10.2,5X,'R = ',F10.2,'CM')
0217     I = M
0218     K = M+1
0219     DEPLAS = DEPL(L,I)*10.0
0220     I = M
0221     K = 1
0222 2500 SIGMOM(I) = E(L,I)*H(L,I)/(2.0*(1.0-AMIU(L,I))*R(K))
0223     I = I-1

```

```

0224 IF(I,L1,Z) GO TO 1017
0225 AB(I)=200
0226 N = I-1
0227 N = I-1
0228 SIGSUP(L,I) = -SIGMOD(I)-SIGRAD(I)+SIGFRE(I)
0229 SIGINF(L,I) = SIGMOD(I)-SIGRAD(N)-SIGFRE(N)
0230 CONTINUE
0231 K = M+1
0232 DO 1020 I=1,M
0233 DEPL(L,I) = 10.0*DEPL(L,I)
0234 CONTINUE
0235 WRITE(6,1021)
0236 FORMAT(6,'58X','RESULTS',/,59X,'*****',/,5X,'E',12X,'H',
17X,'MU',9X,'F',16X,'Y',17X,'SIGVER',17X,'SIGSUP',11X,'SIGINF',/
22X,'KGF/CM2',7X,'CM',30X,'MM',10X,'KGF/CM2',22X,'KGF/CM2',
37,'+8X','MEASURED',3X,'COMP',T'D',3X,'MEASURED',3X,'COMPUTED',
43X,'MEASURED',3X,'COMPUTED',3X,'COMPUTED',/
0237 DO 1022 I=1,M
0238 VAL(I,5,1023) = (I,I),H(L,I),AMT(L,I),FL(I),Y(I),DEPL(L,I)
1,PREVE(L,I),SIGVER(I),ORIZ(L,I),SLOPE(L,I),SIGINF(L,I)
0239 FORMAT(7,'F10.2,1J(2X,F9.4)
0240 CONTINUE
0241 C 1 1023 I=1,M
0242 IF(Y(I),LE=0.0) GO TO 9500
0243 IF(ABS(DEPL(L,I))-0.10) GO TO 9500
0244 RAPDEF(L,I) = DEPL(L,I)/VAL(L,I)
0245 GO TO 9501
0246 RAPDEF(L,I) = 0.0
0247 IF(ABS(Y(I),LE=0.0) GO TO 9502
0248 RAPREV(L,I) = SIGVER(I)/PREVE(L,I)
0249 GO TO 9505
0250 RAPREV(L,I) = 0.0
0251 CONTINUE
0252 WRITE(6,9504) (RAPDEF(L,I),I=1,M)
0253 WRITE(6,9505) (RAPREV(L,I),I=1,M)
0254 FORMAT(6,'58X','RAPDEF',7(F9.3,2X)
0255 45,'+8X','MEASURED',3X,'COMPUTED',3X,'COMPUTED',/
0256 K = I-1
0257 IF(ABS(ORIZ(L,I))-0.0000001) ORIZ(L,I) = 0.0
0258 IF(ABS(ORIZ(L,I))-0.0000001) SIZ(L,N) = 0.0
0259 IF(ABS(ORIZ(L,I))-0.0000001) GO TO 950
0260 RAPDEF(L,I) = SIGSUP(L,I)/ORIZ(L,I)
0261 GO TO 9507
0262 RAPREV(L,I) = 0.0
0263 I = I(L,K),EM=0.0) GO TO 950
0264 RAPREV(L,I) = SIGREV(L,I)/ORIZ(L,I)
0265 GO TO 9507
0266 RAPDEF(L,I) = 0.0
0267 RAPREV(L,I) = 0.0
0268 WRITE(6,9509) RAPDEF(L,I),RAPREV(L,I)
0269 FORMAT(6,'58X','RAPDEF',7(F9.3)
15X,'RAPREV',7(F9.3)
0270 DO 1100 I=1,M
0271 A(I) = 0.0
0272 EXPB(I) = 0.0

```

```

0273 ZECH(I) = 0.0
0274 B(I) = 0.0
0275 SIGVER(I) = 0.0
0276 ALFPAT(I) = 0.0
0277 ALF(I) = 0.0
0278 SIGFRE(I) = 0.0
0279 SIGRAD(I) = 0.0
0280 R(I) = 0.0
0281 SIGMOM(I) = 0.0
0282 DO 1101 J=1,7
0283 DEFL(I,J) = 0.0
0284 DEFPAR(I,J) = 0.0
0285
0286
0287
0288
0289
0290
0291
0292
0293
0294
0295
0296
0297
0298
0299
0300
0301
0302
0303
0304
0305
0306
0307
0308
0309
0310
0311
0312
0313
0314
0315
0316
0317
0318
0319
0320
0321
0322
0323
0324
0325
0326
0327
1101 CONTINUE
1100 CONTINUE
1000 CONTINUE
      NUMAR1 = 0
      NUMAR2 = 0
      NUMAR3 = 0
      NUMAR4 = 0
      SUMRAP = 0.0
      SURAPR = 0.0
      SURADS = 0.0
      SURAJI = 0.0
      DO 9601 L=1,LIMITA
      M = LIST(L)
      DO 9600 I=1,M
      IF(RAPDEF(L,I).EQ.0.0) GO TO 9602
      NUMAR1 = NUMAR1+1
      SUMRAP = SUMRAP+RAPDEF(L,I)
9602 IF(RAPREV(L,I).EQ.0.0) GO TO 9600
      NUMAR2 = NUMAR2+1
      SURAPR = SURAPR+RAPREV(L,I)
9600 CONTINUE
      IF(RAPURS(L).EQ.0.0) GO TO 9604
      NUMAR3 = NUMAR3+1
      SURADS = SURADS+RAPURS(L)
9604 IF(RAPORI(L).EQ.0.0) GO TO 9601
      NUMAR4 = NUMAR4+1
      SURAJI = SURAJI+RAPORI(L)
9601 CONTINUE
      WRITE(6,2600) NUMAR1,NUMAR2,NUMAR3,NUMAR4
2600 FORMAT(' 5X,4(I3,5X)')
      IF(NUMAR1.EQ.0.0) GO TO 1900
      AMDEF = SUMRAP/NUMAR1
      GO TO 1901
1900 AMDEF = 0.0
1901 IF(NUMAR2.EQ.0.0) GO TO 1902
      AMPREV = SURAPR/NUMAR2
      GO TO 1903
1902 AMPREV = 0.0
1903 IF(NUMAR3.EQ.0.0) GO TO 1904
      AMFORS = SURADS/NUMAR3
      GO TO 1905
1904 AMFORS = 0.0
1905 IF(NUMAR4.EQ.0.0) GO TO 1906

```


UNIVERSITY OF MICHIGAN



3 9015 03695 1922